$CD8^+$ T cell priming and provision of $CD4^+$ T cell help are spatially and temporally distinct events

Dissertation

zur Erlangung des Doktorgrades (Dr. rer. nat.)
der Mathematisch-Naturwissenschaftlichen Fakultät
der Rheinischen Friedrich-Wilhelms-Universität Bonn

vorgelegt von

Sarah Eickhoff

aus Walsrode

Bonn, Oktober 2017

Angefertigt mit Genehmigung der Mathematisch-Naturwissenschaftlichen Fakultät der Rheinischen Friedrich-Wilhelms-Universität Bonn

1. Gutachter: Prof. Dr. Wolfgang Kastenmüller

2. Gutachter: Prof. Dr. Waldemar Kolanus

Tag der Promotion: 21.06.18

Erscheinungsjahr: 2018

Erklärung

Diese Dissertation wurde im Sinne von § 6 der Promotionsordnung vom 03.06.2011 im Zeitraum von Februar 2014 bis Oktober 2017 von Herrn Prof. Dr. Kastenmüller betreut.

Eidesstattliche Erklärung

Hiermit versichere ich, dass

- die vorgelegte Arbeit – abgesehen von den ausdrücklich bezeichneten Hilfsmitteln – persönlich, selbständig und ohne Benutzung anderer als der angegebenen Hilfsmittel angefertigt wurde,

- die aus anderen Quellen direkt oder indirekt übernommenen Daten und Konzepte unter Angabe der Quelle kenntlich gemacht sind,

- die vorgelegte Arbeit oder ähnliche Arbeiten nicht bereits anderweitig als Dissertation eingereicht worden ist bzw. sind,

- kein früherer Promotionsversuch unternommen worden ist,

- für die Erstellung der vorgelegten Arbeit und/oder die Gelegenheit zur Promotion keine fremde Hilfe, insbesondere keine entgeltliche Hilfe von Vermittlungs- bzw. Beratungsdiensten (Promotionsberatern/ -vermittlern oder anderen Personen) in Anspruch genommen wurde.

Bonn, den Sarah Eickhoff

Diese Arbeit ging in folgende Publikation ein:

Sarah Eickhoff, Anna Brewitz, Michael Y. Gerner, Frederick Klauschen, Karl Komander, Hiroaki Hemmi, Natalio Garbi, Tsuneyasu Kaisho, Ronald N. Germain, Wolfgang Kastenmüller. Robust Anti-viral Immunity Requires Multiple Distinct T cell-Dendritic Cell Interactions.
Cell (2015), https://doi.org/10.1016/j.cell.2015.08.004

Abstract

The generation of a protective memory $CD8^+$ T cell response requires priming of naïve T cells by dendritic cells and consecutive proliferation and differentiation of $CD8^+$ T cells. In this differentiation process $CD8^+$ T cells integrate multiple signals, including TCR-mediated stimulation, co-stimulation as well as cytokine-mediated activation. Co-stimulation and cytokine-mediated activation are in part dependent on $CD4^+$ T cell helper signals. However, $CD4^+$ T cell help for $CD8^+$ T cells is not directly transmitted but rather provided by an intermediate cell population - dendritic cells.

In this study, I investigated which DC subset serves as the critical communication platform between $CD4^+$ T helper and $CD8^+$ T cells in order to optimize $CD8^+$ T cell priming. Additionally, I aimed to address the spatio-temporal dynamics of such interactions *in vivo*, asking when and where those interactions may take place during an antiviral immune response. Interestingly, I found that $CD4^+$ and $CD8^+$ T cells were initially primed on spatial separated DC. $CD8^+$ T cells were activated on directly infected DC in the periphery of the LN whereas $CD4^+$ T cells were activated on non-infected DC in the LN paracortex. Notably, only during the later phase of infection (> 24h), both $CD4^+$ and $CD8^+$ T cells interacted with antigen-presenting non-infected $XCR1^+$ DC within the paracortex of the LN. This critical activation step happened after the initial DC encounter of both lymphocyte subsets, but before they started to proliferate. On a functional level, I found that anti-viral $CD8^+$ T cell responses activated in the absence of $XCR1^+$ DC failed to differentiate into fully functional memory $CD8^+$ T cells, mimicking the lack of $CD4^+$ T cell help.

In conclusion, this study identifies a new phase of T cell programing that reveals multiple DC interactions during the initial lymphocyte priming step, is critical for the development of a functional memory $CD8^+$ T cell compartment.

Table of Contents

1 Introduction

1.1 The organization of the immune system

The immune system protects us from infections and from the development of cancer. One major characteristic of the immune system is that it is highly dynamic, as its components possess extensive migratory capacities. This feature is indispensible for an effective protection against pathogens, because it allows immune cells to rapidly enter the inflamed tissue. Innate immune cells are either tissue-resident or can be rapidly recruited to the site of inflammation and are able to efficiently eliminate pathogens in an antigen-unspecific manner. Therefore, they possess conserved and specialized pattern recognition receptors (PRR), which allow them to sense pathogen-associated molecular patterns (PAMPs) on pathogens and directly respond with diverse effector mechanisms (Medzhitov and Janeway, 2000).

In contrast, the adaptive immune system detects specific antigens from pathogens and provides specific mechanisms to eliminate pathogens. This specificity results from high numbers of diverse antigen-specific receptors, like the T cell receptor (TCR) on conventional T lymphocytes, which diversity is based on gene rearrangement. This variability in the TCR allows for the existence of a broad repertoire of T cells with diverse antigen-specificities and at once is limited in low numbers of precursors (Davis and Bjorkman, 1988). Another fact is that only antigen-experienced T cells perform efficient effector functions. For initial activation, naïve T cells need contact with its cognate antigen, presented by an antigen-presenting cell (APC), which in most cases is a dendritic cell (DC) (Banchereau et al., 2000; Mempel et al., 2004; Mescher et al., 2006; Arens and Schoenberger, 2010). Hence, for an effective adaptive immune response, cell - cell interactions between different immune cells are necessary. These interactions are initiated in secondary lymphoid organs like lymph nodes (LN), the spleen and the mucosa-associated lymphoid tissues (MALT) and require co-localization of specific cells in order to exchange signals. In other words, for a T cell response, rare T cell precursors need to interact with a few DC presenting their specific foreign antigen. Thus, two different kinds of cells need to be together in space and time

demonstrating again their indispensability of the migratory capacity (Qi et al., 2014). Secondary lymphoid organs provide the environment for an efficient scanning strategy and antigen-specific cell - cell interactions and therefore recruit lymphocytes and collect pathogen/antigens and antigen-bearing DC from peripheral tissues (Andrian and Mempel, 2003; Steinman, 2012). Through that procedure, the spleen purges the blood of pathogens; the MALTs get the pathogen information from epithelial surfaces and LN from the epithelial surfaces, skin barriers and internal organs (Murphy and Weaver, 2016). Further, to accomplish the task of the specific functions of different immune cells and the dynamic cell encounter interactions, the structure of lymphoid organs is highly organized and will be discussed in the following section with a focus on the LN.

1.1.1 Lymph nodes architecture

The antigens/pathogens either freely drain or are transported by dendritic cells (DC) via the lymphatic network to the lymph nodes (Randolph et al., 2005). Over the afferent lymphatic vessels it is conducted to the subcapsular sinus (SCS) and the cortical sinus (CS)/interfollicular area (IFA) passes the medullary sinus (MS) and leaves the LN over the efferent lymphatic vessels (Figure 1.1). Around the sinusoid areas, innate immune cells are strategically positioned and are poised to detect pathogens immediately to initiate and support the adaptive immune response. Associated with these innate cells are macrophages and innate-like lymphocytes, like γδ T cells, natural killer cells (NK cells) or natural killer T cells (NKT cells). Along the sinusoids, macrophages are localized, filtering and eliminating the pathogens from the lymph and thereby preventing the spreading of the infection (Kastenmüller et al., 2012). After sensing pathogens, the macrophages release e.g. interleukin 18 (IL-18), which can rapidly activate the surrounding innate-like lymphocytes. In turn, the innate-like lymphocytes secrete e.g. interferon γ (IFNγ) leading to antimicrobial resistance of the macrophages (Mantovani et al., 2002; Benoit et al., 2008; Kastenmüller et al., 2012).

Besides the innate component on the entry sides, the LN is also the site for the initiation of the adaptive immune response. Therefore, lymphocytes constantly recirculate to lymph nodes, which they enter via high endothelial venules (HEV) and leave via the lymphatics (Gowans and Knight, 1964). In between, they migrate through the LN parenchyma guided by

a network of stromal cells (Bajénoff et al., 2006). These stromal cells basically build the backbone of LN architecture, containing a network of fibroblastic reticular cells (FRC) and the follicular DC (FDC). By producing different chemokines, these stromal cells enable the separation into roughly two zones: the B cell zone (B cell follicles) and the T cell zone (paracortex), which contain B and T cells, respectively. The B cell follicles contain follicular dendritic cells (FDC) producing the chemokine CXCL13. In turn, the receptor CXCR5 is expressed on naïve B cells and reflects the reasons for B cell recruitment into the follicles. T cells express the CC chemokine receptor type 7 (CCR7) and are recruited to the paracortex by FCR producing its ligands CC-chemokine ligand 21 and 19 (CCL21 and CCL19) (Cyster, 2005). In steady state, B and T cells constantly move along the stromal network while mainly remaining in their compartments (Bajénoff et al., 2006). Whereas naïve $CD8^+$ T cells are located in the deeper paracortex, memory $CD8^+$ T cells are preferentially located in the peripheral paracortex, allowing them the advantage to quickly respond to an infection (Kastenmüller et al., 2013).

Upon inflammation, before migratory DC arrive in the LN, soluble antigens reach the LN and are transported through a conduit system into the lymph node cortex. This conduit system is based on the network of fibroblastic reticular cells (FRC) and further resident DC are connected to the FCR network, collecting the antigens from the conduit´s lymph (Sixt et al., 2005). Resident DC can be subdivided into a $XCR1^+$ DC subset that is mainly localized in the paracortex but is also present in the IFA and SCS where it is prepared to ingest and transport antigens to the paracortex. It was shown, that $CD8^+$ T cell priming occurs in this areas. In contrast, resident $CD11b^+$ DC are primarily located close to the lymphatic sinuses, especially the medulla, which is the area where mainly $CD4^+$ T cell priming occurs (Dorner et al., 2009; Gerner et al., 2012). Later during the infection, antigen-bearing, migratory DC enter the LN and end up preferentially in different areas. Dermal ($CD103^+$) or $XCR1^+$ DC migrate in the cortical ridge close to the high endothelial venules (HEV), the main entry side of the lymphocytes. In contrast, migratory $CD11b^+$ DC are mainly found in the IFA, while Langerhans cells migrate towards the paracortex (Bajénoff et al., 2003; Kissenpfennig et al., 2005; Gatto et al., 2013).

In summary, the structure of the lymph node is highly organized, in order to support rapid and effective, innate and adaptive immune responses against infections. It provides the

spatial-temporal conditions that are needed for specific cell-cell interactions of highly dynamic immune cells. Furthermore, upon inflammation, the immune cells get activated, allowing them to reorganize their behavior/position within the LN.

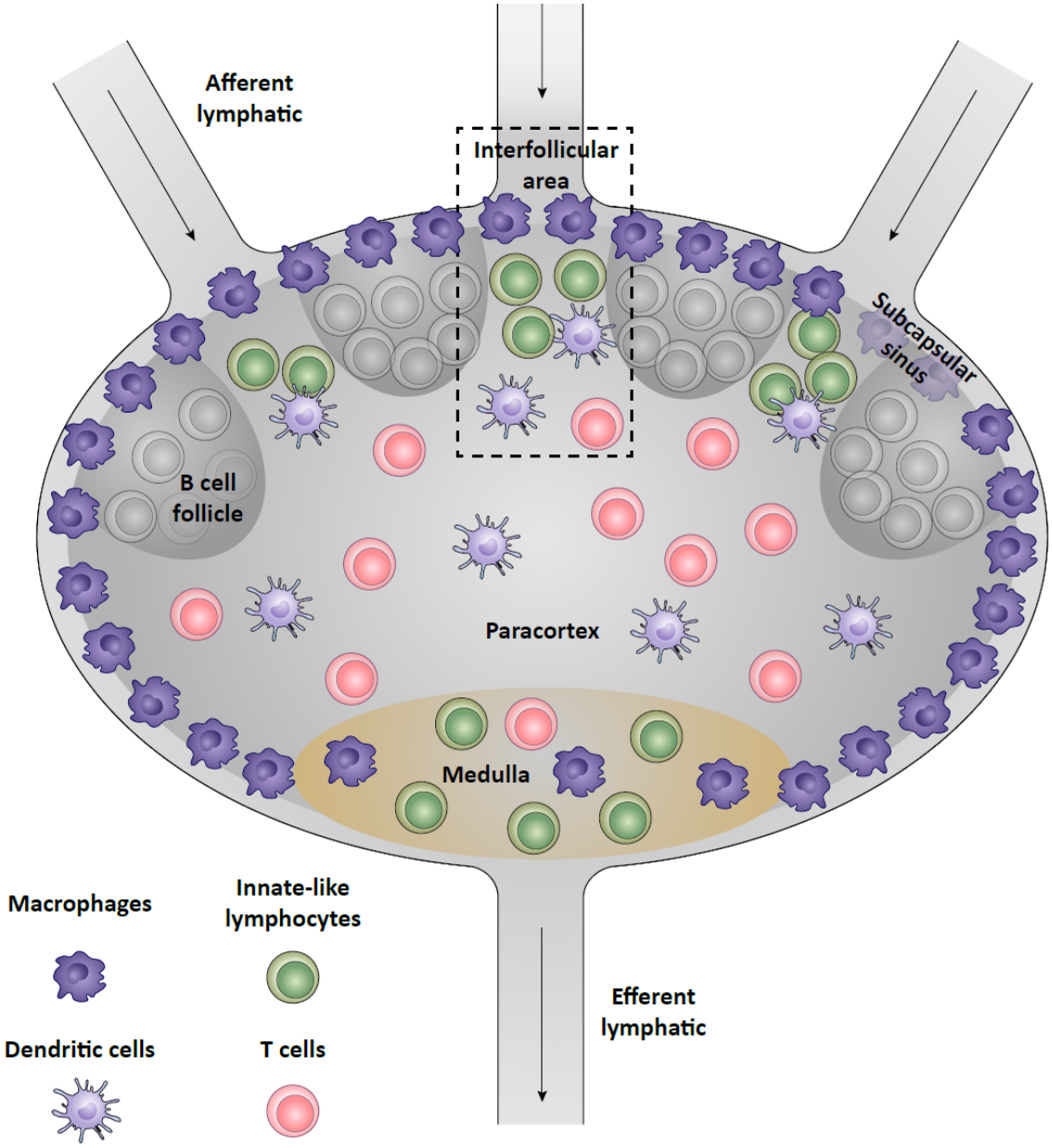

Figure 1.1. Lymph nodes architecture.
Spatial organization of the LN shows different areas with strategically pre-positioning of certain immune cells. Innate immune cells are positioned at the pathogen entry/egress sides allowing them to response immediately to infectious agents. Macrophages are localized along the sinusoid areas (subcapsular sinus, medulla) filtering the lymph, whereas innate-like lymphocytes are preferentially localized in the interfollicular areas and medulla. Adaptive immune cells are separated into two zones: the B cell follicle harboring B cells and the paracortex harboring T cells. Figure is adapted from Eickhoff et al., 2015 and Kastenmüller et al., 2012.

1.2 T cell mediated immunity

Within the adaptive immune response, T cells play an important role. After the activation of T cells through T cell receptor (TCR) mediated recognition of their cognate antigen, the T cells undergo clonal proliferation and differentiation into effector cells. Therefore, the antigen has to be presented as a complex of peptide and major histocompatibility complex (MHC). As T cells only recognize antigens (peptides) on MHC molecules on cell surfaces, they do not interact with the pathogen itself (Garcia and Adams, 2005). Additionally to the TCR, conventional T cells express a co-receptor determining their MHC restriction. On the one hand there are $CD4^+$ T cells, which recognize peptides presented through MHC class II molecules, on the other hand $CD8^+$ T cells recognize peptides via MHC class I molecules (Rudolph et al., 2006). The difference in the MHC restriction is also related to the different functions of $CD4^+$ and $CD8^+$ T cells. The MHC class II molecules are primarily expressed on APC, like macrophages, B cells and DC. $CD4^+$ T cells support these APC in their attempts to eliminate or to respond to pathogens, they promote ´help´ and are therefore also called $CD4^+$ T helper cells (Bluestone et al., 2009). In contrast, MHC class I molecules are expressed on all nucleated organism cells, constantly presenting cytosolic peptides. Upon intracellular infection, foreign antigens are presented on MHC class I molecules and can be recognized by antigen-specific effector $CD8^+$ T cells that promote killing of these intracellular infected cells by the release of cytotoxic effector molecules, which earned them the name cytotoxic T cells (CTL) (Trambas and Griffiths, 2003). The effector functions of CTL include a wide range of different mechanisms like granzyme/perforin and tumor necrosis factor alpha (TNFα) production or Fas ligand/TRAIL interactions (Ratner and Clark, 1993; Hirst et al., 2003; Brincks et al., 2008; Hassin et al., 2011). Another characteristic of activated effector $CD8^+$ T cells is the production of interferon gamma (IFNγ) leading to an activation of other effector cells (Cruz-Guilloty et al., 2009).

After antigen-specific activation, $CD8^+$ T cells undergo clonal expansion and upon clearance of the pathogen population - contraction and the formation of memory cells (Kaech and Cui, 2012). The development of an immunological memory is a hallmark of the adaptive immune system. Memory cells are characterized by long-term survival and differ from the naïve lymphocytes insofar that they are antigen-experienced and provide an increased pool of antigen-specific cells, which additionally allow for a more rapid and effective response upon

reinfection. The long-term survival of memory $CD8^+$ T cells is largely independent of TCR-mediated activation and is promoted through the cytokines IL-7 and IL-15 (Surh and Sprent, 2008). Their ability to rapidly respond to secondary infections results also from the fact that memory $CD8^+$ T cells can be activated through cytokines.

1.2.1 T cell migration in lymph nodes

T cells are continually searching for their specific antigen and for that purpose circulate between the blood and lymphoid organs like lymph nodes (Butcher and Picker, 1996). They enter the lymph nodes mostly via high endothelial venules (HEV) through interactions with selectins, whereby L-selectin (CD62L) is expressed on lymphocytes leading to a loose binding on peripheral node addressins (PNAD) expressed by the endothelium. This process is described as rolling. The expression of CD62L is the cause of specific homing from T cells to lymphoid organs. However, to enter the LN, CD62L is not sufficient on its own. It requires further interactions between integrins and chemokines. To arrest at the lymphoid HEV, the integrin leukocyte function-associated antigen 1 (LFA-1) must be activated on T cells. This activation is facilitated by CCR7 - CCL21/19 interactions, which are constantly expressed by naïve T cells and the endothelial cells, respectively. Once activated, LFA-1 interacts with the intracellular adhesion molecule 1 (ICAM1) leading to a proper adhesion which is followed by transmigration into the LN (Andrian and Mempel, 2003).

When T cells arrive in the LN, they migrate along a filament network of FRC (Bajénoff et al., 2006). Together, DC and FRC attract T cells by the production of CCL21/CCL19 (Stachowiak et al., 2006; Woolf et al., 2007). Searching for its cognate antigen, naïve T cells scan many DC with a contact time about 3-5 minutes for every DC and remain 12-21 hours in the LN (Miller et al., 2004; Mandl et al., 2012). If T cells do not encounter their cognate antigen, they leave the lymph node through the efferent lymph. For the egress of the LN, naïve T cells require sphingosine 1-phosphate receptor 1 (S1PR1) to sense the lipid molecule S1P. The efferent lymph contains a higher level of S1P compared to the lymph node tissue, thereby forming a gradient of S1P. In the end, this leads the naïve T cells to egress the lymph node into lymphatic vessels (Matloubian et al., 2004; Pham et al., 2010).

As mentioned above, T cells are searching for their specific antigen and if they find it, they are activated. In the case of naïve T cells, the initial encounter with their specific antigen is

called priming. T cell priming is separated into three distinct phases (Mempel et al., 2004). In the first phase after entering the LN, T cells have short encounters with a lot of different DC. Once they find their specific antigen, presented by a mature DC, they move into phase two, characterized by long-term interactions (12-24 h) between DC and T cell and initiation of cytokine production (Miller et al., 2002; Stoll et al., 2002; Bousso and Robey, 2003). In the third phase, DC and T cells return to short interactions and T cells start to proliferate and differentiate into various effector cells.

During their activation and proliferation, T cells remain in the lymph node for several days. This is caused by the upregulation of CD69 on T cells induced by TCR signaling (Cebrian et al., 1988). The surface protein CD69 leads to an internalization of S1PR1 and consequently to a loss of chemotaxis in response to S1P. After proliferation, T cells loose CD69 expression and regain the S1PR1, allowing them to egress the LN (Shiow et al., 2006). Because CD69 is rapidly upregulated after TCR signaling, it is often used as an activation marker for T cells after antigen-specific activation.

1.2.2 Activation of naïve T cells

If naïve T cells encounter their specific antigen, presented by a professional APC usually in lymphoid organs, they start to proliferate and differentiate into effector cells. These newly developed effector cells leave the lymphoid organs and migrate into inflamed tissue. After re-encountering the antigen, the antigen-experienced T cells then rapidly and efficiently perform their effector functions, like induction of apoptosis of infected cells (Weninger et al., 2001; Zhang and Bevan, 2011).

Before naïve T cells develop to functional effector cells, they require priming by a professional APC because naïve T cells need co-stimulatory signals to become fully activated. For a successful activation, naïve T cells require three signals mediated by APC, typically DC. The first signal is the interaction between the TCR and the peptide:MHC (p:MHC) complex on APC. If the affinity of the TCR is high enough, meaning if the TCR is specific for the antigen, it a stable interaction is formed and induces proliferation of antigen-specific T cells (Brownlie and Zamoyska, 2013). The co-stimulatory molecules expressed by the APC provide the second essential signal. In addition to that, an APC expresses the co-stimulatory molecules only when it is activated by innate receptors. Hence, it is implicated to an infection or

inflammation. Without any co-stimulatory signals, a strong TCR – p:MHC interaction may induce tolerance by e.g. elimination of the reactive T cell or the induction of anergy (Harding et al., 1992; Tan et al., 1993). However, in an inflammatory context, the co-stimulatory signals are mediated by the molecules CD80 and CD86 (B7 family) on APC through binding to CD28 on T cells. These interactions induce survival and expansion signals to the T cells by promoting the expression of the α chain of interleukine-2 receptor (IL-2Rα, also known as CD25) on T cells. Further, the stimulation of CD28 leads to IL-2 production by T cells, hence they increase their own proliferation capacity (Allison, 1994; Lenschow et al., 1996). In addition to the CD80/86 – CD28 interaction, further co-stimulatory interactions are involved in the T cell proliferation and survival, like 4-1BBL – 4-1BB interactions. The 4-1BB molecules are expressed on activated T cells and belong to the tumor necrosis factor superfamily. The stimulation through 4-1BB induces cell division and IL-2 production of T cells and further is important for the survival of activated T cells (Williams and Bevan, 2007). The molecule CD70 is expressed on mature DC and binds through the CD27 receptor on T cells (Hendriks et al., 2000; 2003). Aside from CD27, 4-1BB and CD28, another pair of co-stimulating molecules is OX40 on DC and OX40 ligand on activated T cells that enhance T cell survival and proliferation. In contrast to the pro-survival and pro-proliferation signals described so far, binding of cytotoxic T-lymphocyte-associated protein 4 (CTLA4) has an inhibitory effect on T cells. Activated T cells express CTLA4, which competes with CD28 for the CD80/86 interaction and thereby regulates the proliferation of T cells (Greenwald et al., 2005; Watts, 2005).

For an initial activation the signals 1 (TCR-p:MHC) and 2 (co-stimulation) are sufficient but an optimal T cell response also need a third signal (van Stipdonk et al., 2001). The signal 3 is represented by the T cell stimulation through cytokines, produced by the APC itself or other activated immune cells (Haring et al., 2006). It has been demonstrated that different cytokines influence the T cell response in various ways. As an example, IL-12 promotes the cytotoxicity and production of IFNγ of effector $CD8^+$ T cells and IFNα influences the $CD8^+$ T cell differentiation and proliferation (Curtsinger et al., 2003a; 2005; Kolumam et al., 2005). The variation and strength of the three signals is dependent on the infection and on the interacting cells themselves and is essential for the T cell differentiation (Stemberger et al., 2007; Gerlach et al., 2010). Thus, the population of T cells is heterogeneous, including

different effector cells, memory precursors and finally various memory cells (Williams and Bevan, 2007; Kaech and Cui, 2012).

1.2.3 The differentiation and heterogeneity of CD8$^+$ T cells

The majority of the effector CD8$^+$ T cells develop into short-lived effector cells (SLEC), which are not able to proliferate after re-encountering their antigen and are therefore also called terminal effector cells (TEC) (Parish and Kaech, 2009). It has been shown that different circumstances promote the differentiation into TECs, like an increased amount of inflammatory cytokines, e.g. IL-2, type I IFN and IL-12, and the constant presence of antigen (Curtsinger et al., 2003b; Kolumam et al., 2005; Pearce and Shen, 2007; Kalia et al., 2010). Furthermore, after activation, naïve CD8$^+$ T cells upregulate expression of chemokine receptors, like CXCR3. It has been demonstrated that CXCR3 guides CD8$^+$ T cells to infected cells - into an inflammatory environment - and in turn enhances the differentiation into TECs (Hu et al., 2011; Kurachi et al., 2011). In contrast, the differentiation into memory CD8$^+$ T cells is enhanced through the expression of the chemokine receptor CCR5 (Castellino et al., 2006; Prlic et al., 2006). Additionally, the homeostatic cytokines, IL-7 and IL-15, promote the formation of memory CD8$^+$ T cells (Kennedy et al., 2000; Ma et al., 2006). Several markers are used to define different CD8$^+$ T cell populations at the peak of the primary response (in this work referred to 8 days after Vaccinia virus infection). While expression of killer cell lectin-like receptor G1 (KLRG1) is used as a marker for TECs, the expression of the α-chain of the IL-7 receptor (IL-7R or CD127) is used to identify those cells, which have a high potential to differentiate into memory cells. Therefore, during the primary response, the IL-7R expressing CD8$^+$ T cells are called memory precursor effector cells (MPEC) (Cui and Kaech, 2010).

Most of the cells die during the contraction phase (≥ 8-30 days after infection) while a small population of memory CD8$^+$ T cells survives. Memory CD8$^+$ T cells can be characterized by different phenotypic markers and can be separated roughly into central memory T cells (T_{CM}) and effector memory T cells (T_{EM}). Central memory T cells express high levels of the chemokine receptor CCR7 and the selectin CD62L, which causes them to recirculate between the blood and secondary lymphoid organs. Furthermore, their functional feature is a high proliferative potential after re-stimulation, while the development of their effector functions

requires a certain amount of time. In contrast, effector memory T cells are characterized through low expression levels of CCR7 and CD62L and recirculate between peripheral tissues. They have a low proliferative potential but can mediate effector functions immediately. Effector memory T cells can be subdivided further by the expression of CD103 and CD69. Memory T cells expressing CD103/CD69 basically remain within peripheral tissues and are referred to as tissue-resident memory T cells (T_{RM}) (Williams and Bevan, 2007; Kaech and Cui, 2012).

Moreover, memory $CD8^+$ T cells can be further classified through the expression of the fractalkine receptor CX_3CR1, as a high expression of CX_3CR1 correlates with the cytotoxic effector functions of $CD8^+$ T cells memory cells and a low homeostatic proliferative capacity. However, it was shown that an intermediate expression of CX_3CR1 on memory $CD8^+$ T cells identifies the population with a higher proliferate capacity, which simultaneously fill up the niche of the CX_3CR1 high expressing cells (Böttcher et al., 2015; Gerlach et al., 2016).

The generation of the heterogeneous $CD8^+$ T cell differentiation is an ongoing field of research. There are currently four main different models to explain the diversity of $CD8^+$ T cells. The first model is based on the separate-precursor theory, where naïve T cells are pre-programmed during their development in the thymus. However, experiments using single cell transfer or barcoding of $CD8^+$ T cells have already disproved this hypothesis (Stemberger et al., 2007; Gerlach et al., 2010). Another model is supported by studies demonstrating that the division of T cells is asymmetric, meaning that the division of one mother cell results into two daughter cells with different fates (Chang et al., 2007). The asymmetric cell fate model suggests that the daughter cell that is closer to the APC receives stronger TCR and co-stimulatory signals and develops into a TEC. In contrast, the daughter cell that is further away from the APC develops into a memory cell. Indeed, *in vivo* T cells do not have contact to their activating APC during division. Two other models propose the theory of different cell fate based on the strength of the stimulation. The decreasing potential model suggests that repetitive stimulation through signals 1-3 leads to terminal differentiation. Studies, which support this hypothesis, demonstrated that truncated stimulation leads to an enhanced formation of memory T cells. The final model proposes that the fate of a T cell is determined the overall signal strength during the initial priming (Lanzavecchia and Sallusto, 2002; D'Souza and Hedrick, 2006; Ahmed et al., 2009; Kaech and

Cui, 2012). Together, these models assume different scenarios to explain the fate of $CD8^+$ T cell differentiation during activation, in which a combination of the models cannot be excluded.

In summary, during infection, $CD8^+$ T cells differentiate into diverse types of effector and memory cells and can be exposed to large range diverse signals, which explains the heterogeneity of effector and memory $CD8^+$ T cells. Thereby, the heterogeneity of memory $CD8^+$ T cells builds the basis for a comprehensive protection against reinfection.

1.3 Dendritic Cells

Dendritic cells (DC) are professional antigen-presenting cells (APC) and were first described by their distinct morphological features, the dendrites (Steinman and Cohn, 1973). Dendritic cells can be activated through tissue injury and the presence of pathogens and are specialized in presentation of antigens to naïve and memory T cells (Steinman and Cohn, 1974). Therefore, they present the interface between the innate and the adaptive immune response with the ability to induce either immunity or tolerance.

1.3.1 Antigen presentation and maturation of dendritic cells

Dendritic cells populate most tissues including barrier tissues such as lung and skin and internal organs such as liver and lymphoid tissues. They constantly take up, process and present antigen. Dendritic cells are able to present antigen through different mechanisms (Banchereau et al., 2000). One route of antigen-presentation is through direct presentation of cytosolic antigen via MHC class I. Dendritic cells are susceptible to infections by some viruses, which leads to the synthesis of viral proteins by DC. Cytosolic proteins are processed to a size of 8-10 amino acids, loaded on MHCI heavy chain and β2-microglobin and transported to the cell surface. Consequently, viral peptides are presented on MHC class I, allowing for recognition by $CD8^+$ T cells (Miles et al., 2005). However, there are situations, in which DC are not infected like influenza virus infection or tumors (Helft et al., 2012). In order to enable the generation of a robust $CD8^+$ T cell response under these circumstances, the immune system needs to transfer exogenous antigens onto MHC class I molecules in a process called cross-presentation (Kurts et al., 1996). This is facilitated by a subset of DC,

which is characterized by the expression of XCR1. Several molecules that are critical for optimal cross-presentation have been identified. However, a unique cell biological, mechanistic concept of cross-presentation has so far not been discovered (Gutierrez-Martinez et al., 2015).

Apart from that, antigen-presentation via MHC class II is also largely restricted to APC, including macrophages, B cells and DC. Here, exogenous antigen is ingested and processed by the APC (Itano and Jenkins, 2003). After processing peptide fragments of 13-20 amino acids are presented via MCHII on the cell surface, allowing for the activation of antigen-specific $CD4^+$ T cells (Rudensky et al., 1991).

Presenting the cognate antigen to T cells is necessary for their initial activation. But as mentioned above, for a successful and optimal activation of naïve T cells, DC require co-stimulatory molecules. In steady state, DC are immature, do not express co-stimulatory molecules and to this end not able to properly activate T cells. Upon infection or inflammation, DC locally ingest antigens and sense `danger´ signals, such as inflammatory cues from infected cells or pathogens themselves through specialized pathogen recognition receptors (PRR), like toll-like receptors (TLRs) (Matzinger and Kamala, 2011). The sensing of danger signals induces maturation and migration of DC to the draining lymph node. Arrived there, DC can present the antigens to high numbers of lymphocytes. Furthermore, stimulation through danger signals activates DC resulting in their maturation. Additionally, receiving signals from antigen-specific $CD4^+$ T cells can further activate DC. Matured DC upregulate the expression of co-stimulatory molecules on their surface and further start the production of cytokines. The expression of co-stimulatory molecules allows DC to activate antigen-specific naïve T cells (see also 1.2.2) and the released cytokines guide the differentiation of the T cells (Merad et al., 2013).

1.3.2 Dendritic cell subsets

Since their discovery, multiple distinct DC subsets have been characterized and they can be distinguished by their specialized function and surface marker expression. Clearly distinct populations are plasmacytoid DC (pDC) and conventional DC (cDC) (Figure 1.2). Plasmacytoid DC have a limited potential to take up antigen (Villadangos and Young, 2008) and are rather

known for their type I interferon production capabilities after viral infections (Merad et al., 2013).

In contrast, the major function of cDC is to phagocytose and process antigen. In mice, cDC are characterized as $CD11c^{hi}$ and $MHCII^{+}$ cells and can be subdivided into migratory and lymphoid tissue-resident DC (Figure 1.2). In steady state, spleen and LN harbor lymphoid-resident DC that express either $CD4^{+}$ or $CD8\alpha^{+}$ or neither of both $CD4^{+}/CD8\alpha^{+}$ and are therefore often referred to as double negative (DN) DC. Migratory DC consist of $CD11b^{+}$ DC, $CD103^{+}$ DC (dermal) and Langerhans cells and transport antigens from peripheral tissues to the draining LN via the afferent lymphatic vessels. Consequently, in contrast to the spleen, LNs contain both migratory and lymphoid-resident DC (Belz and Nutt, 2012). Unraveling the different groups of DC by surface markers, there is also functional specialization of DC regarding their antigen-presentation. Whereas $CD8\alpha^{+}$ DC and $CD103^{+}$ DC are known for their capacity to cross-present antigen, $CD4^{+}$ and DN DC are more efficient in presenting antigen via MHCII. Therefore, $CD8\alpha^{+}$ DC are more efficient in activating $CD8^{+}$ T cells, and $CD4^{+}$ and DN efficiently provoke $CD4^{+}$ T cell responses (Caminschi, 2012).

Additionally, the majority of $CD8\alpha^{+}$ DC and $CD103^{+}$ DC can be characterized by the chemokine receptor expression of XCR1 (Shortman and Heath, 2010). The ligands of XCR1 are XCL1 and XCL2, which are produced by activated $CD8^{+}$ T cells, Th1-polarized $CD4^{+}$ T cells and natural killer (NK) cells (Dorner et al., 2002; 2004). It has been shown that XCL1 is a specific chemoattractant for XCR1 and that a loss of XCL1 leads to a decreased specific $CD8^{+}$ T cell response (Dorner et al., 2009). Furthermore, it has been demonstrated that $XCR1^{+}$ DC are specialized in the uptake of dead cells and cross-presentation of antigen to $CD8^{+}$ T cells (Iyoda et al., 2002). In this work, in some experiments $XCR1^{+}$ DC are referred to as $CD8\alpha^{+}$ DC whenever CD8α was used as marker to distinguish DC subsets.

Another factor to be mentioned in the context of cross-presenting DC is the basic leucine zipper transcription factor, ATF-like 3 (Batf3). In the spleen, deficiency of Batf3 has been described to lead to a lack of cross-presenting $CD8\alpha^{+}$ DC and $CD103^{+}$ DC (Hildner et al., 2008).

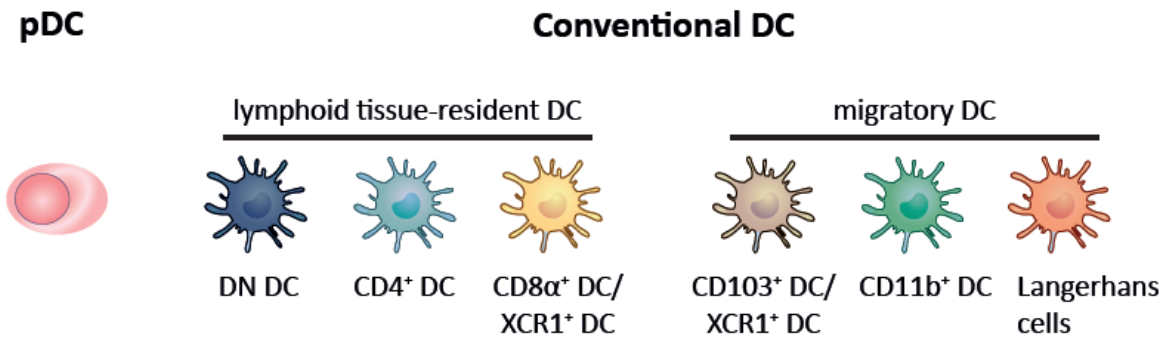

Figure 1.2. Dendritic cell subsets.
Conventional dendritic cells (cDC) are subdivided into migratory and lymphoid tissue-resident DC. Detailed characterization of DC is based on the expression of CD4, CD8α, CD11b, CD103 or XCR1 and their functional specialization. pDC: plasmacytoid dendritic cell; cDC: conventional dendritic cell Figure is adapted from Belz and Nutt, 2012.

1.4 CD4$^+$ T cell help for CD8$^+$ T cell immunity

The generation of an effective CD8$^+$ T cell immunity is dependent on the help of CD4$^+$ T cells, which requires interaction between these cells. There is no evidence for direct cell - cell interactions between CD8$^+$ and CD4$^+$ T cells. The CD4$^+$ T cell help of CD8$^+$ T cells is dependent on a third cell compartment to serve as communication platform. It was shown that the coordination of the help is permitted through DC, which receive the CD4$^+$ T cell helper signals and are then able to prime CD8$^+$ T cells (Mitchison and O'Malley, 1987; Ridge et al., 1998). For that purpose, foreign antigens need to be presented on the same DC via MHCI and MHCII in order to stimulate both CD4$^+$ and CD8$^+$ T cells (Cassell and Forman, 1988; Bennett et al., 1997). Since the discovery of a three-cell interaction axis, many researchers investigated how DC receive helper signals and how DC mediate helper signals. Early *in vitro* studies showed that the CD4$^+$ T cells supply a high amount of IL-2 and that IL-2 was essential for the growth of CD8$^+$ T cells in culture flasks. These facts lead to the assumption that IL-2 represent a primary helper signal, which means that the nature of help is provided by CD4$^+$ T cells and in turn means that the CD4$^+$ and CD8$^+$ T cells need to be in close proximity at the same time (Bevan, 2004; Castellino and Germain, 2006). This theory was disproved when several groups discovered the mechanism how CD4$^+$ T cells provide the help to DC or how CD4$^+$ T cells license the DC (Ridge et al., 1998; Schoenberger et al., 1998). They demonstrated that the provision of CD4$^+$ T cell help to DC happens through CD40 and CD40L interactions, which leads to the upregulation of the co-stimulatory molecules CD80/CD86

and to the production of cytokines by the DC. Further, it was demonstrated that *in vitro* stimulation with CD40 antibody alone, led to DC licensing and further to an effective priming of antigen-specific $CD8^+$ T cells. According to this, there would be no need of a three-cell interaction at the same time as the DC itself provides the helper signals. It should be noted though that the cytokines provided by the DC are dependent on the model system studied. For example, for an antigen-specific $CD8^+$ T cell response, it was shown that during Vaccinia virus (VV) and adenovirus infection $CD4^+$ T cell help induces the type I IFN and IL-15 production by DC, respectively. Furthermore, IL-12 was shown to be a strong amplifier of $CD8^+$ T cell response in $CD4^+$ T cell help dependent systems (Bedoui et al., 2016). In other words, $CD4^+$ T cell help for $CD8^+$ T cells means that $CD4^+$ T cells activate or license DC in an antigen-specific manner in order to prime antigen-specific $CD8^+$ T cells via these DC.

However, the requirement of help has been described in several models, it has especially been demonstrated that all secondary responses are dependent on $CD4^+$ T cell help. Hence, without $CD4^+$ T cells during the priming of $CD8^+$ T cells, the formation of memory $CD8^+$ T cells is impaired, which is reflected by lower numbers as well as by functional defects of memory $CD8^+$ T cells. In contrast, the primary $CD8^+$ T cell response can be either dependent on or independent of $CD4^+$ T cell help depending to the strength of the inflammation. Upon viral or bacterial infection, the microenvironment contains high levels of inflammatory cues and PAMPs. Consequently, DC can be directly activated through these infectious agents and differentiate from an immature to a mature state and may bypass the need of $CD4^+$ T cell help (Behrens et al., 2004; Williams and Bevan, 2007). For example, lymphocytic choriomeningitis virus (LCMV) infections induce a strong type I IFN response and do not require $CD4^+$ T cell help to induce the primary $CD8^+$ T cell response (Bourgeois and Tanchot, 2003). In contrast, in a non-inflammatory scenario like priming against tumors antigens or when viruses evolved strategies to evade $CD8^+$ T cell activation or recognition, some studies showed that the priming of $CD8^+$ T cells is dependent on $CD4^+$ T cell help (Behrens et al., 2004). In this work, Vaccinia virus was used as model system as its primary antigen-specific $CD8^+$ T cell response is optimized via the help of $CD4^+$ T cells.

1.5 Aim of the study

A well-characterized example for $CD4^+$ T cell help is the help for B cells. $CD4^+$ T cell help for B cells includes that antigen-specific helper T cells find the antigen-bearing B cells. The dynamic mechanism of this rare two-cell encounter is a well-known concept and contains multiple cell-cell interactions. Thereby, DC prime naïve $CD4^+$ T cells in the paracortex of the LN (T cell zone) and the B cells previously encounter their specific antigen in the B cell follicle. After antigen-recognition, B and $CD4^+$ T cells change their chemokine receptor expression, which leads to their re-localization towards the T-B border in the LN and in turn increases the ability of a specific cell-cell interaction. Finally, $CD4^+$ T cell help for B cells is required for a germinal center reaction, including isotype class switching and affinity maturation, factors that are essential for immunity against secondary infections (McHeyzer-Williams et al., 2006; Qi et al., 2014).

In line with this, the development of a functional and effective memory $CD8^+$ T cell response is also influenced through the help of $CD4^+$ T cells. In this process, the provision of help was considered to be a three-cell encounter of rare antigen-specific $CD4^+$ and $CD8^+$ T cells and antigen-bearing DC, which were thought to interact simultaneously in space and time. The establishment of the DC licensing model, where $CD4^+$ T cells migrate from DC to DC and activate these through CD40/CD40L interaction, offered a solution for the unlikely case of a simultaneous three-cell cluster (Castellino and Germain, 2006). At the same time, the antigen-specific licensing of DC prevents $CD4^+$ T cells randomly activating DC, but does not solve the problem of how naïve antigen-specific $CD8^+$ T cells find the licensed DC. Similar to the $CD4^+$ T cell help for B cells, it has been demonstrated that chemokine receptors guide the $CD8^+$ T cells to a licensed DC, which produce the chemokines CCL3/CCL4 and CCL17 and attracts the $CD8^+$ T cells via CCR5 and CCR4, respectively (Castellino et al., 2006; Semmling et al., 2010). Nevertheless, this chemokine guidance model introduced new unresolved issues. Following a chemokine gradient, $CD8^+$ T cells would encounter non-licensed DC, presenting their specific antigen, which in turn leads to long-term interactions with this DC (12-24 h) (Miller et al., 2002; Stoll et al., 2002; Bousso and Robey, 2003). Consequently, they are delayed in finding their common licensed DC. Moreover, naïve $CD8^+$ T cells do not express high levels of the receptors CCR5 and CCR4 (ImmGen database; search term: CCR4 and CCR5 (Heng and Painter, 2008)).

Based on the knowledge of multiple cell-cell interactions during the $CD4^+$ T cell help for B cells and the knowledge that different DC subsets are specialized in their functions and their interactions with either $CD4^+$ or $CD8^+$ T cells, I wanted to understand how the $CD4^+$ T cell help for $CD8^+$ T cells is organized. Therefore, I aimed to address two major questions. First, how is $CD4^+$ T cell help organized in a spatial-temporal dimension, or in other words: Where and when does $CD4^+$ T cell help take place? And second, which DC subset is delivering the helper signals to $CD8^+$ T cells? Unraveling this questions promises to provide novel basis insights into the exact steps of lymphocyte priming, which may be critical for future vaccines aimed to optimally induce cytotoxic $CD8^+$ T cell responses.

2 Materials and Methods

2.1 Materials

2.1.1 Equipment

Equipment	Name and Company
Anesthetic apparatus	Tec3, Eickemeyer, Tuttlingen
Balances	CP224S-0CE and CP2201, Sartorius, Göttingen
Centrifuge	Multifuge 3 S-R, Heraeus, Hanau
	Sprout mini centrifuge, Biozym, Hessisch Oldendorf
	Mikro 200R centrifuge, Hettich, Tuttlingen
Cryostat	CM 3050S, Leica, Hamburg
Flow cytometer	FACSCanto™ II, LSRFortessa™, FACSAria™, Becton-Dickinson, Heidelberg
Freezer -20°C	Bosch, Munich
Freezer -80°C	Heraeus, Hanau
Incubator	HeraCell, Heraeus, Hanau
Infrared lamp	HP3616, Philips, Hamburg
Lasers	Tunable Chameleon laser, Coherent, Santa Clara
MACS cell separator	QuadroMACS, Miltenyi Biotec, Bergisch-Gladbach
Microscopes	Olympus CKX31, Olympus, Düsseldorf
	LSM 780, Zeiss, Jena
	LSM 710, Zeiss, Jena
Mouse cages	Tecniplast Smartflow, Hohenpeißenberg
Neubauer Chamber	Assistent, Karl Hecht GmbH, Sondheim
Pipette boy	Integra, Zizers
Pipets	Research plus (10, 20, 200, 1000), Eppendorf, Hamburg
Preparation instruments	Bochem, Weilburg; Hammacher, Solingen; F.S.T., Heidelberg
Refrigerator 4°C	Bosch, Munich
Sieves, steel	Mechanical Workshop, University Hospital Bonn

Stages for microscopy	Feinmechanik-Werkstatt, University of Bonn
Waterbath	TW8, Julabo, Seelbach
Workbench (sterile)	HeraSafe, Heraeus, Hanau
Vortex	neolab, VortexMixer, Heidelberg

2.1.2 Consumables

Consumables	Name and Company
Canula	100 Sterican, B. Braun, Melsungen
Cover slips	controlled thickness 0.17 ± 0.01 mm, CE, Assistent, Karl Hecht GmbH, Sondheim
Cryomolds	Tissue-Tek®, Sakura, Alphen aan den Rijn
FACS tubes	Sarstedt, Nümbrecht
FALCON tubes	15 ml, Greiner bio-one, Solingen
	50 ml, Sarstedt, Nümbrecht
Glas pipets	Greiner, Nürtingen
Microtome	blades stainless steel, Feather
Nylon gauze	Labomedic, Bonn
Object slides	Superfrost® Plus, VWR, Darmstadt
pH value indicator	stripes pH fix 4.5-10.0, Macherey-Nagel
Pipet tips	sterile pipette tips 200 µl, 10 µl, VWR, Darmstadt
	Ultratip 1000 µl, Greiner bio-one, Frickenhausen
	TipOne 200 µl, STARlab, Hamburg
	Pipette Tip 10 µl neutral, Sarstedt, Nümbrecht
Reaction tubes	microtubes 0.5 ml, 1.5 ml, 2 ml, Sarstedt, Nümbrecht
Sterile filter	AcroVac Filter Unit PES 0.2 µm Supor, Pall Life Sciences, Dreieich
Syringes	2 ml, 5 ml, BD Discardit II, Becton-Dickinson, Heidelberg
Tissue culture plates	TPP Tissue culture testplates 96, 24, 6 wells, Trasadingen

2.1.3 Chemicals and Reagents

Chemicals and Reagents	Name and Company
Ammonium chloride (NH_4Cl)	Merck, Darmstadt
$B8R_{20}$ peptide	Xaia custom peptides, Göteborg
β-Mercaptoethanol (C_2H_6OS)	Aldrich, St. Louis
Brefeldin A	Sigma Aldrich, München
Bovine serum albumin (BSA)	Roth, Karlsruhe
Cell labelling dyes	CFSE, CFDA SE cell tracer kit, Invitrogen, Eugene Cell tracker Orange (CMTMR), ThermoFisher Scientific, Eugene Cell Tracker Blue, Invitrogen, Eugene Cell Tracker Green, LifeTechnologies, Rockford
Collagenase D	Roche Diagnostics, Mannheim
Dimethylsulfoxid (DMSO)	AppliChem, Darmstadt
Diphtheria Toxin	calbiochem, San Diego
DNAse I	recombinant, Grade I, Roche, Mannheim
Disodium phosphate (Na_2HPO_4)	AppliChem, Darmstadt
Ethanol 70% (v/v)	Otto Fischar, Saarbrücken
Ethylene diamine tetraacetic acid (EDTA)	0.5M pH 8.0, Applichem, Damstadt
Fcγ block	Privigen, CSL Behring, Marburg
Embedding medium	Tissue-Tek® O.C.T.™ Compund, Sakura, Alphen aan den Rijn
Ethidium monoazide bromide E1374 (EMA)	ThermoFisher, Eugene
Fetal bovine serum (FBS)	Good Filtrated Bovine Serum, PAN Biotech
Fluoromount-G®	ebioscience, San Diego
Gelatine from cold water fish skin (GCWFS)	Sigma Aldrich, München
Hydrochloric acid (HCl)	Roth, Karlsruhe
Hydrophobic Barrier (PAP) Pen	ImmEdge™ Pen (H-4000), Vector Laboratories,

	Burlingame
Isofluran	Forene®, AbbVie, Ludwigshafen
Lipopolysaccharid (LPS)	*Escherichia coli* type 0111.B4, Sigma Aldrich, München
L-Lysine	Sigma Aldrich, München
LPS-free Ovalbumin	Hyglos, Bernried
Medium	RPMI medium 1640 1x, life technologies, Rockford
Monosodium phosphate (NaH_2PO_4)	Merck, Darmstadt
Normal Mouse Serum (NMS)	LifeTechnologies, Rockford
Normal Rat Serum (NRS)	LifeTechnologies, Rockford
Normal Rabbit Serum (NRaS)	LifeTechnologies, Rockford
Ovalbumin (OVA), grade V	Sigma Aldrich, München
Paraformaldehyd (PFA)	AppliChem, Darmstadt
Phosphate buffered Saline (PBS)	Biochrom AG, Berlin
Potassium bicarbonate ($KHCO_3$)	Merck, Darmstadt
Penicillin/Streptomycin/Glutamine	Thermo Fisher Scientific, Waltham
Pluronic® F-127	LifeTechnologies, Eugene
Propidiumiodid (PI)	ThermoFisher, Eugene
SIINFEKL peptide	IBA, Göttingen
Sodium azide (NaN_3)	Sigma Aldrich, München
Sodium hydroxide (NaOH)	Roth, Karlsruhe
Sodium periodate ($NaIO_4$)	Sigma Aldrich, St. Louis
Sucrose	Sigma Aldrich, München
Tris base	AppliChem, Darmstadt
Triton-X	GERBU, Gaiberg
Trypan Blue	0.4%, 0.85% NaCl, BioWhittaker®, Lonza

2.1.4 Antibodies

Antigen	Application, Dilution	Clone	Company
CD3ε	F, 1:200	145-2C11	eBioscience, San Diego
CD4	F, 1:200	GK1.5	BD Biosciences, Heidelberg
	IV, 500 µg	GK1.5	BioXcell, West Lebanon
CD8α	F, 1:200	5H10	ThermoFisher, Eugene
	H, 1:200	2G9	Caltag, Buckhingham
CD11b	F, 1:200	M1/70	eBioscience, San Diego
CD11c	F, 1:200	N418	eBioscience, San Diego
	H, 1:100		
CD25	F, 1:200	3C7	BD Biosciences, Heidelberg
CD44	F, 1:200	IM7	eBioscience, San Diego
CD45.R	H, 1:300	RM2628	ThermoFisher, Eugene
CD62L	IV, 100 µg	MEL-14	BioXcell, West Lebanon
CD69	F, 1:200	H1.2F3	eBioscience, San Diego
	H, 1:500	AF2386	R&D Systems, Wiesbaden
CD127	F, 1:200	A7R34	eBioscience, San Diego
ERTR7	H, 1:100	sc-73355	Santa Cruz, Santa Cruz
F4/80	H, 1:200	BM8	ThermoFisher, Eugene
GFP	H, 1:500	A21311	ThermoFisher, Eugene
IFNγ	F, 1:300	XMG1.2	ThermoFisher, Eugene
IL-2	F, 1:250	JES6-5H4	eBioscience, San Diego
Isotyp control	IV, 500 µg	LTF-2	BioXcell, West Lebanon
	IV, 100 µg	2A3	BioXcell, West Lebanon
KLRG1	F, 1:200	2F1	eBioscience, San Diego
MHCII	F, 1:200	M5/114.15.2	BD Biosciences, Heidelberg
MHC Dextramer H-2Kb/	F, 1:20	JD3267	Immudex, Kopenhagen
TSYKFESV			Dirk Busch, TU Munich
NK1.1	F, H 1:100	PK136	BD Biosciences, Heidelberg

Secondary antibodies Alexa Fluor®-conjugated	H, 1:1000		Invitrogen, Carlsbad
TNFα	F, 1:300	MP6-XT22	BD Biosciences, Heidelberg
XCR1	F, 1:200	ZET	Biolegend, San Diego

Application: F: flow cytometry; IV: *in vivo*, intraperitoneal injection; H: histology

2.1.5 Kits

Name	Company
CD4 T cell Isolation Kit, mouse	Miltenyi Biotec, Bergisch Gladbach
$CD8a^+$ T cell Isolation Kit, mouse	Miltenyi Biotec, Bergisch Gladbach
CD11c MicroBeads, mouse	Miltenyi Biotec, Bergisch Gladbach
Cytofix/Cytoperm	BD Biosciences, Heidelberg

2.1.6 Software

Software	Company
Adobe Creative Suite CS6	Adobe, San José
BD FACSDiva 8.0.1	BD Biosciences, Heidelberg
FlowJo X 10.0.7	Tree Star, Inc., Ashland
Imaris 8.2.1	Bitplane, Belfast
Microsoft Office 2011	Microsoft, Unterschleißheim
GraphPad Prism 6	GraphPad Software, La Jolla
Papers 2.3	Mekentosj B.V., Aalsmeer

2.1.7 Bacteria and viruses

Name	Description and Reference
Ad OVA GFP	Adeno Virus expressing GFP and OVA; provided by Percy Knolle, TU, Munich
L.m.-B8R	*Listeria monocytogenes* expressing B8R; provided by Ross Kedl, University of Colorado, Denver
MVA GP	Modified Vaccinia Virus Ankara expressing GP; provided by Gerd Sutter, LMU, Munich
MVA GP Venus	Modified Vaccinia Virus Ankara expressing GP and Venus
MVA OVA	Modified Vaccinia Virus Ankara expressing OVA; provided by Ingo Drexler, Institute of Immunology, Düsseldorf
MVA OVA GFP	Modified Vaccinia Virus Ankara expressing OVA and GFP
MVA OVA Kb	Modified Vaccinia Virus Ankara expressing OVA and Kb
MVA WT	Modified Vaccinia Virus Ankara, wild type
VV OVA	Vaccinia Virus expressing OVA; provided by Jonathan Yewdell, National Institute of Allergy and Infectious Diseases, Bethesda

2.1.8 Buffers, Media and Solutions

All stock solutions and buffers are filtered sterile or are autoclaved. Afterwards the solutions, media and buffers are kept under sterile conditions.

Name	Compounding
Cell culture and isolation	
10x ACK buffer (Ammonium – Chloride – Potassium)	1.5 M NH_4Cl, 100 mM $KHCO_3$, 10 mM Na_2EDTA in distilled water (pH value 7.2)
Cell medium	8% heat-inactivated FBS, 50 µM β-Mercaptoethanol, 4 mM L-Glutamin, 100 U/ml Penicillin und 100 µg/ml Streptomycin in RPMI 1640 medium
MACS buffer	0.5% (v/v) BSA, 2 mM EDTA in 1x PBS

Digestion medium	1 mg/ml Collagenase D, 15 µg/ml DNAse type I (105 U/ml), in cell medium with 1% FBS, preparation directly before use
Immunhistology and cytometry	
Blocking buffer	1% (v/v) FBS, 1% (m/v) GCWFS, 0.3% (v/v) Triton-X in 0.1 M Tris, 1% NMS is added directly before use
FACS buffer	2% (v/v) FBS, 0.02% (v/v) NaN_3 in 1x PBS
Fixation buffer (PLP)	2.12 mg $NaIO_4$ in 3.75 ml P-buffer, 3.75 ml L-Lysine and 2.5 ml 4% PFA (pH value 7.4, adjusted with 10 M NaOH), preparation directly before use
L-Lysin solution	0.2 M L-Lysine in P-buffer
Na_2HPO_4 solution	0.2 M Na_2HPO_4 in distilled water
NaH_2PO_4 solution	0.2 M NaH_2PO_4 in distilled water
P-buffer	40.5% (v/v) 0.1 M Na_2HPO_4, 9.5% (v/v) NaH_2PO_4 in distilled water (pH value 7.4)
PFA solution	4% (w/v) PFA in PBS, gradually heated (pH value 7.4)
Sucrose solution	30% (w/v) Sucrose in P-buffer
Tris buffer	1 M Tris base in distilled water (pH value 7.5, adjusted with 10 M HCl)

2.1.9 Mouse strains

C57BL/6J were purchased from Charles River, Harlan or Janvier, France. All mice were maintained under specific pathogen-free conditions at an Association for Assessment and Accreditation of Laboratory Animal Care-accredited animal facility (HET, House of Experimental Therapy, University of Bonn) or maintained at in-house facilities in accordance with the institutional animal guidelines of the HET. The knockout (KO) and transgenic mice used for this work are listed below. All transgenic and knockout mice are on the genetic

background of C57BL/6J. Mice were used at an age of 8-15 weeks. For some experimental procedure, strains were inter-crossed to fluorescent reporters.

Mouse strain	Publication	Description
Batf3$^{-/-}$	(Hildner et al., 2008)	This mouse strain lacks the transcription factor *Batf3* and thus ablated development of CD8α^{+} DC.
Kbm1	(Schulze et al., 1983)	This mouse strain has a point mutation in the MHC class I molecule that prevents presentation of the OVA-peptide$_{257\text{-}264}$ SIINFEKL to CD8^{+} T cells.
CD11c YFP	(Lindquist et al., 2004)	The mouse strain expresses eYFP under the control of the CD11c promotor.
IFNγ eYFP	(Reinhardt et al., 2009)	The mouse strain is an IFNγ reporter strain that expresses eYFP under the control of the IFNγ promotor. GREAT-mice: IFN-gamma reporter with endogenous polyA transcript.
MHCII KO	(Madsen et al., 1999)	This mouse strain is deficient of four of the classical murine MHC-II genes.
OT-I	(Hogquist et al., 1994)	This mouse strain has a transgenic TCR that recognizes the OVA$_{257\text{-}264}$ peptide SIINFEKL in MHC I molecules.
OT-II	(Barnden et al., 1998)	This mouse strain has a MHCII-restricted transgenic TCR that is specific for OVA.
P14	(Pircher et al., 1989)	This mouse strain has a transgenic TCR that recognizes the parts of the LCMV glycoprotein (GP) in MHC I molecules.
SMARTA	(Oxenius et al., 1998)	This mouse strain has a transgenic TCR that recognizes the parts of the LCMV glycoprotein in MHC II molecules.

tdTomato	(Kastenmüller et al., 2013)	The mouse strain expresses the fluorescent protein tdTomato under the ubiquitin promotor.
UbGFP	(Schaefer et al., 2001)	The mouse strain expresses the fluorescent protein eGFP under the ubiquitin promotor.
$XCR1^{DTRvenus/+}$	(Yamazaki et al., 2013)	The mouse strain expresses the human diphtheria toxin receptor (DTR) and the fluorescent protein venus under the XCR1 promotor.

2.2 Methods

2.2.1 Bacteria and viruses

Bacteria: Recombinant *Listeria monocytogenes*-B8R was maintained as a –80°C stock in 1:1 ratio in brain-heart infusion (BHI) and glycerol. Before each experiment, recombinant *L.m.*-B8R was grown in BHI at 37°C with aeration. The used bacteria were purified out of their log phase.

Viruses: Highly purified viruses were used for this study. Adenovirus (Stabenow et al., 2010) was purified using a Cesium Chloride density gradient. MVA and Vaccinia viruses were purified using two consecutive sucrose cushions. MVA GP (Frenz et al., 2010) and MVA WT, MVA OVA, MVA OVA GFP, MVA OVA tdTomato have been previously described (Kastenmüller et al., 2013). MVA GP Venus and MVA OVA Kb were generated based on standard methods (Staib et al., 2004).

2.2.2 Treatment of mice

Pathogens, reagents and cells were diluted in PBS injected in the footpad (f.p.; foothock (Kamala, 2007)), intravenously (i.v.) or intraperitoneal (i.p.). Footpad injections were performed in a total volume of 30 µl, intravenous injections in a volume of 100 µl and in a volume of 200 µl for intraperitoneal injections.

Infections/Immunization: 10^7-10^8 IU recombinant MVA, 10^6 -10^7 PFU VV OVA, 2x 10^7 PFU Ad OVA GFP or 5x 10^3 CFU *L.m*.-B8R were injected in the f.p., i.v. or i.p.. Soluble OVA (50 µg) and LPS (1 µg) were injected in the footpad.

Depletions: For depletion of $CD4^+$ T cells, mice received 500 µg of anti-CD4 or isotype control (LTF-2) antibodies i.p. on d-3 and d-1. For depletion of $XCR1^+$ DC, transgenic mice and control littermates were treated i.p. with 0.5 µg diphtheria toxin (DTX) on d-2, d-1 and d0, unless indicated otherwise.

Entry blockade: 12 and 36 hours after infection, mice received either 100 µg anti-CD62L or isotype control (2A3) antibodies i.p. to block the entry of naïve T cells (lymphocytes) into the LN.

Mixed bone marrow chimeras: For generations of chimeric mice, the mice were irradiated with 9 Gy from a ^{137}Cs source. For reconstitution of the bone marrow (BM), the mice received a 1:1 mixture of total 2x 10^6 BM cells 4 h after irradiation. Eight weeks after transplantation, the used chimeric mice had a 50% ± 10% ratio of bone marrow of each type.

2.2.3 Adoptive T cell transfer and labeling

Isolation of naïve T cells: For the isolation of naïve polyclonal or transgenic T cells, spleens and lymph nodes were harvested and homogenized through a metal cell strainer. After lysis of erythrocytes with 4 min incubation in ACK buffer, cell suspensions were washed with PBS. After counting, $CD8^+$ or $CD4^+$ T cells were purified using MACS CD4 or CD8 negative selection kits (Miltenyi) combined with biotinylated anti-CD44 (diluted 1:10000). The isolation of cells was performed according to manufacturer´s instructions.

Labeling: Non-fluorescent T cells were labeled either with 1 µM Cell Tracker Green (CTG), 100 µM Cell Tracker Blue (CTB) or 10 µM Cell Tracker Orange (CTO). For CTO labeling, cells were incubated for 10 min at 37°C in cell medium containing CTO. The reaction was stopped by centrifugation of the labeled cells into FBS. For CTG or CTB labeling, cells were incubated for 10 min at 37°C in a PBS containing CTG or CTB and 1 µM Pluronic®, respectively. The reaction was stopped by the addition of FBS containing cell medium. Cells were washed with PBS and 2-4x 10^6 cells were transferred in volume of 100 µl intravenously.

2.2.4 *In vitro* proliferation assay

Isolation and sorting of DC: Spleens were harvested and incubated in digestion medium for 30 min at 37°C. After generation of single cell suspensions, DC were enriched according to manufacturer´s instruction using MACS CD11c positive selection kit (Miltenyi). Different populations of DC were separated based on CD11c, MHCII, CD8α and CD11b staining using a FACSAria cell sorter. Cellular purity was >95%.

Isolation and labeling of T cells: Naïve OT-I T cells were purified as described above (2.2.3). Purified OT-I T cells were stained in PBS containing 5 µM CFSE for 10 min at 37°C. Adding PBS stopped the reaction and cells were washed twice with PBS.

In vitro proliferation: Isolated DC and 1x 10^6 OT-I cells were co-incubated in different ratios in 200 µl cell medium on a 96-well plate at 37°C and a content of 5% CO_2. After 72 h cell surfaces were stained in FACS buffer with anti-CD8, anti-CD44, anti-CD3, anti-CD11c and live/dead marker for 30 min on ice. After 2x washing with FACS buffer, the proliferation profile of OT-I T cells was analyzed using flow cytometers and FlowJo software.

2.2.5 Flow cytometry

The $B8R_{20}$ tetramer staining was used to determine the number of endogenous T cells specific for the immuno-dominant epitope of Vaccinia virus. Restimulation/ intracellular staining for IFNγ, TNFα and IL-2 was performed in order to assess T cell activation *in vivo*. For analysis of T cells, LN and spleens were harvested and single cell suspensions were generated as described above (2.2.3).

Tetramer/ Surface staining: In total 2x 10^6 cells were stained in FACS buffer, beginning with an incubation containing Fcγ block (1:66) and EMA (1:2000) in order to fill unspecific binding sites and Fc receptors and to discriminate live/dead cells. Cell suspensions were incubated for 20 min on ice under direct lighting. Afterwards, cells were stained with surface markers in FACS buffer, 30 min on ice followed by washing with FACS buffer. For $B8R_{20}$ tetramer staining, cells were incubated with the tetramer for 30 min at room temperature (RT), followed by adding the surface markers and incubation for 30 min on ice.

Restimulation/ Intracellular cytokine staining: In a total amount of 2x 10^6 cells were taken up in cell culture medium. Afterwards, $B8R_{20}$ peptide was added at a concentration of 5 µg/ml in order to restimulate specific $CD8^+$ T cells. Moreover, Brefeldin A reagent was added at a concentration of 5 µl/ml to prevent secretion of newly synthesized cytokines. The cells were incubated for 5 h at 37°C, 5% CO_2. The cells were then washed with PBS and stained with surface markers as described above. The intracellular staining was performed using the Cytofix/Cytoperm kit (BD Biosciences) according to the manufacturer´s instructions. The samples were collected on flow cytometers and analyzed with FlowJo software.

2.2.6 Immunofluorescence staining

Preparations of cryosections: LN and spleens were harvested and fixed using PLP buffer for 12 h, then dehydrated in 30% sucrose for 12 h, prior to embedding in OCT freezing media. Frozen samples were cut in 30 µm serial sections, adhered on Superfrost® Plus object slides. *Immunofluorescence staining:* Sections were rehydrated with 0.1 M Tris buffer for 10 min on RT, followed by permeabilization and blocking in blocking buffer for 30 min on RT. The sections were stained fluorescent labeled antibodies in blocking buffer on 4°C over night. After washing, the sections were mounted with Fluoromount-G®. Serial lymph node sections were visually inspected using epifluorescent light microscopy, and several representative sections from different LN areas were acquired using confocal microscopy for detailed analysis.

2.2.7 Intravital two-photon imaging

Mice were anesthetized with isoflurane (2.5% for induction, 1-1.5% for maintenance, vaporized in an 80:20 mixture of O_2 and air), popliteal LN was exposed and intravital microscopy (IVM) was performed. The microscope was enclosed in an environmental chamber in which anesthetized mice were warmed by heated air and the surgically exposed LN was kept at 36-37°C with warmed PBS. For dynamic imaging, a z-stack of 57 µm and 3 µm step size was used and acquired every 40 sec.

2.2.8 Cluster formation as a readout for antigen-presentation

Conventional naïve T cell priming by DC is separated into three phases (Mempel et al., 2004). During the second phase, when naïve T cells recognize their specific peptide upon TCR–MHC interaction, the T cells and DC get into long-term (12-24 h) interactions (Miller et al., 2002; Stoll et al., 2002; Bousso and Robey, 2003). These interactions were used as readout, for identification of a certain antigen-presenting cell. Therefore fluorescent or labeled naïve T cells, expressing a clonal TCR, were transferred in high amounts (2-4x 10^6) into different recipient mice. The animals were infected with pathogens additionally encoding for the specific antigen. According to the long-term interaction and the high numbers of naïve, antigen-specific T cells, a lot T cells arrest and build clusters around the specific antigen-

presenting DC. Using confocal microscopy and intravital microscopy, these cluster formation was analyzed *in vivo* in LNs and on spleen and LN sections. Thus, cluster formation is used to visualize the place of antigen-presentation and to identify on which DC the antigen is presented. Using transgenic $CD4^+$ and $CD8^+$ T cells also allows distinguishing between antigen-presentation by either MHCI or MHCII or both.

2.2.9 Analysis of imaging data

Images were systematically analyzed with the Imaris software tools using a semi-automated approach.

Distance quantification: Both infected cells and the various T cell populations were localized using Imaris spot function and relative distance was calculated using Excel software calculating the minimal distance in 3D. To calculate the distance to the LN capsule spots outlining the capsule were placed manually using ERTR7 staining as guidance.

Co-localization and cluster quantification: T cell clusters were defined semi-automated using a surface generation tool (Imaris) and incorporated at least 3 cells. Co-localization with other cell populations were counted manually.

2.2.10 Statistical Analysis

Student t test (two-tailed) and Mann-Whitney test were used for the statistical analysis of differences between two groups with normal and non-normal distribution. Stars indicate significances (* $p \leq 0.05$, ** $p \leq 0.01$, *** $p \leq 0.001$).

3 Results

3.1 Initial activation of OT-I T cells occurs on directly infected cells and is independent of XCR1$^+$ DC

Naïve CD8$^+$ T cells are activated by antigen-presenting cells (APC) upon an antigen-specific interaction between the T cell receptor (TCR) and major histocompatibility complex I (MHCI). This activation or priming leads to the proliferation and differentiation into effector and memory CD8$^+$ T cells. An optimal CD8$^+$ T cell response requires help from CD4 T cells (Bevan, 2004), which is transmitted via dendritic cells. The DC transmits its helper signals to CD8$^+$ T cells after it has presented antigens to CD4$^+$ T cells and has received activating signals in return. This implicates that CD4$^+$ and CD8$^+$ T cells co-recognize antigen on the same DC. It has been previously shown that different DC subsets are specialized to interact with either CD4$^+$ or CD8$^+$ T cells (Merad et al., 2013). Therefore, I aimed to study which DC subset is critical to mediate CD4$^+$ T cell helper signals in order to optimize CD8$^+$ T cell priming or whether this function is redundant among all DC´s. In our previous work, we found that early (< 12 h) after viral infection, pDC and XCR1$^+$ DC - together with activated, antigen-specific CD8$^+$ T cells - form a cluster of cells that co-localize and co-arrest around an infected antigen-presenting conventional DC (Brewitz et al., 2017). This cluster formation creates a special microenvironment that optimizes the XCR1$^+$ DC maturation in a type I IFN dependent manner. To understand if XCR1$^+$ DC present antigen to the CD8$^+$ T cells during the initial activation, we examined the role of XCR1$^+$ DC during the initial activation of CD8$^+$ T cells in cooperation with Anna Brewitz. For this purpose, we made use of CD8$^+$ OT-I T cells expressing a MHCI restricted transgenic T cell receptor (TCR) recognizing the OVA-peptide SIINFEKL and of a modified Vaccinia virus Ankara encoding ovalbumin (MVA OVA), a replication deficient model pathogen. We infected WT mice intravenously (i.v.) with MVA OVA, and 8 hours later we sorted splenocytes for CD8α$^+$ DC (a population also referred as XCR1$^+$ DC) and CD11b$^+$ DC and cultured the DC with CFSE labeled naïve OT-I T cells. The proliferation profile of the OT-I T cells revealed that both XCR1$^+$ DC and CD11b$^+$ DC activate CD8$^+$ T cells if they were directly infected (Figure 3.1 A). To clarify if XCR1$^+$ DC are obligatory for the initial activation of CD8$^+$ T cells *in vivo,* I employed XCR1 DTR mice expressing the

human diphtheria toxin receptor (DTR) under the XCR1 promoter. To deplete the XCR1$^+$ DC, I treated the mice with diphtheria toxin (DTX) starting two days (d-2, d-1, d0) before the infection. One day before the infection, I transferred naïve OT-I and OT-II T cells - the CD4$^+$ transgenic counterpart of OT-I T cells - into XCR1 DTR mice and their control littermates (WT), which obtained the same treatment but do not express the DTR. Twelve hours after footpad infection, I analyzed the OT T cells in the draining popliteal lymph node (pLN) and found no difference regarding the early activation markers CD69 and CD25 on OT-I T cells in the absence or presence of XCR1$^+$ DC (Figure 3.1 B/C). Interestingly, the activation of OT-II T cells was slightly reduced in the absence of XCR1$^+$ DC.

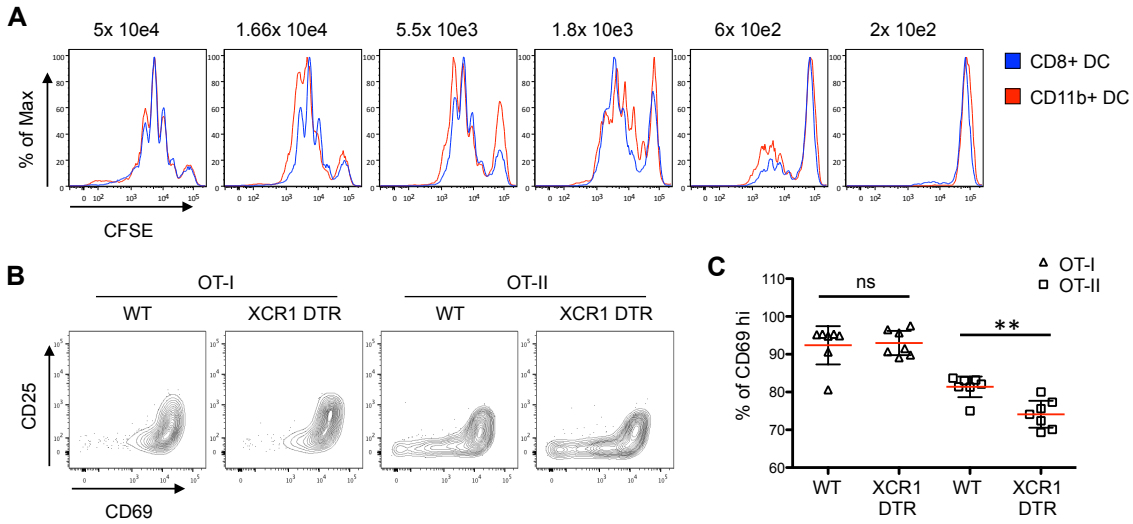

Figure 3.1. Initial activation of OT-I T cells is independent of XCR1$^+$ DC.
(A) Analysis of OT-I proliferation after co-incubation (72 h) with *ex vivo* sorted splenic DC subsets after 8 h MVA OVA i.v. infection. (B/C) Analysis of activation markers (CD69/CD25) on pLN´s OT-I and OT-II T cells in presence or absence of XCR1$^+$ DC, 12 h after MVA OVA f.p. infection. (B) Representative plots and (C) statistical analysis of CD69 upregulation. Both XCR1 DTR mice and WT littermate controls were treated with 500 ng DTX two days before infection (d-2, d-1, d0). A. Brewitz generated proliferation assays. Data are representative of three (n=3 A) and two (n=7 B/C) independent experiments. (C) Red bars indicate mean values ± 95% confidence interval. **p≤0.01; ns, non-significant. See also Movie 1. Figures are paneled (A/B) and modified (C) from Eickhoff et al., 2015.

After having observed that early during the infection XCR1$^+$ DC are not obligatory antigen-presenters, the question arose which antigen-presenting cell (APC) activates the CD8$^+$ T cells. To visualize the CD8$^+$ T cell priming sites and thereby identifying the specific-antigen presenting cell, Anna Brewitz and I transferred high numbers of OT-I T cells and analyzed via confocal microscopy and intravital two photon microscopy (IVM) on which APC the antigen-specific T cells build clusters due to long-term interactions during their initial activation (see

also 2.2.8). Eight hours after footpad infection with MVA OVA GFP, I observed that OT-I T cells were interacting and clustering around directly infected CD11c$^+$ DC indicated by virally driven GFP expression (Figure 3.2 A, Movie 1). To examine the possibility that early after viral infection the activation of CD8$^+$ T cells is dependent on directly infected APC, I employed Kbm1 mice. This mouse line harbors a point mutation in the Kb molecule and therefore is not able to directly present the SIINFEKL peptide via MHCI to CD8$^+$ T cells. Usage of MVA OVA and MVA OVA Kb allowed me to distinguish if the activation is dependent on directly infected cells because in the Kbm1 mice only APC that are directly infected with MVA OVA Kb are able to present antigens. To test the hypothesis, DC were sorted 8 hours after *in vivo* infection from Kbm1 mice and further DC were co-incubated with CFSE labeled, naïve OT-I T cells. Only the DC that were obtained from the MVA OVA Kb infected mice were able to activate the OT-I T cells and induce their proliferation (Figure 3.2 B). I verified this finding *in vivo* by analyzing the activation markers CD69 and CD25 of OT-I T cells in Kbm1 mice, infected 12 hours with either MVA OVA Kb or MVA OVA footpad infection (Figure 3.2 C/D).
Hence, even though XCR1$^+$ DC build clusters with and around antigen-specific CD8$^+$ T cells during the early phase of MVA infection, they are not obligatory for the initial activation of naïve antigen-specific CD8$^+$ T cells. Further, the activation of antigen-specific CD8$^+$ T cells does not rely on a special DC subset. It occurs on directly infected APC including different dendritic cell subsets.

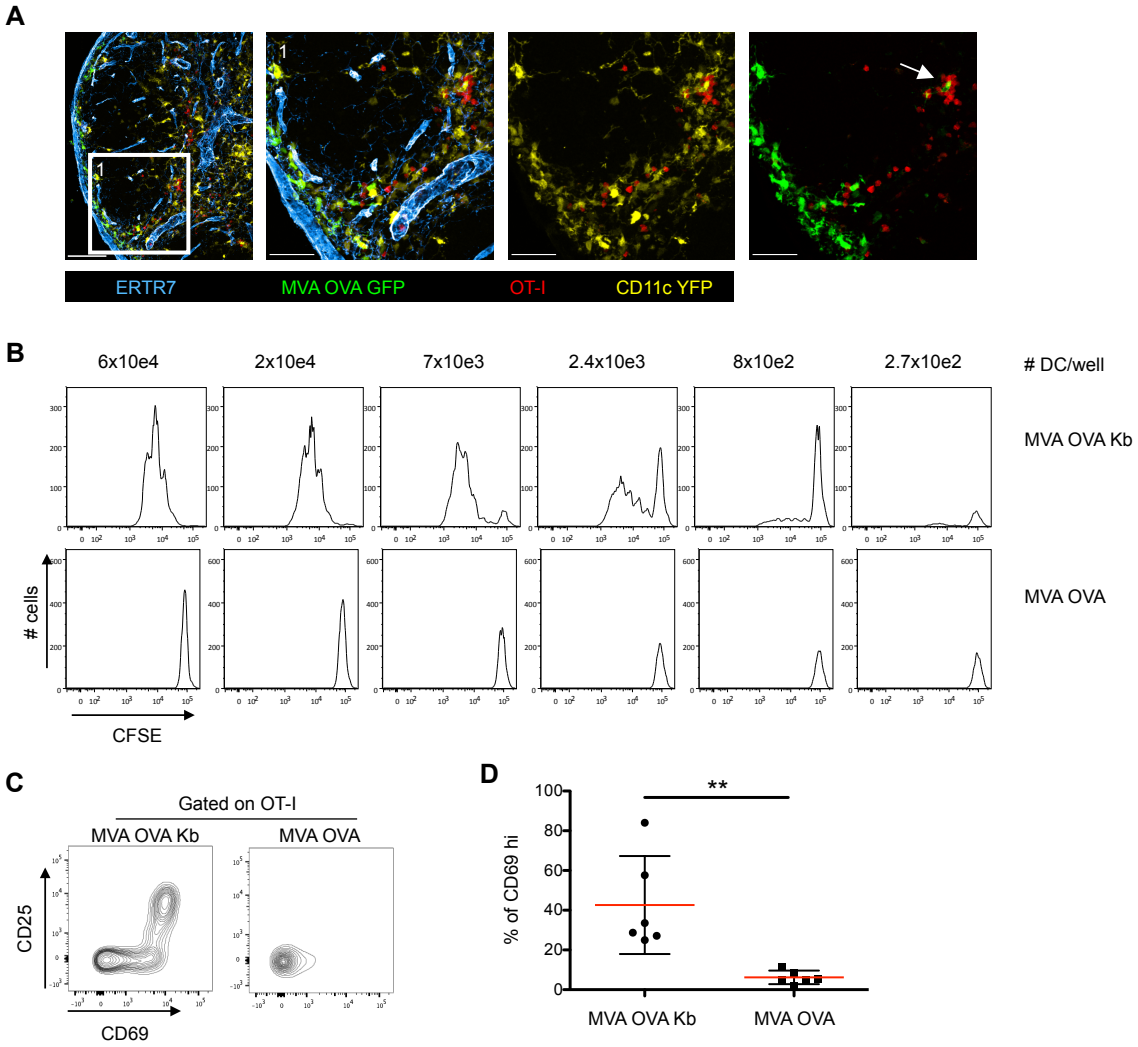

Figure 3.2. Initial activation of OT-I T cells occurs on directly infected cells.
(A) Immunofluorescence (IF) images of pLN showing OT-I T cells clustering around direct infected DC, 8 h after MVA OVA GFP f.p. infection, see also Movie 1. (B) Analysis of OT-I proliferation after co-incubation (72 h) with *ex vivo* sorted splenic DC subsets from Kbm1 mice infected with either MVA OVA or MVA OVA Kb i.v. (8 h p.i.). (C/D) Analysis of activation markers (CD69/CD25) on pLN´s OT-I T cells prior transferred into Kbm1 mice, 12 h after either MVA OVA or MVA OVA Kb f.p. infection. (C) Representative plots and (D) statistical analysis of CD69 upregulation. A. Brewitz generated proliferation assays and IF image data. Data are representative of three (n=3 A/B) and two (n=6 C/D) independent experiments. (D) Red bars indicate mean values ± 95% confidence interval. Scale bars, 100/50 µm. **p≤0.01. See also Movie 1. Figures are paneled (A/B) from Eickhoff et al., 2015.

3.2 Initial activation of OT-I and OT-II T cells is on different DC

As mentioned above, I wanted to investigate which DC transmits the helper signals of $CD4^+$ T cells to the $CD8^+$ T cells. MVA infection is known to be dependent on $CD4^+$ T cell help and to support all antigen-presentation pathways (Norbury et al., 2001). To visualize the common cellular platform that presents foreign antigen via both MHCI and MHCII, I transferred OT-I and OT-II cells and control polyclonal $CD4^+$ T cells into WT mice and analyzed cluster formation 10 hours after infection through confocal microscopy. The analysis of LN sections showed that OT-II T cells and control $CD4^+$ T cells do not cluster at OT-I priming sites (Figure 3.3 A/B). This data suggests that during the early phase of infection, $CD4^+$ T cells might not interact with the same DC as $CD8^+$ T cells. Nevertheless, missing co-localization between arrested antigen-specific $CD4^+$ and $CD8^+$ T cells on tissue sections is not a definitive proof of lacking interactions. In order to obtain more conclusive data, I performed intravital two-photon microscopy (IVM) on the pLN with OT-I, OT-II and polyclonal $CD4^+$ T cells transfer prior to infection. Early after MVA OVA infection, OT-I T cells arrested at their priming sites, which is reflected by their cluster formation (Figure 3.3 C, Movie 2). Interestingly, OT-II T cells did not arrest at the OT-I priming sites early after the infection even though some OT-II T cell were in direct proximity to the OT-I T cell cluster (e.g. Figure 3.3 C, Movie 2: 3h:28min:40sec). In addition, analysis of T cell velocity showed no difference between OT-II T cells and polyclonal $CD4^+$ T cells dynamics (Figure 3.3 D) at this time point.

To investigate if OT-II T cells are activated early during the infection, in cooperation, Anna Brewitz and I analyzed the kinetics of CD69 upregulation on transferred OT-I and OT-II T cells after infection. Twelve hours after infection, I found that about 89% of the OT-I T cells and 84% of the OT-II T cells were activated in an antigen-specific manner with a slight delay of OT-II T cell activation (Figure 3.3 E). Further, I performed co-cluster analysis using IVM at later time-points (≤ 12 h), but the OT-II T cells still did not cluster around the OT-I T cell priming sites (data not shown). Thus, OT-I and OT-II T cells are primed on different DC.

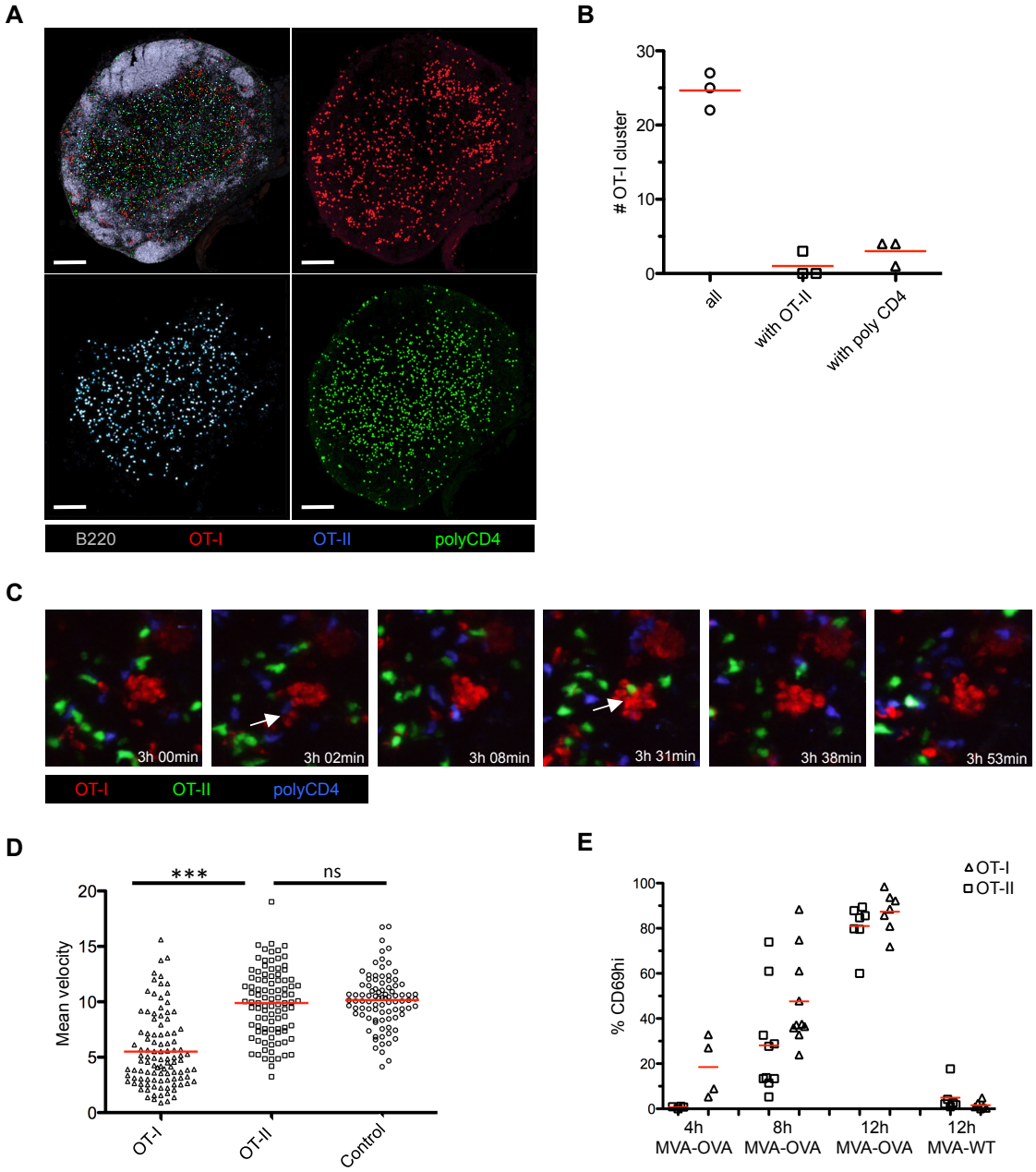

Figure 3.3. Initial activation of OT-I and OT-II T cells is on different DC.
(A) IF images of pLN showing OT-I cluster without OT-II and polyclonal CD4$^+$ T cells 10 h after MVA OVA f.p. infection. (B) Semi-automated analysis of counts of OT-I T cell co-clusters with OT-II and polyclonal CD4$^+$ T cells in pLN 10 h after MVA OVA f.p. infection using IF images from A. (C) IVM images of pLN 3-4 h after MVA OVA f.p. infection, T cells were transferred 24 h prior to infection. Arrows indicate brief interactions between OT-I T cell cluster and OT-II T cell or polyclonal CD4$^+$ T cell, see also Movie 2. (D) Analysis of mean velocity of T cells using the IVM Movie 2. (E) Kinetic of CD69 upregulation on OT-I and OT-II T cells in pLN after MVA OVA or MVA WT f.p. infection. Analysis of CD69 upregulation was performed in cooperation with A. Brewitz. Data are representative of three (n=3 A/B) and two (n=10 C/D) (n=4-8 E, pooled data) independent experiments. Scale bars, 200 µm. (D/E) Red bars indicate mean values. ***p≤0.001; ns, non-significant. Figures are paneled (B-E) and from Eickhoff et al., 2015.

3.3 Initial activation of CD4$^+$ and CD8$^+$ T cells is on spatially separated DC

After having resolved that OT-I T cells are activated via directly infected cells after MVA infection and that OT-II T cells are activated on different non-infected DC, I aimed to gain further insights into localization of CD4$^+$ T cell priming. Moreover, I wanted to address whether my observed results can be generalized across different T cell specificities, different viruses and different SLO´s. After the infection, MVA freely drains via the lymphatics in the lymph node and infects phagocytosing cells in the subcapsular sinus (SCS) and the interfollicular areas (IFA). In the LN, T cells are usually located in the T cell zone, the paracortex. Hence, CD8$^+$ and CD4$^+$ T cells might not only be activated on different DC but also on spatially separated DC. To examine this possibility, I infected mice with MVA OVA expressing GFP after OT-I and OT-II T cells transfer and analyzed the localization of both cell subsets via confocal microscopy 10 hours later. The analysis of the lymph node sections showed that the OT-I T cells translocated to the infected APC and the OT-II T cells were primed in the paracortex of the LN (Figure 3.4 A). On the assumption that CD4$^+$ and CD8$^+$ T cells are primed on spatially separated DC, I sought to verify this finding in different experimental systems. First, I aimed to address whether segregated priming of CD4$^+$ and CD8$^+$ T cells is specific to LN or is a general feature of T cell activation. Therefore, I infected mice intravenously with MVA OVA GFP after OT-I and OT-II transfer and analyzed their positioning in the spleen 8 hours later. As in the LN, OT-I T cells translocated towards infected APC in the marginal zone, while OT-II T cells remained in the T cell zone (Figure 3.4 B). To examine the independence of the transgenic TCR in the OT system, I made use of transgenic P14 (CD8$^+$) T cells and SMARTA (CD4$^+$) T cells, which express a TCR specific for the glycoprotein (GP) of LCMV. Ten hours after footpad infection with MVA GP Venus, transferred P14 T cells translocated towards the infected APC in the SCS and IFA, whereas the SMARTA T cells were clustering in the paracortex (Figure 3.4 C). Upon infection, some viruses are known to downregulate antigen-presentation via MHCII and so they prevent recognition from antigen specific CD4$^+$ T cells (Maudsley and Pound, 1991). In order to address whether a separated activation of lymphocyte subsets is general mechanism after viral infection, I immunized the mice with adenovirus, encoding OVA and GFP. In accordance with my previous results using Vaccinia virus infections, I observed translocation of OT-I T cells towards Adeno-virally infected cells (Figure 3.4 D). Finally, when using a protein based

vaccine consisting of OVA and LPS, I also observed activation of OT-I and OT-II cells on different DC, even though both T cell subsets were activated in the paracortex of the LN in this setting (Figure 3.4 E, Movie 3). Together, a separated activation of $CD4^+$ and $CD8^+$ T cells is robust within different experimental systems.

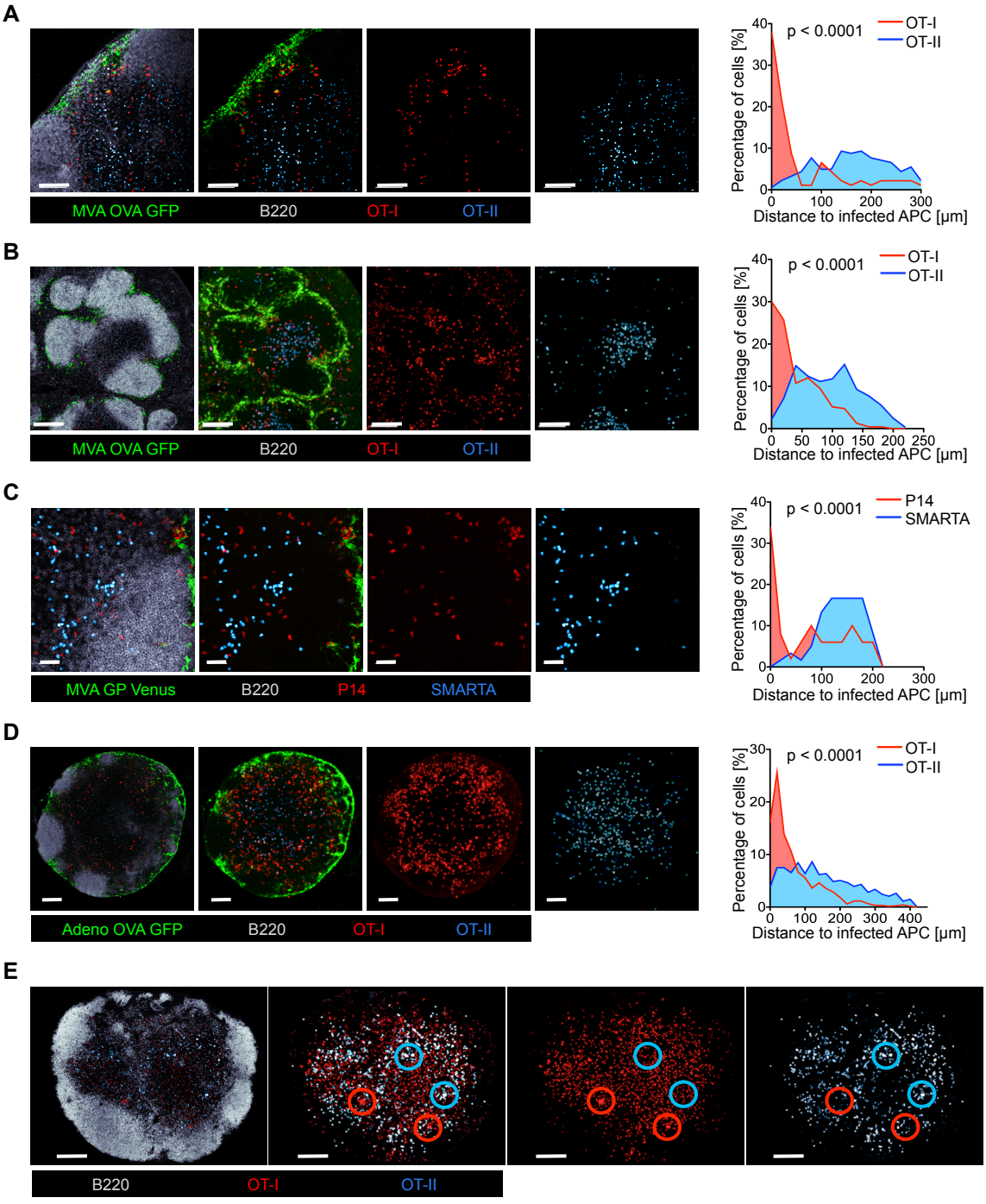

Figure 3.4. Initial activation of $CD4^+$ and $CD8^+$ T cells is on spatially separated DC.
(A-E) IF images showing localization of T cells and (A/C/D) histograms showing distance of T cells from infected APC. (A) OT-I and OT-II T cells, pLN 10 h after MVA OVA GFP f.p. infection. (B) OT-I and OT-II T cells, spleen 8 h after MVA OVA GFP i.v. infection. (C) P14 and SMARTA T cells, pLN 10 h after MVA GP Venus f.p. infection. (D) OT-I and OT-II T cells, pLN 10 h after Adeno OVA GFP f.p. infection. (E) OT-I and OT-II T cells, pLN 6 h after LPS

and OVA f.p. immunization, see also Movie 3. Data are representative of three (n=3 B/D/E) and two (n=10 A/C) independent experiments. Scale bars, 100 µm (A/C), 200 µm (B/D/E). Figures are paneled from Eickhoff et al., 2015.

3.4 $CD4^+$ and $CD8^+$ T cell interaction on the same DC occurs later during viral infection

The finding that the activation of $CD4^+$ and $CD8^+$ T cells is mediated via spatially separated DC during the early phase of the infection was unexpected. Given the $CD4^+$ T cell help dependency of the immune response against Vaccinia virus infections, I hypothesized that $CD4^+$ T cell help for $CD8^+$ T cells is taking place at later time-points of the infection and hence, $CD4^+$ and $CD8^+$ T cells interact later during the infection with the same dendritic cell. To test this hypothesis, I modified the experimental system. I infected mice with MVA OVA before I transferred antigen-specific and control naïve T cells. During the first activation, naïve T cells arrested at the APC for about 8-12 hours in an antigen specific manner, which allowed me to visualize the antigen-presenting DC due to cluster building even at later time-points. So, after 30 hours of footpad infection, I transferred naïve OT-I and OT-II T cells and 8 hours later I harvested the pLN (Figure 3.5 A). Analysis of serial LN sections showed that OT-I and OT-II cells formed co-clusters later during the infection in the paracortex of the LN (Figure 3.5 B). In comparison, polyclonal naïve $CD4^+$ T cells do not form co-cluster with OT-I or OT-II T cells. Furthermore, a staining of CD69 indicated that both OT-I and OT-II T cells are activated and are co-localized around dendritic cells (Figure 3.5 C). In order to distinguish the place of antigen-presentation at earlier and later time-points of the infection, I quantified the localization of transferred T cells in relation to the LN capsule after infection with MVA encoding their foreign antigen. The analysis of clusters of transgenic $CD4^+$ and $CD8^+$ T cells showed that early during the infection (< 12 h) the antigen-presenting cells for $CD8^+$ T cells are located in the periphery (IFA, SCS) of the LN structure and later in the LN paracortex (Figure 3.5 D). In contrast, the DC presenting the antigen for $CD4^+$ T cells are located in the paracortex of the LN early and later during the infection (Figure 3.5 D). Further, control polyclonal $CD4^+$ T cells showed no difference in positioning during viral infection.

In conclusion, $CD4^+$ T cell help for $CD8^+$ T cells takes place later during MVA infection and their common DC is located in the paracortex of the LN. Further, usage of a replication

deficient virus allowed the distinction between different antigen-presentation pathways. One the one hand early during MVA infection (< 12 h), naïve $CD8^+$ T cells are activated by directly infected APC, which involves direct antigen-presentation pathway by the APC. On the other hand later during MVA infection (> 24 h), directly infected cells die - as a replication deficient virus was used - and no further cells could be infected. Phagocytes, including DC, take the apoptotic/necrotic material from the dead cells and DC present the viral antigens via cross-presentation to the $CD8^+$ T cells. Hence, the common DC for $CD4^+$ and $CD8^+$ T cells is a cross-presenting DC. Interestingly, the antigen-presentation through migratory, cross-presenting DC ($CD103^+$) could be excluded by verifying the co-cluster formation in Batf3 KO mice, which lack the migratory DC but not the cross-presenting DC ($XCR1^+$ DC) in the LN. Furthermore, I observed co-cluster formation in mice, after lymphatic vessel obliteration, which fully blocks the entry of migratory of DC into the LN (data not shown). This verifies again that the common DC for $CD4^+$ and $CD8^+$ T cells is a cross-presenting, lymphoid tissue-resident DC.

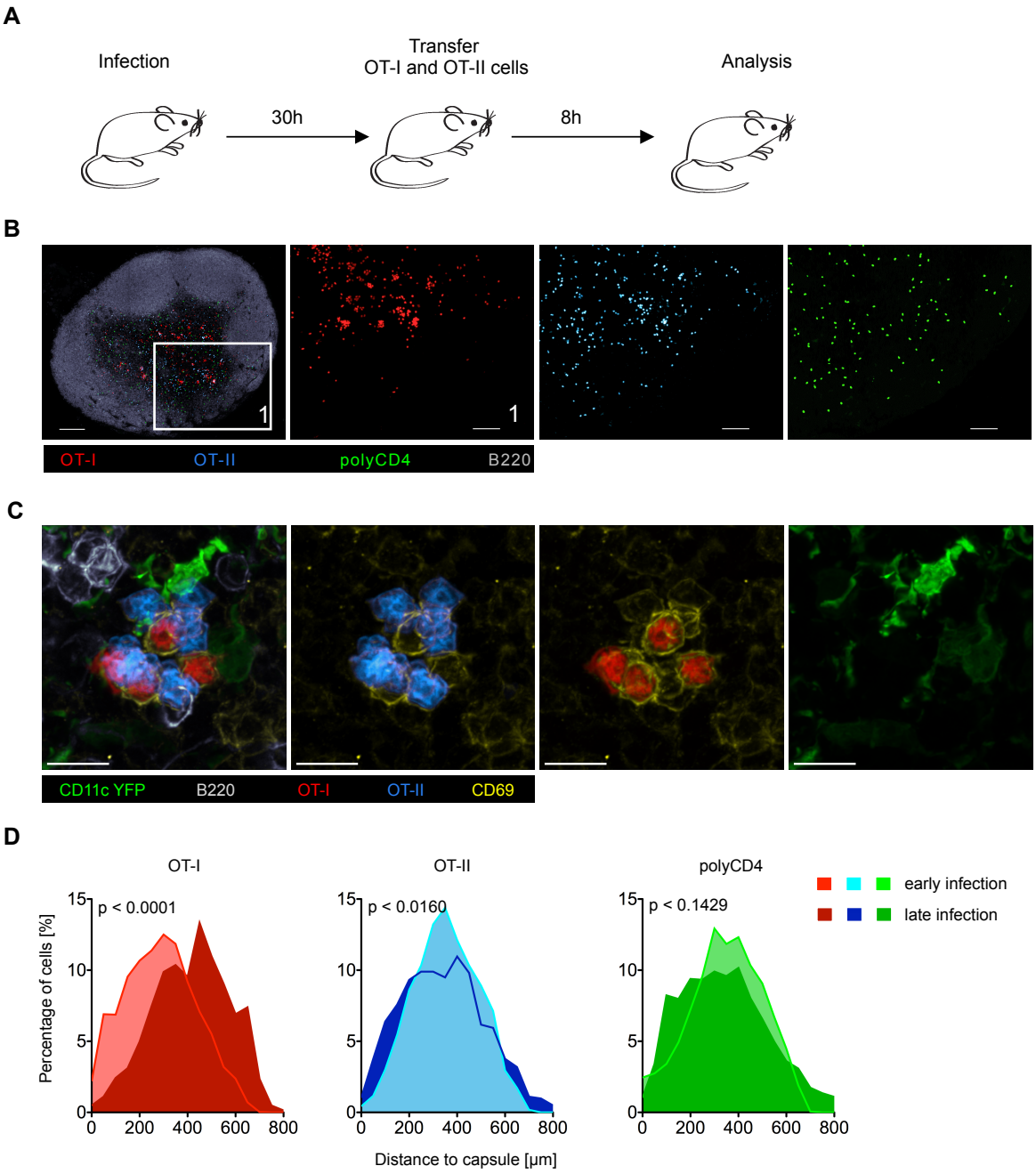

Figure 3.5. CD4⁺ and CD8⁺ T cell interaction on the same DC occurs later during viral infection.
(A) Experimental setup to manifest place of antigen-presentation and antigen-bearing cells in the later phase of infection. (B) IF images of the pLN showing the localization of T cells after 30+8 h MVA OVA f.p. infection. (C) IF image of the pLN showing activation (CD69) of co-clustering OT-I/OT-II T cells. (D) Histograms showing OT-I and OT-II T cell localization in pLN 10 h (see also Figure 3.4) or 30+8 h after MVA f.p. infection. A. Brewitz acquired IF images from (C). Data are representative of 10 (n=20 B/C) or three (n=3 D) independent experiments. Scale bars, 200/100 µm (B) and 10 µm (D). Figures are paneled from Eickhoff et al. 2015.

3.5 XCR1$^+$ DC present antigen to both CD4$^+$ and CD8$^+$ T cells during viral infection

In the next step, I aimed to identify the DC subset permitting the CD4$^+$ T cell helper signals. Based on the previously obtained data and the knowledge that XCR1$^+$ DC are a critical cross-presenting DC, I investigated if XCR1$^+$ DC present antigen to both CD4$^+$ and CD8$^+$ T cells later during the infection. In order to analyze the co-cluster formation of CD4$^+$ and CD8$^+$ T cells in the absence of XCR1$^+$ DC, I used XCR1 Venus DTR mice. Using the experimental setup described above (Figure 3.5 A), I additionally treated those mice with either DTX or PBS. Strikingly, the analyses of LN sections obtained in this experiment indicated that without XCR1$^+$ DC, OT-I and OT-II T cells do not form co-cluster on the same DC (Figure 3.6 A/B). Additionally, semi-automated quantification of the LN sections showed that OT-I T cells are barely clustering in the absence of XCR1$^+$ DC (Figure 3.6 B). This suggested that antigen presentation to CD8$^+$ T cells at later time-points of MVA infection is a unique function of XCR1$^+$ DC. To verify this finding, I analyzed the activation of OT T cells by the expression of CD69 using flow cytometry 40 hours after infection and 12 hours after T cell transfer. Depleting XCR1$^+$ DC decreased OT-I activation from 80% to 10%, and OT-II activation from 60% to 40% (Figure 3.6 C) after MVA OVA infection. The infection with the MVA WT showed that the activation is antigen-specific since there was no upregulation of CD69 after using MVA WT (Figure 3.6 C). To confirm that XCR1$^+$ DC are the critical antigen-presenting DC for CD8$^+$ T cells during the later course of infection, Anna Brewitz performed an *in vitro* proliferation assay of naïve OT-I T cells. To that end, she sorted splenic CD11b$^+$ and CD8α$^+$ DC (XCR1$^+$ DC) 36 hours after i.v. infection and co-cultured naïve OT-I T cells with either CD11b$^+$ or CD8α$^+$ DC. Indeed, OT-I T cells only proliferated in the presence of CD8α$^+$ DC (XCR1$^+$ DC) (Figure 3.6 D).

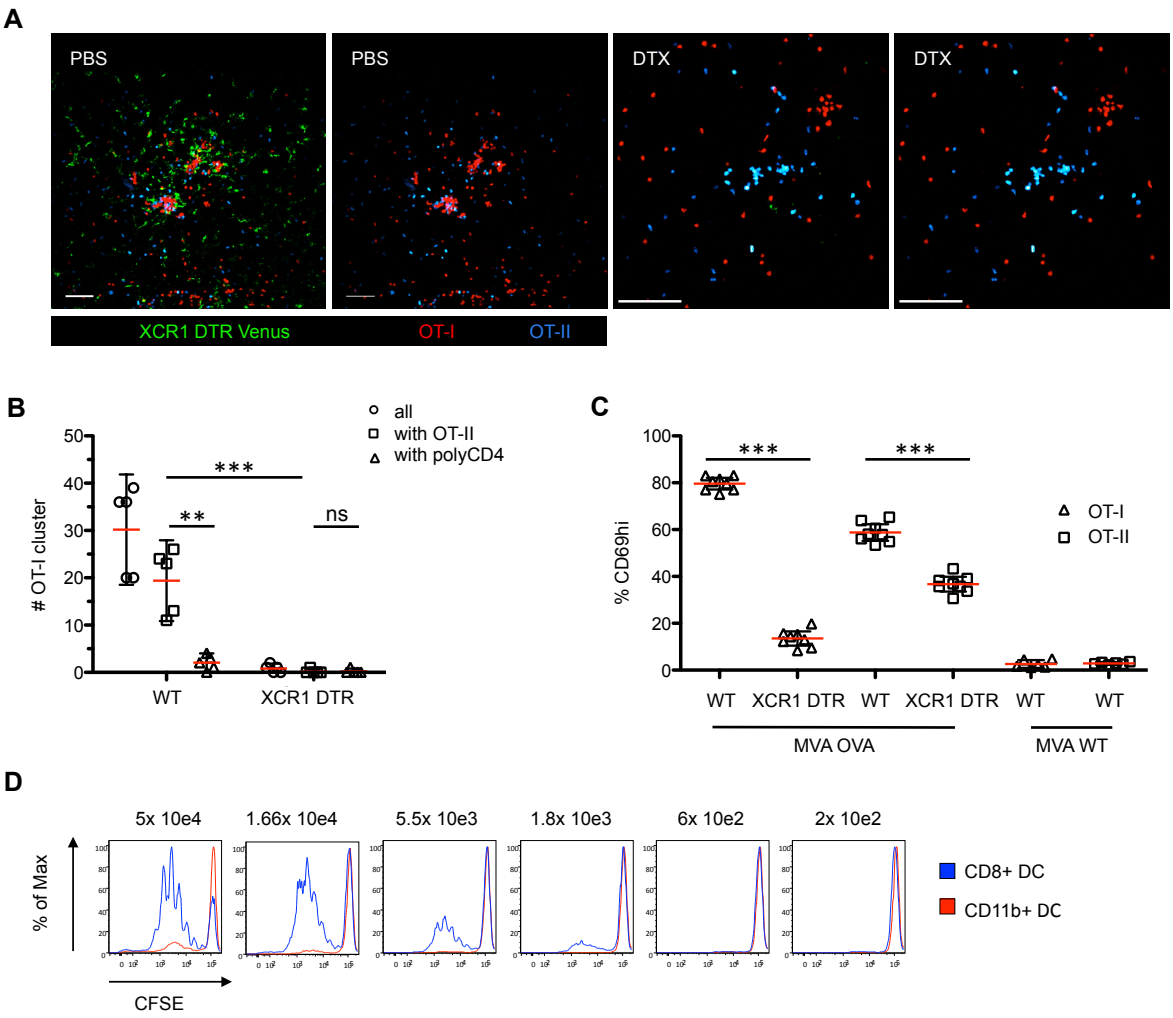

Figure 3.6. XCR1$^+$ DC present antigen to both CD4$^+$ and CD8$^+$ T cells during viral infection.
(A) IF images of pLN 30+8 h after MVA OVA infection, showing OT-I and OT-II T cell co-cluster in the presence and absence of XCR1$^+$ DC using the experimental setup from Figure 3.5 A. (B) Quantitative semi-automated analysis of IF images of pLN´s OT-I T cell co-cluster with OT-II and polyclonal CD4$^+$ T cells in the presence or absence of XCR1$^+$ DC. (C) In the presence and absence of XCR1$^+$ DC, analysis of CD69 upregulation on OT-I and OT-II T cells, transferred 28 h post-infection (MVA OVA/MVA WT; f.p.) and analyzed 12 h later in the pLN. (D) Proliferation of OT-I T cells after *ex vivo* co-incubation (72 h) with sorted splenic DC subsets after 36 h MVA OVA i.v. infection. XCR1 DTR Venus mice were treated with PBS or DTX (A/B) or littermates (WT) were also treated with 500 ng DTX (C), two days before infection (d-2, d-1, d0). A. Brewitz performed proliferation assays. Data are representative of three independent experiments (n=8). (A) Scale bars, 50 µm. (B/C) Red bars indicate mean values ± 95% confidence interval. ***p≤0.001; **p≤0.01; ns, non-significant. Figures are paneled (A/D) and modified (B/C) from Eickhoff et al., 2015.

3.6 Initial activation of CD4$^+$ and CD8$^+$ T cells and co-recognition of antigen are distinct events during Vaccinia virus infection

Since I found separated activation of CD4$^+$ and CD8$^+$ T cells early (< 12 h) during MVA infection and since XCR1$^+$ DC are the DC presenting antigen to both CD4$^+$ and CD8$^+$ T cells later during MVA infection, I wanted to corroborate these findings in a replicating viral system. As a non-replication system, MVA infection requires cross-presenting XCR1$^+$ DC for continuous antigen-presentation. Hence, it remains unclear whether cross-presentation is required per se during a continuous infection. To elucidate this, I used Vaccinia virus expressing OVA (VV OVA) and analyzed the priming sites of CD4$^+$ and CD8$^+$ T cells early and later during the infection. By applying IVM, I observed separated, arrested OT-I and OT-II cells in the pLN 10 hours after infection (Figure 3.7 A, Movie 4). Similarly to the MVA infection, analysis of the LN sections also determined that CD8$^+$ T cells are clustering and translocating to the periphery of the LN early during VV infection (Figure 3.7 B), while CD4$^+$ T cells again remained in the paracortex (Figure 3.7 B). Usage of the late T cell transfer approach showed that the common DC for CD4$^+$ and CD8$^+$ T cells is located in the paracortex of the LN and presents the antigen later in VV infection as well (Figure 3.7 C). After XCR1$^+$ DC depletion, I detected only a few T cell clusters and co-clusters on the LN sections (Figure 3.7 D). To test whether the clustering cells are activated in the XCR1$^+$ DC depleted mice, I stained for CD69 and observed that within the single clusters the T cells are activated. Importantly however, within the co-cluster either OT-I or OT-II T cells are activated in the absence of XCR1$^+$ DC (Figure 3.7 D). Semi-automated analysis of OT-I T cell clusters on LN sections verified that without XCR1$^+$ DC no co-clusters are present (Figure 3.7 E). In the end, the results after VV infection are in line with the results after MVA infection and encourage the notion that the CD4$^+$ T cell help for CD8$^+$ T cells occurs on XCR1$^+$ DC within the paracortex of the LN.

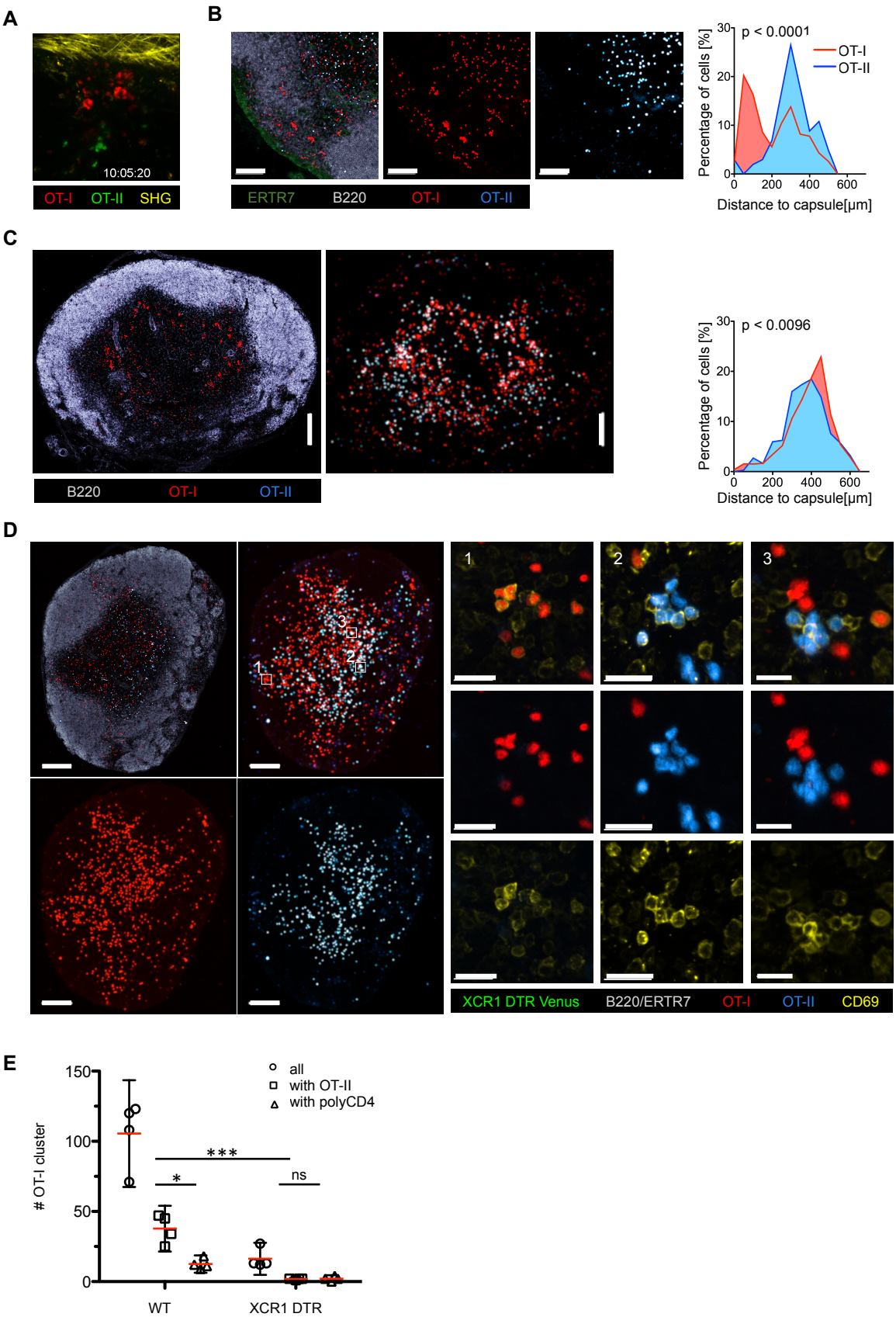

Figure 3.7. Initial activation of CD4⁺ and CD8⁺ T cells and co-recognition of antigen are distinct events during Vaccinia virus infection.

(A) IVM images of pLN 10-11 h after VV OVA f.p. infection, T cells were transferred 24 h prior to infection. Circles indicate separated activation between OT-I and OT-II T cell cluster, second harmonic generation signal (SHG) indicates distance to LN capsule, see also Movie 4. (B) IF images showing localization of T cells and histogram showing distance of T cells from capsule (infected cells). (C/D) IF images of 30+8 h after VV OVA infection, showing OT-I and OT-II T cell co-cluster in the LN paracortex in the presence (C) and absence (D) of $XCR1^+$ DC using the experimental setup from Figure 3.5 A, histogram (C) showing distance of T cells from capsule and CD69 staining indicating T cell activation (D). (E) Quantitative analysis of IF images of pLN´s OT-I T cell co-cluster with OT-II and polyclonal $CD4^+$ T cells in the presence or absence of $XCR1^+$ DC using semi-automated analysis after 30+8 h VV OVA f.p. infection. XCR1 DTR Venus mice or littermates (WT) were treated with 500 ng DTX (D/E) two days before infection (d-2, d-1, d0). Data are representative of three independent experiments (n=4). Scale bars, 50 µm (A), 100 µm (B), 200 µm (C) and 200/20 µm (D). (B/C) Red bars indicate mean values ± 95% confidence interval. ***p≤0.001; **p≤0.01; *p≤0.05; ns, non-significant. Figures are paneled (A-D) and modified (E) from Eickhoff et al., 2015.

3.7 Endogenous activated $CD8^+$ T cells are located in the area of $CD4^+$ T cell help during viral infection

After having established that during the early phase of viral infection naïve $CD4^+$ and $CD8^+$ T cells are activated on spatially separated DC and at later stages of viral infections $XCR1^+$ DC are presenting the antigen to both subsets within the LN paracortex, I aimed to confirm these finding regarding endogenous $CD8^+$ T cells. To assess the role of the localization of endogenous $CD8^+$ T cell – DC interactions *in vivo*, I employed interferon-γ (IFNγ) reporter mice indicating cells (eYFP expression), which produced IFNγ within the last 24 hours. Interferon-γ production of $CD4^+$ and $CD8^+$ T cells is a result of activation. To characterize the IFNγ producing cells after viral infections, I analyzed the cells via flow cytometry. Thirty-eight hours after VV infection (f.p.), I observed an increase of IFNγ-producing cells in the draining LNs (Figure 3.8 A). Analysis of the IFNγ high producing cells revealed that about 40% of the population are NK cells ($NK1.1^+/CD3^-$), 30% are $CD8^+$ T cells ($CD8^+/CD3^+$), 20% are $CD4^+$ T cells ($CD4^+/CD3^+$) and 10% are double negative (DN) T cells ($CD8^-/CD4^-/CD3^+$) (Figure 3.8 B). Furthermore, $IFNγ^+$ $CD8^+$ T cells had a brighter eYFP signal and additionally a bigger cell volume (blasted) compared to the other cellular subsets, which indicates that they were about to go into cell division (Figure 3.8 C/D). To visualize the localization of endogenous activated $CD8^+$ T cells, I analyzed pLN sections after VV f.p. infection. To ensure that the endogenous, activated $CD8^+$ T cells did not enter the LN after the early phase of infection, I treated the IFNγ reporter mice 14 hours after infection with CD62L antibodies in order to block the entry of naïve T cells. In total 40 hours after infection, I characterized the localization of IFNγ-producing (YFP^+) cells. In line with the flow cytometry data, the majority

of the bright and blasted YFP positive cells were also positive for CD8 staining, whereas small and dim YFP positive cells were rather positive for NK1.1 and CD4 (Figure 3.8 E).

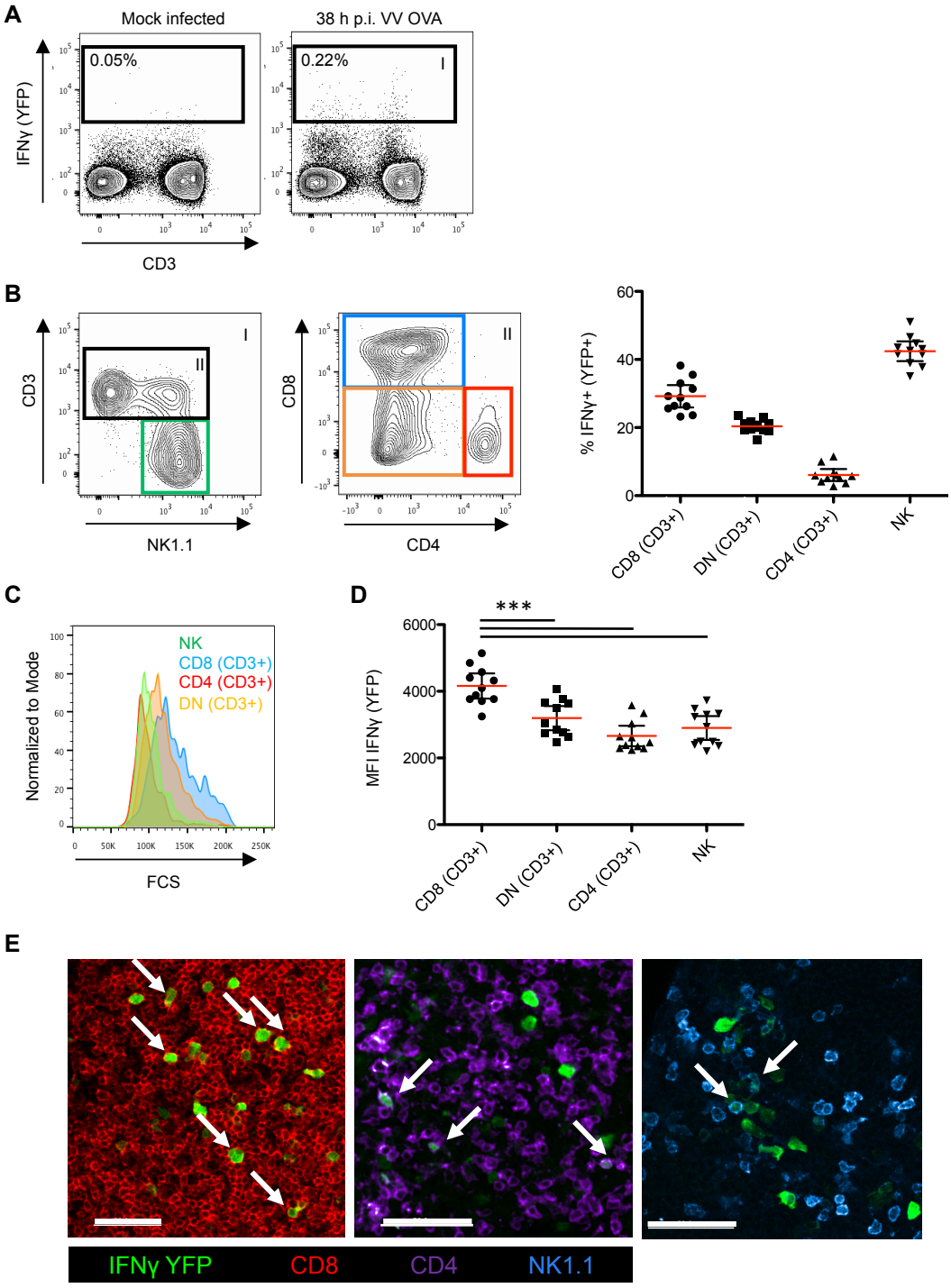

Figure 3.8. Endogenous activated CD8+ T cells have an increased cell volume 38 h after viral infection.
(A-D) Characterization of IFNγ reporter mice (YFP$^+$) by flow cytometry 38 h after VV OVA f.p. infection. Representative plots showing the gating strategy (A/B), the quantification of cellular frequencies (B), the size (C) and the mean fluorescence intensity (MFI) of the YFP signal from different cellular populations (D). (E) IF images showing pLN of IFNγ reporter mice (YFP$^+$) 40 h after VV OVA f.p. infection, 14 h after infection mice were treated with 100 µg αCD62L i.p. to block entry of naïve lymphocytes. Blasted and bright YFP$^+$CD8$^+$ cells compared to small and dim YFP$^+$CD4$^+$ and YFP$^+$NK1.1$^+$ cells. Data are representative of two (n=11 B/D) or three

(n=3 E) independent experiments. Scale bars, 50 µm. (B/D) Red bars indicate mean values ± 95% confidence interval. ***p≤0.001. Figures are paneled (A-D) and modified (E) from Eickhoff et al., 2015.

During the early phase of infection, I found endogenous activated ($CD69^+$) cells at the priming sites of OT-I T cells indicating that endogenous lymphocytes are primed at the same DC (Figure 3.9 A). To track the localization of the endogenous activated $CD8^+$ T cells, I infected IFNγ reporter mice with VV OVA and 32 hours later transferred naïve OT-I T cells in order to visualize if the endogenously activated cells localized at the place of antigen-presentation, more precisely the place of the $CD4^+$ T cell help. Indeed, I detected $IFN\gamma^+$ (YFP^+) cells in the LN paracortex and found that they co-localized with activated, transferred OT-I T cells (Figure 3.9 B). Finally, I intercrossed the IFNγ reporter mice with the XCR1 DTR-Venus reporter mice, and analyzed the co-localization of the blasted YFP^+ cells and $XCR1^+$ DC. Usage of CD62L block as described above, I found blasted, $CD8^+$, YFP^+ cells that co-localized with $XCR1^+$ DC (Figure 3.9 C).

In summary, this data indicate that during their priming, $CD8^+$ T cells could have multiple interactions with DC in an antigen-specific manner, because activated $CD8^+$ T cells (YFP^+) cells, which are shortly before cell division (blasted), seek out and interact/co-localize with $XCR1^+$ DC within the LN paracortex.

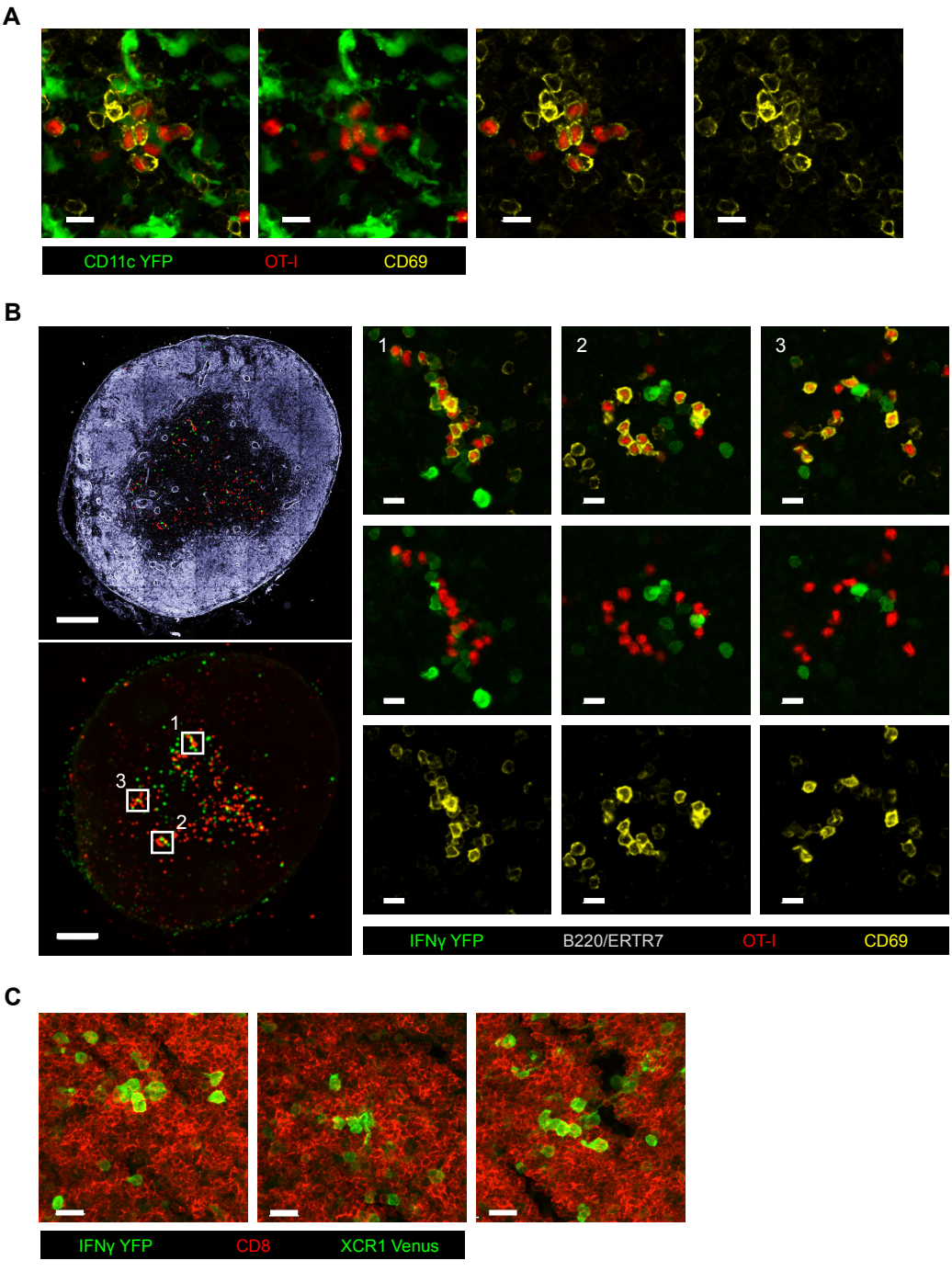

Figure 3.9. Endogenous activated CD8⁺ T cells are located in the area of CD4⁺ T cell help during viral infections.
(A) IF images of pLN of CD11c YFP reporter mice 8 h after VV OVA f.p. infection. Images showing co-localization of transferred, activated OT-I T cells with endogenous activated cells (CD69⁺). (B-C) Localization analysis of YFP-positive cells in IFNγ reporter mice (YFP⁺) 40 h after VV OVA f.p. infection. (B) 32 h post infection IFNγ reporter mice received OT-I T cells and 8 h later localization of activated (CD69⁺) OT-I T cells and YFP positive cells were analyzed. IF images showing co-localization between activated OT-I T cells and YFP positive cells. (C) IF images of intercrossed XCR1⁺ DTR Venus x IFNγ reporter mice 40 h after VV OVA f.p. infection and after treatment with 100 µg αCD62L 14 h post infection. Images showing co-localization of paracortical XCR1⁺ DC with blasted, YFP positive cells. Data are representative of two (n=4 B) and one (n=4 A/C) independent experiments. Scale bars, 10 µm (A), 200/10 µm (B), 20 µm (C). Figures are paneled (A/B) from Eickhoff et al., 2015.

3.8 Primary CD8$^+$ T cell response is impaired without XCR1$^+$ DC

Based on the findings that exclusively XCR1$^+$ DC are presenting antigen to both T lymphocyte subsets, I investigated CD4$^+$ T cell help to the endogenous CD8$^+$ T cell response in the absence of XCR1$^+$ DC on a functional level. In order to test if CD4$^+$ T cell help influences the primary CD8$^+$ T cell response of our viral system, I depleted CD4$^+$ cells (d-3, d-1 post infection) and determined the specific, endogenous CD8$^+$ T cell response 8 days after VV infection. Tetramer staining for the immuno-dominant VV epitope B8R$_{20}$ showed decreased numbers of specific CD8$^+$ T cells in the absence of CD4$^+$ cells compared to the PBS treated group (Figure 3.10 A). Having established that CD4$^+$ T cell help dependency impacts on the primary response to VV infection, I aimed to gain detailed insights into the differentiation and function of antiviral CD8$^+$ T cells primed in the absence of XCR1$^+$ DC. To remove the XCR1$^+$ DC during the priming phase of CD8$^+$ T cells, I treated XCR1 DTR mice and their littermate controls (WT) with DTX (d-2, d-1, d0 prior infection) before I infected the mice with Vaccinia virus. Eight days after the infection, I observed a decrease in the numbers of antiviral CD8$^+$ T cells primed without XCR1$^+$ DC (Figure 3.10 B). Additionally, within CD4$^+$ cells depleted animals, the specific CD8$^+$ T cell response did not alter in presence or absence of XCR1$^+$ DC (Figure 3.10 C). This data indicate that the observed reduced CD8$^+$ T cells response is a consequence of XCR1$^+$ DC lacking CD4 helper signals. To test the hypothesis XCR1$^+$ DC are the cells that receive and translate CD4 helper signals to CD8$^+$ T cells, I employed mixed bone marrow chimeras. The irradiated mice got a 1:1 mixture from bone marrow of MHCII KO mice and XCR1 DTR mice. As a result, the chimeric mice possessed two kinds of XCR1$^+$ DC, those that carry a DTR and those that do not express MHC II and consequently are not able to interact with CD4$^+$ T cells in an antigen-specific manner (Figure 3.10 D). I treated the chimeric mice with either DTX or PBS, meaning that in the DTX treated group, only those XCR1$^+$ DC are left which can not interact with CD4$^+$ T cells in an antigen-specific manner. The analysis revealed again a decrease of specific CD8$^+$ T cell numbers in the absence of ´helped` XCR1$^+$ DC after VV infection on day 8 (Figure 3.10 E).

As CD4$^+$ T cell licensing of XCR1$^+$ DC occurs later during the infection, I hypothesized that depletion of XCR1$^+$ DC after the infection should also be followed by a decreased specific CD8$^+$ T cell response. Therefore in cooperation, Karl Komander and I started the DTX-treatment of XCR1 DTR mice 12 hours after the infection. In line with my previous findings,

the inducted antigen-specific CD8$^+$ T cell response was also decreased if XCR1$^+$ DC were depleted after initial infection and initial T cell priming (data not shown).

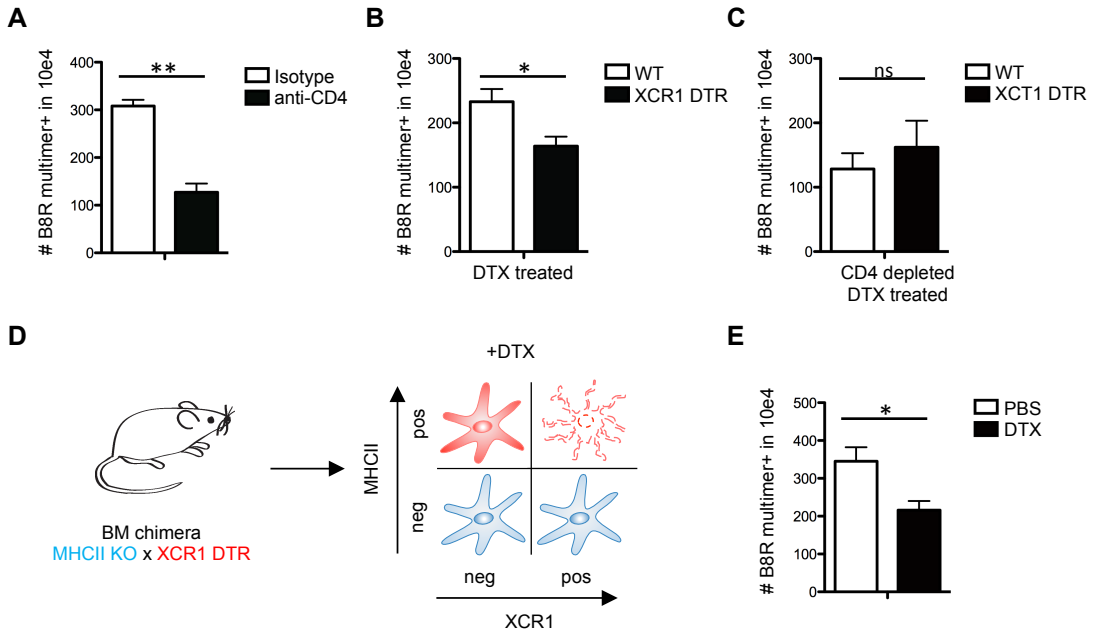

Figure 3.10. Primary CD8$^+$ T cell response is impaired without XCR1$^+$ DC.
(A-C) Numbers of splenic specific CD8$^+$ T cell response 8 days after VV OVA i.p. infection in presence or absence of CD4$^+$ T cells (A), XCR1$^+$ DC (B) or w/o CD4$^+$ T cells in presence or absence of XCR1$^+$ DC (C). Mice were treated with 500 µg αCD4 or isotype control (A/C) prior to infection (d-3, d-1). XCR1 DTR mice or littermates (WT) were treated with 500 ng DTX (B/C), prior to infection (d-2, d-1, d0). (D) Experimental design of mixed BM chimeric mice. (E) Numbers of splenic specific CD8$^+$ T cell response from mixed BM chimeric mice 8 days after VV OVA i.p. infection and after either 500 ng DTX or PBS treatment (d-2, d-1, d0). Data are representative of three (n=4) independent experiments. Graphs show mean +SEM. ***p≤0.001; **p≤0.01; *p≤0.05; ns, non-significant. Figures are paneled (A-E) from Eickhoff et al., 2015.

3.9 Secondary CD8$^+$ T cell response depends on XCR1$^+$ DC

The previously obtained data suggest a diminished primary CD8$^+$ T cell response in absence of XCR1$^+$ DC permitting the CD4$^+$ T cell helper signals. However, CD4$^+$ T cell help not only optimizes the primary immune response, but is also critical for a robust memory formation of CD8$^+$ T cells (Bevan, 2004). Thus, I tested whether the absence of XCR1$^+$ DC influences the differentiation of antigen-specific CD8$^+$ T cells on day 8. Here, I detected a decrease of the frequency of CD127$^+$ (IL-7R) antigen-specific CD8$^+$ T cells after XCR1$^+$ DC depletion during the early phase of infection (Figure 3.11 A). As CD127 is a surrogate marker for memory precursors, I expected a loss of the antigen-specific memory CD8$^+$ T cells after the CD8$^+$ T cell contraction phase. To address the question whether memory CD8$^+$ T cells are lost, I analyzed the amount of antigen-specific CD8$^+$ T cells 60 days after VV infection. Interestingly, the

numbers of $B8R_{20}$-positive (antigen-specific) $CD8^+$ T cells were only slightly reduced when $XCR1^+$ DC were missing during the initial priming (Figure 3.11 B). After re-stimulating the cells with the $B8R_{20}$ peptide, the amount of IFNγ-producing $CD8^+$ T cells was similar between the $XCR1^+$ DC depleted and non-depleted group (Figure 3.11 C). However, the polyfunctionality (TNFα and IL-2 production) of the IFNγ-producers was significantly impaired. The capacity of $CD8^+$ T cells to produce IL-2 was remarkably reduced in $XCR1^+$ DC depleted animals (Figure 3.11 D). One hallmark of memory cells is a rapid response after a second exposure to the antigen and further they need IL-2 for an efficient proliferation (Cui and Kaech, 2010). Based on the functional defect of IL-2 production, I predicted a limited response after a second antigen challenge. In order to test this notion, I infected $XCR1^+$ DC depleted and non-depleted mice with VV and 60 days after VV infection and re-challenged the mice with *Listeria monocytogenes* expressing the Vaccinia virus epitope B8R (L.m.-B8R). In fact, five days after the second antigen challenge, I detected a significant reduction of antigen-specific $IFN\gamma^+$ $CD8^+$ T cells if $XCR1^+$ DC were depleted during priming with Vaccinia virus (Figure 3.11 E).

In conclusion, my data resolve that $XCR1^+$ DC are the DC translating CD4 helper signals to $CD8^+$ T cells. The absence of $XCR1^+$ DC during priming leads to a functional defect of $CD8^+$ memory T cells, which leads to an impaired memory response upon secondary antigen exposure.

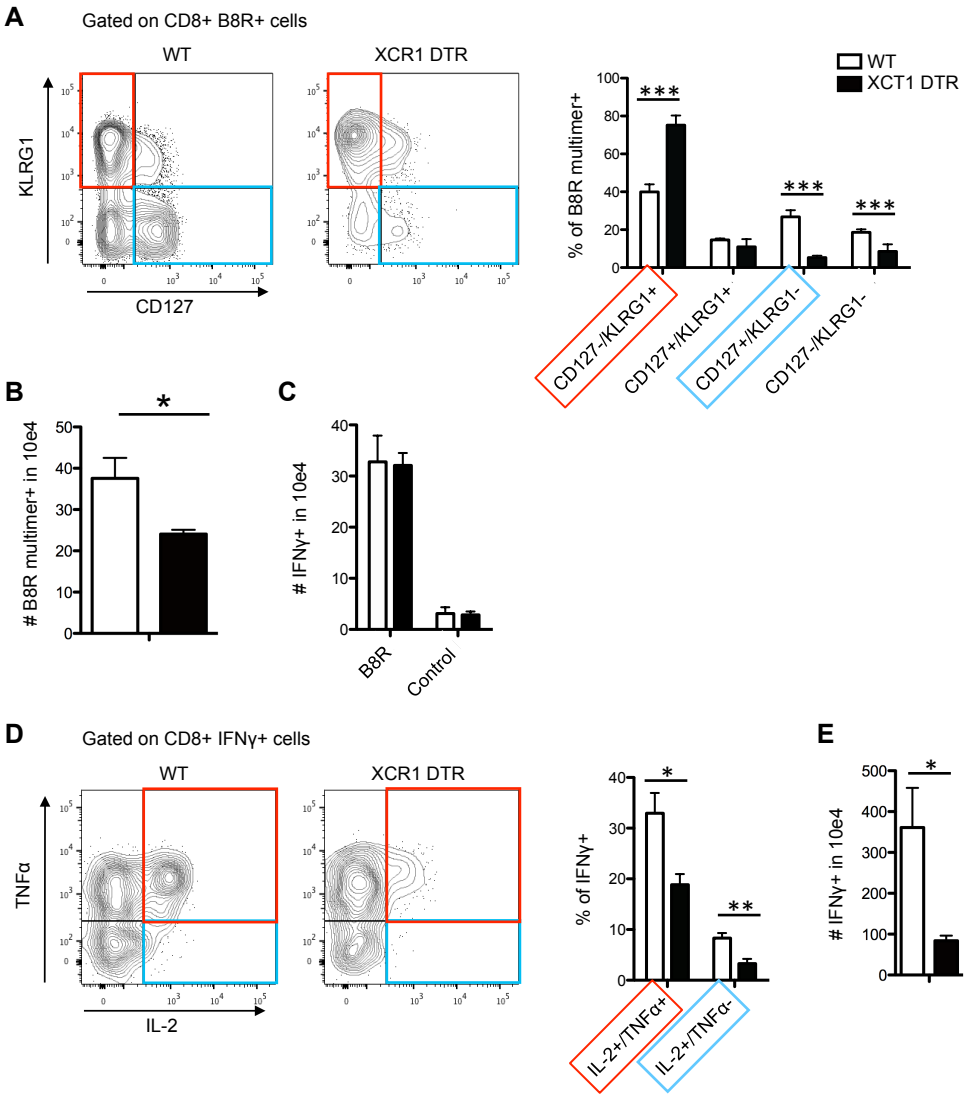

Figure 3.11. Secondary CD8⁺ T cell response depends on XCR1⁺ DC.
(A) Analysis of KLRG1 and CD127 positive specific splenic CD8⁺ T cell response (B8R-positive) 8 days after VV OVA i.p. infection in DTX treated XCR1 DTR mice or littermate control mice (WT). Representative plots showing gating strategy and frequencies of different populations. (B-D) Analysis of splenic specific CD8⁺ T cell response 60 days after VV OVA i.p. infection in presence or absence of XCR1⁺ DC during the acute infection. Graphs showing absolute numbers of antigen-specific memory CD8⁺ T cells (B), absolute numbers of IFNγ producing CD8⁺ T cells (C) after 5 h peptide (B8R) restimulation and representative plots and frequencies (D) of polyfunctionality of restimulated IFNγ-producing CD8⁺ T cells. Control shows responding cells without B8R restimulation. (E) Rechallange of VV OVA primed (60d i.p.) DTX treated XCR1 DTR mice or littermate controls (d-2, d-1, d0) with L.m.-B8R (5d i.v.). Graph shows absolute numbers of splenic IFNγ-producing CD8⁺ T cells after 5 h restimulation with peptide (B8R). Data are representative of three or two (E) (n=4) independent experiments. Graphs show mean +SEM. ***p≤0.001; **p≤0.01; *p≤0.05; ns, non-significant. Figures are paneled (A-E) from Eickhoff et al., 2015.

Discussion

In this work, I investigated the spatio-temporal dynamics of $CD4^+$ T cell help for $CD8^+$ T cell responses in the LN and addressed which DC subset delivers the helper signals during viral infections. I showed that during the early phase of infection, the initial activation of $CD4^+$ and $CD8^+$ T cells occurred on spatially separated DC. $CD8^+$ T cells were activated through directly infected APC, which were primary located at the lymphatic entry sides, specifically in the subcapsular sinus and the interfollicular areas of the LN. In contrast, $CD4^+$ T cells were activated through non-infected APCs, which were located in the paracortex of the LN. Being aware of the fact that Vaccinia virus infection is dependent on $CD4^+$ T cell help, I hypothesized that at some point a DC subset presents antigen to both $CD4^+$ and $CD8^+$ T cells. Indeed, I found that later during the infection, $CD4^+$ and $CD8^+$ T cells arrested at a non-infected DC subset in the paracortex of the LN. Further, I identified $XCR1^+$ DC as this non-redundant DC subset, which presented antigens to both $CD4^+$ and $CD8^+$ T cells and thereby served as a meeting point. Finally, I showed that early-activated, endogenous $CD8^+$ T cells co-localized with the $XCR1^+$ DC at the later stage of infection. Having defined that $XCR1^+$ DC are the DC, which transmit the helper signals, I verified the delivery of help through $XCR1^+$ DC during primary responses and its impact on secondary antiviral $CD8^+$ T cell responses on a functional level. Overall, my data suggest that during the initial activation phase, $CD8^+$ T cells have multiple interactions with different DC in order to generate functional memory $CD8^+$ T cells. Further my data provide insights into how the highly dynamic immune system could organize a three-cell interaction event (consecutive or simultaneous). The key findings of my work are illustrated in Figure 4.1.

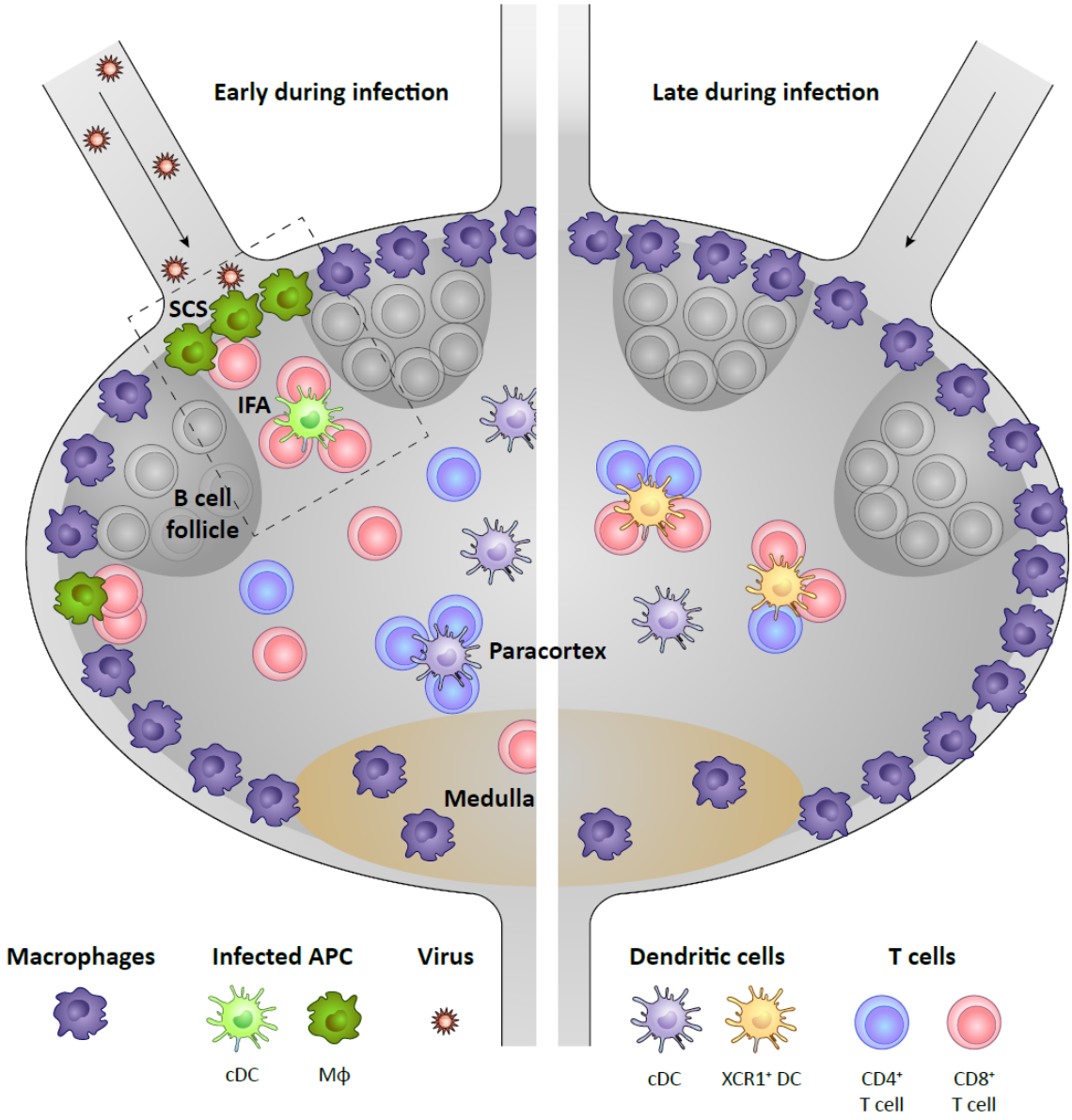

Figure 4.1. CD8⁺ T cell priming and provision of help are spatially and temporally separated events.
The graphical abstract shows on the left side of the LN spatially separated initial activation of CD4⁺ and CD8⁺ T cells, in which after viral infection CD8⁺ T cells were primed on directly infected cells within the SCS and IFA. The right side illustrates that later during viral infection, XCR1⁺ DC present foreign antigen to both CD4⁺ and CD8⁺ T cells within the LN paracortex. IFA: interfollicular area; SCS: subcapsular sinus; APC: antigen-presenting cell; Mϕ: macrophage; cDC: conventional dendritic cell. Figure is adapted from Eickhoff et al., 2015.

3.10 Spatio-temporal organization in lymph nodes during CD8$^+$ T cell response

3.10.1 Separated initial activation of CD4$^+$ and CD8$^+$ T cells is followed by co-recognition of antigen on XCR1$^+$ DC

Delivery of CD4$^+$ T cell help for CD8$^+$ T cells requires foreign antigen presentation on the same DC via MHCI and MHCII in order to allow cognate interaction with both CD4$^+$ and CD8$^+$ T cells (Cassell and Forman, 1988; Bennett et al., 1997). In my work, I found that early during viral infections, initial CD8$^+$ and CD4$^+$ T cell activation is orchestrated on spatially separated DC followed by co-recognition of antigen on XCR1$^+$ DC within the LN paracortex at the later stage of infection. This finding in the context of viral infections was surprising and has been missed by previous studies based on the use of peptide-pulsed DC during the simultaneous analysis of CD4$^+$ and CD8$^+$ T cell dynamics. More precisely, I found a separation in activation of CD8$^+$ T cells on directly infected dendritic cells *versus* activation of CD4$^+$ T cells on non-infected dendritic cells. One possible explanation for this finding could be that some viruses have evolved evasion mechanism that target MHCII for downregulation. If this were the case, antigen presentation towards CD4$^+$ T cells by directly infected cells would be inhibited. Within this work, I showed priming of CD8$^+$ T cells after contact with adenovirus and Vaccinia virus infected cells. Vaccinia virus has been demonstrated to interfere on the MHCII antigen presentation pathway, whereas adenovirus has not been demonstrated to affect the MHCII presentation pathway (Maudsley and Pound, 1991). Nevertheless, the reason for the separated activation could lay in the nature of the virus. In contrast to this assumption is that I also observed a separated activation of CD8$^+$ and CD4$^+$ T cells early after pathogen-free, sterile immunization with protein (OVA) and LPS. This observation supports the notion that separated lymphocyte activation early during infection is a general phenomenon. This hypothesis is line with several functional studies on antigen-presentation, which show that different DC subsets are specialized in their capacity to present antigen through either MHCI or MHCII (Merad et al., 2013). Besides their functional specialization in antigen-presentation, DC subsets also occupy distinct anatomical niches and are located in preferential anatomical areas of the LN and the spleen (Gerner et al., 2012; Calabro et al., 2016). In line with that notion such Calabro *et al*. observed a preferentially occupation of CD4$^+$ and CD8$^+$ T cells in the spleen in areas that are enriched for

XCR1$^+$ DC and CD11b$^+$DC, respectively. This biased localization could support a separated activation on a spatial level. Moreover, a recently published work by Gerner *et al.* confirmed my finding of separated activation of CD4$^+$ and CD8$^+$ T cells after protein immunization and also linked lymphocytes activation through different DC subsets with different DC localization in the LN as well as antigen availability (Gerner et al., 2017). In that study, it was shown that DC, which preferentially present via MHCI, are located in deeper areas of the paracortex of the LN and therefore have limited antigen availability so subcutaneously applied vaccines draining via the lymph. Hence, the CD8$^+$ T cell response in this experimental condition was lower compared to the CD4$^+$ T cell response. Using herpes simplex virus 1 (HSV-1) infections, Scott Mueller's group showed an asynchronous activation of CD4$^+$ and CD8$^+$ T cells on a temporal level (Hor et al., 2015). In this model, the virus does not freely drain to the LN. Thus, CD4$^+$ T cell priming occurs on migratory DC and later (> 24 h) CD8$^+$ T cell priming occurs on XCR1$^+$ DC, which at this time-point present antigen to both CD4$^+$ and CD8$^+$ T cells. Nevertheless, in a former publication the authors described that they also observed early CD8$^+$ T cell priming by directly infected cells after subcutaneous inoculation with HSV, where, in contrast to the former model, virus freely drains to the LN (Bedoui et al., 2016). From the results of other studies and my own work, I can conclude that separated activation of CD4$^+$ and CD8$^+$ T cells is a robust phenomenon observed in various experimental models and therefore represents a basic concept of adaptive cellular immunity.

A central finding of my study is that later during viral infection both, CD4$^+$ and CD8$^+$ T cells are able to interact with XCR1$^+$ DC. In other words, the provision of help is organized in a temporal sequence after the initial priming of the naïve lymphocytes. The dynamics of the adaptive humoral immune responses fully reflects my findings seen during the induction of cellular immunity. Naïve CD4$^+$ T cells and naïve B cells are primed separately in distinct areas through cognate antigen recognition, before they directly interact supporting the provision of help of CD4$^+$ T cells to B cells. In more detail, within 48 hours after initial priming, CD4$^+$ T cells change their chemokine receptor profile allowing them to migrate to the border of T and B cell zones (T-B border). Similarly, primed B cells change their chemokine receptor profile followed by the guidance to the T-B border and increase the chance to get helper signals of activated T cells in an antigen-specific manner (McHeyzer-Williams et al., 2006; Qi

et al., 2014). Reminiscent to the biology of B cells by data also argues that activated rather than naïve $CD8^+$ T cells are the recipients of helper signals.

Overall, I suggest a new spatio-temporal model for $CD4^+$ T cell help for $CD8^+$ T cells, in which initially a separated activation of the T lymphocyte subsets on specialized DC allows a quick and effective activation of $CD4^+$ and $CD8^+$ T cells. These activation signals alter the chemokine receptors expression profiles of $CD4^+$ and $CD8^+$ T cells (ImmGen database (Heng and Painter, 2008)), fostering interactions with a shared DC platform (Castellino et al., 2006). The proposed model of pre-activation implies that $CD8^+$ T cells have multiple interactions with dendritic cells. My own data and previous published work support this notion and will be further discussed in the following chapter.

3.10.2 $CD8^+$ T cells have multiple DC interactions during their priming

In a Vaccinia virus infection model, I delineated that directly infected DC prime $CD8^+$ T cells during the early phase of infection. The present study indicates that after initial activation, $CD8^+$ T cells (IFNγ-producers) translocate into the paracortex interacting there with the helper platform, $XCR1^+$ DC, before they start their clonal proliferation (blasted IFNγ-producers co-localize with $XCR1^+$ DC; Figure 3.8 and 3.9). Forty hours after infection, blasted (activated) antigen-specific $CD8^+$ T cells interact with $XCR1^+$ DC in the paracortex of the LN. But, why do $CD8^+$ T cells require multiple interactions with DC? Before TCR stimulation, the expression of CCR5 on naïve $CD8^+$ T cells is very low (Oppermann, 2004). Encountering foreign antigen leads to an upregulation of CCR5 and therefore guides $CD8^+$ T cells to the licensed DC. This notion is supported by the work of different groups. First, Ronald Germain´s group found that $CD4^+$ T cell help leads to the production of CCL3 and CCL4 by cognate antigen-bearing DC, which recruits $CCR5^+$ $CD8^+$ T cells to the licensed DC (Castellino et al., 2006). Second, Sammy Bedoui´s group found that licensed $XCR1^+$ DC produce higher amounts of CCL3 and CCL4, allowing them to augment the recruitment of $CCR5^+$ cells (Bedoui et al., 2016).

However, not only $CD8^+$ T cells get pre-activated before they receive help. $CD4^+$ T cells also require activation in order to optimally provide help. On a molecular level this is reflected by the upregulation of CD40L on activated CD4 T cells - a critical molecule for help-delivery, which is absent on naive $CD4^+$ T cells. Similar to the help provided to B cells, previous

activation of $CD4^+$ T cells is required in order to stimulate the $XCR1^+$ DC via CD40/CD40L interactions and consecutively prime $CD8^+$ T cells. The well-established model of the three priming phases during T cell activation (Mempel et al., 2004), further supports the notion of multiple DC interactions as the basis for optimal $CD8^+$ T cell responses. After phase 2, which is characterized by long-term interactions (12-24 h) between T cells and cognate antigen-bearing DC (Miller et al., 2002; Stoll et al., 2002; Bousso and Robey, 2003), activated T cells enter phase 3. During this phase $CD8^+$ T cells show short-term interactions with DC followed by clonal proliferation of $CD8^+$ T cells. My results argue that during phase 3, $CD8^+$ T cells integrate helper signals via consecutive interactions with licensed DC.

3.10.3 $CD4^+$ T cell help for $CD8^+$ T cells is mediated via $XCR1^+$ DC

When, where and on which DC subset help is provided to $CD8^+$ T cells is a central discovery of my study. I identified non-infected $XCR1^+$ DC as the critical helper platform, being crucial for the formation of functional memory $CD8^+$ T cells. Interestingly, $XCR1^+$ DC were not required for the optimal initial activation/priming step. Instead, I found that directly infected DC, irrespectively of their subset, mediate the initial $CD8^+$ T cell activation. Only at a later stage of infection, $CD4^+$ T cell help for $CD8^+$ T cells is provided through $XCR1^+$ DC within the paracortex of the LN. Notably, the common $XCR1^+$ DC in the paracortex were not infected at this time-point. Since those $XCR1^+$ DC interacted with both $CD4^+$ and $CD8^+$ T cells in a cognate manner, $XCR1^+$ DC were presenting exogenous antigen via MHCI and MHCII pathways. Indeed, based on numerous studies, $XCR1^+$ DC are specialized in the uptake and presentation of antigen from dead cells (Iyoda et al., 2002). So the question arises, where do XCR1 DC efficiently acquire foreign antigen? During my previous study in collaboration with Anna Brewitz, we found that $XCR1^+$ DC get recruited to the initial $CD8^+$ T cell priming sites around infected DC (Brewitz et al., 2017). Activated $CD8^+$ T cells orchestrate this recruitment through the T cell derived chemokine XCL1. Being recruited of the initial activation cluster, close to the infected DC, $XCR1^+$ DC are in prime position to take up pathogenic antigens once the infected cell succumbs to death (Brewitz et al., 2017). In other words, $XCR1^+$ DC within the early clusters are predisposed for being the helper platform at the later phase of infection. On a conceptual level, upon activation $CD8^+$ T cells lay the ground for consecutive DC encounters to optimize their own activation that includes helper signals by $CD4^+$ T cells.

But what are those signals on a molecular level? Regarding the input signal ($CD4^+$ T cells → $XCR1^+$ DC) the field has largely come to a consensus. In line with the licensing model and paralleling B cell help, the critical molecular interactions between $CD4^+$ T cells and $XCR1^+$ DC are based on CD40L - CD40 (Ridge et al., 1998; Schoenberger et al., 1998). In contrast, regarding the output signal, which means signals that are transmitted from licensed $XCR1^+$ DC to $CD8^+$ T cells ($XCR1^+$ DC → $CD8^+$ T cells), several molecules have been implicated. One interesting candidate that can transmit CD4 helper signals to $CD8^+$ T cells via $XCR1^+$ DC are CD70/CD27 interactions (Feau et al., 2012). Further, the group of Ross Kedl showed that *in vivo* upregulation of CD70 on DC is dependent on both innate and CD40 stimulation pathways arguing for a second signal that may be required to fully license $XCR1^+$ DC. Interestingly, their data indicate a slight delay of CD70 upregulation compared to the upregulation of CD80/86 and CD40 (Sanchez et al., 2007), which delineates chronological sequence of upregulation and stimulation of co-stimulatory molecules on DC (CD40 upregulation, allowing CD40/CD40L interactions, followed by CD70 upregulation).

Sammy Bedoui´s group showed that after co-stimulation with type I IFN and CD40 stimulatory antibodies, $XCR1^+$ DC produced higher amounts of the chemokines CCL3 and CCL4 and cytokines IL-15 and IL-6 (Bedoui et al., 2016; Greyer et al., 2016), molecules also related to the output signals of $CD4^+$ T cell help. Again, CD40 stimulation alone did not lead to the production of those chemokines and cytokines. This argues that $CD4^+$ T cell help may act as an amplification mechanism, if innate signals are insufficiently strong to fully support an optimal adaptive immune response. Together, all these findings related to the $XCR1^+$ DC helper platform support the spatio-temporal model of help and augment it to pre-activation and preparation of lymphocytes as well as pre-activation and preparation of the helper platform.

3.10.4 Role and dynamics of accessory cells during $CD8^+$ T cell activation

Several cell types that modulate antiviral $CD8^+$ T cell responses but are not directly involved in the priming process (signal 1 and 2) have been identified. Among those accessory cells are plasmacytoid DC (pDC) and NK cells. In following paragraph I will discuss how and when those cells participate in the $CD8^+$ T cell activation and/or programming phase.

As discussed above, we recently found that early after infection, $CD8^+$ T cells recruit together $XCR1^+$ DC in the interfollicular areas of the LN through the production of XCL1 (Brewitz et al., 2017). Additionally, within 4-8 hours after priming, these activated $CD8^+$ T cells also recruited pDC through CCL3/4 to the sites of their activation. We showed that pDC deliver type I IFN and thereby optimize the maturation of $XCR1^+$ DC, like the upregulation of the co-stimulatory molecule CD40 (Brewitz et al., 2017). The early clusters of antigen-specific $CD8^+$ T cells, pDC and $XCR1^+$ DC provide an optimal exchange of cytokines, like type I IFNs. This finding clarifies the critical source of type I IFN that is required to fully license $XCR1^+$ DC (besides CD40L from $CD4^+$ T cells) and optimizes their ability to cross-present antigen. In summary, pDC support antiviral $CD8^+$ T cell response early after priming by locally delivering type I IFN signals that act on $XCR1^+$ DC.

Natural killer (NK) cells can eliminate virally infected cells and malignant cells through different cytotoxic effector functions in a similar manner as effector $CD8^+$ T cells. However, NK cells perform their effector functions largely in an antigen-independent manner, e.g. through killer lectin like receptors (KLR´s). Upon infection, NK cells become activated and are able to influence the T cell response through different mechanisms. As such, it has been shown that NK cells are able to directly modulate T cell responses through cell-cell interactions, via cytokine production and possibly cytokine competition. Further, NK cells are able to indirectly affect the T cell response through the regulation of the APC activity (Cook et al., 2014).

From a spatio-dynamic perspective, I observed that NK cells co-localized with $CD8^+$ T cell at their activation sites early after viral infections (< 12 h) similar to pDC. This is somewhat expected given the shared chemokine receptor expression pattern between pDC and NK cells (e.g. CXCR3 and CCR5). In contrast to pDC, NK cells also co-localized with $CD8^+$ T cells at later phases after infection (> 24 h). At this later time-point, I found high numbers of NK cells in the paracortex of the LN (unpublished observations). This was an interesting finding as NK cells are usually not located in the paracortex of the LN. Instead, they are typically found at the pathogen entry sites like medullary and interfollicular region of the LN (Garcia et al., 2012; Kastenmüller et al., 2012). Thus, NK cells seem to be re-localized to the different activation sites of $CD8^+$ T cell response, the place where $CD8^+$ T cells get their helper signals. So what is the functional role of NK cells early (< 12 h) and later (> 24 h) after infection

regarding the modulation of $CD8^+$ T cells responses? Combining my concept of $CD8^+$ T cell activation with known mechanisms of NK cell function, several concepts how NK cells impact on $CD8^+$ T cell responses can be hypothesized. For example, Zecher *et al.* suggested competition of IL-15. In particular their data indicate that in steady state, NK cells suppress homeostatic proliferation of $CD8^+$ T cells through IL-15 competition (Zecher et al., 2010). I propose that a similar mechanism may be at play during infection and activation of both CD8 and NK cells. Strikingly, licensed $XCR1^+$ DC are known to produce CCL3/4 and IL-15. Additionally, NK cells express CCR5 and the IL-15 receptor complex. Hence, NK cells are likely to be recruited to the licensed $XCR1^+$ DC, where they would be activated through IL-15. In line with this notion, it was shown that after viral infection, NK cells were recruited to LN´s and activated through type I IFN and $XCR1^+$ DC-derived IL-15 (Lucas et al., 2007). Moreover, several publications delineate that IL-15 signals promote memory $CD8^+$ T cell differentiation (Manjunath et al., 2001; Kaech and Cui, 2012; Mathieu et al., 2015). The group of Stephen N. Waggoner has shown that in the absence of NK cells, increased numbers and altered functionality of memory $CD8^+$ T cells can be observed after viral infections. Further, they showed a NK cell dependent control of $CD4^+$ T cell responses, which, in turn, could also lead to an impaired $CD8^+$ T cell memory formation due to the reduced numbers of helper $CD4^+$ T cells (Rydyznski et al., 2015). However, this data do not exclude the hypothesis of a NK cell dependent IL-15 competition during $CD8^+$ T cell differentiation. Besides the competition of cytokines, NK cells are known to rapidly produce cytokines upon viral infection. The most prominent secreted cytokine is IFNγ, which is also known to affect $CD8^+$ T cell differentiation (Martín-Fontecha et al., 2004). However, the effects of NK cell-driven IFNγ on $CD8^+$ T cell responses are very variable and dependent on the experimental model (Cook et al., 2014). In addition, it was demonstrated that NK cells are able to eliminate activated $CD8^+$ T cells in a perforin-dependent manner early during persistent LCMV infection (Waggoner et al., 2012). The questions remain open, whether NK cells influence $CD8^+$ T cell differentiation during the initial priming and during the helper phase and if so, how? Are those NK cells, which are found later in the paracortex, the same NK cells from the initial priming sites? Do LN-resident NK cells migrate towards the paracortex or are they newly recruited from the blood during the infection? Is the differential localization of NK cells linked to their different functional behavior? The above questions as well as how NK

cells influence CD8+ T cell differentiation are currently under investigation. Overall, my data illustrate the complexity of spatial-temporal CD8+ T cell interactions during their priming and thereby provide a new perspective on how CD8+ T cells develop into different specialized populations.

3.11 A spatio-temporal model for CD8+ T cell differentiation

A single naïve antigen-specific CD8+ T cell has the potential to differentiate into a range of effector and memory CD8+ T cell subsets. The question of when, where and how a heterogeneous CD8+ T cells response can be generated, has been intensively researched and is an ongoing field of study. Nevertheless, it is well established that help is critical for the differentiation of memory CD8+ T cells. In the present work, I found changes in CD8+ T cell differentiation, in which the absence of XCR1+ DC led to a decrease of memory CD8+ T cell precursors and further to an impaired proliferative capacity of memory CD8+ T cells. In the following chapter, in order to combine my model with memory CD8+ T cell differentiation, I highlight previous observations and models of effects influencing the CD8+ T cell programming.

It is well established that the fate of CD8+ T cell differentiation is influenced by the presence or absence of inflammatory stimuli. Thereby, a pro-inflammatory milieu promotes effector CD8+ T cell differentiation (TEC), whereas a milieu with low level inflammation rather promotes memory CD8+ T cell differentiation (Haring et al., 2006; Zhang and Bevan, 2011). For example, it was shown that the ´late-incomers` of foreign CD8+ T cells preferentially develop into central memory CD8+ T cells due to a decreased antigen availability and inflammation (D'Souza and Hedrick, 2006). Another model, which considers the role of inflammation as well as repetitive signals during CD8+ T cell differentiation, is the model of decreasing potential (Kaech and Cui, 2012; see also 1.2.3). This model implicates that repetitive foreign antigen stimulations in a pro-inflammatory area promote effector CD8+ T cell differentiation, whereas stimulation through lower doses of antigens in an anti-inflammatory area promote memory CD8+ T cells differentiation. How can these findings be integrated into a spatio-dynamic model of CD8+ T cell differentiation?

Upon infection, pathogens arrive via the lymphatics in the subcapsular sinus (SCS) and the interfollicular and medullary areas of the LN. Here, a layer of macrophages forms a physical

barrier to prevent pathogen spread (Kastenmüller et al., 2012). These subcapsular sinus and medullary macrophages produce high levels of inflammatory cytokines, like type I IFN, TNF and inflammasome dependent cytokines like IL-1β and IL-18. On these grounds, the antigen availability and inflammatory cues are very high in these areas. In my work, I showed that the provision of memory-promoting help occurs later in the less-inflamed deeper paracortical areas of the LN, which support the proposed models of $CD8^+$ T cell differentiation (Haring et al., 2006; Kaech and Cui, 2012; Kim and Harty, 2014). In other words, $CD8^+$ T cells that linger in the LN periphery are disposed to become effector cells based on their high exposure to inflammatory cues and antigen. In contrast $CD8^+$ T cells that predominantly migrate into the paracortex are less exposed to inflammatory cytokines.

This spatio-temporal concept of $CD8^+$ T cell differentiation is further supported by studies analyzing the role of chemokine receptors on effector *versus* memory $CD8^+$ T cells differentiation. In particular, those studies found that in the absence of the inflammatory chemokine receptor CXCR3, T cells remain in the white pulp of the spleen and are skewed towards memory $CD8^+$ T cell differentiation (Hu et al., 2011; Kurachi et al., 2011). In the LN, this receptor guides the $CD8^+$ T cells through CXCL9 and CXCL10 to the infected cells and further into the pro-inflammatory microenvironment (IFA, SCS and medulla). In contrast, the receptor CCR5 promotes interaction with licensed DC and therefore its absence led to impaired memory development (Castellino et al., 2006). Interestingly, both receptors are not expressed on naïve $CD8^+$ T cells (ImmGen database; search term: CXCR3 and CCR5 (Heng and Painter, 2008)) and hence support the model I propose in this study that pre-activated rather than naïve $CD8^+$ T cells are the recipients of help and that this process involves the interaction with multiple DCs.

Bringing together various aspects of $CD8^+$ T cells differentiation with my results on spatio-temporal aspects of T cells priming, I hypothesize that $CD8^+$ T cell differentiation depends on the localization of the second round of DC interactions (inflammation area *versus* helping area or LN periphery *versus* LN paracortex). In line with previous publications, it is well established that the initial activation of naïve $CD8^+$ T cells occurs in the inflamed SCS and IFA of the LN (Bajénoff et al., 2003; Hickman et al., 2008; John et al., 2009). The strength of this initial priming step likely determines the expression level of chemokine receptors which in turn determine the likelihood for activated T cells to be present in the inflamed LN periphery

versus help-enriched paracortical environment. CCR5 appears to have a two-sided role based on current literature (Castellino et al., 2006; Kohlmeier et al., 2011). On one hand, CCR5 promotes recruitment to helped XCR1$^+$ DC, on the other hand its absence (in combination with loss of CXCR3) was also shown to promote memory development. Currently, the recruitment of activated CD8$^+$ T cells to the paracortex appears to be largely mediated by the absence/or level expression by inflammatory chemokine receptors. However, it is likely that also active chemokine receptor-mediated guidance, similar to CXCR5 and CCR7 for B cells and CD4$^+$ T cells that promote encounters, play are role. Elucidating such factors will be an important goal for future studies, because they may be suitable targets to promote memory CD8$^+$ T cell development in order to optimize vaccine approaches.

In summary, I delineated a spatially separated activation of CD4$^+$ and CD8$^+$ T cells during the early phase of infection and identified XCR1$^+$ DC as the critical helper platform for CD8$^+$ T cell help. Further encounters between CD4$^+$ and CD8$^+$ T cells in the LN paracortex during the later phase of infection are orchestrated on XCR1$^+$ DC. The elucidation of the spatio-temporal dynamics of CD4$^+$ T cell help for CD8$^+$ T cells enabled me to develop a new concept when and where CD4 helper signals are mediated. Moreover, in combination with signaling-based models on CD8$^+$ T cell differentiation, I conceptualized a new localization based model of CD8$^+$ T cell differentiation. An overview of this model is illustrated in Figure 4.2.

My data strongly indicates that under physiological conditions, multiple interactions are taking place and that these interactions are required for an optimal immune response. In my current model CD8$^+$ T cell differentiation is linked to the localization of activated CD8$^+$ T cells within the LN. However, CD8$^+$ T cell differentiation could be further influenced by heterogeneity within the licensed XCR1$^+$ DC pool that reside in similar LN areas. Such DC could receive and provide a range of different signals and produce varying chemotactic and inflammatory cues, which may further contribute to CD8$^+$ T cell recruitment and differentiation. Together, these scenarios help to explain the diversity of CD8$^+$ T cell differentiation. Future studies are required however to analyze (I) if the three-cell encounter (XCR1$^+$ DC, CD4$^+$ T cell, CD8$^+$ T cell) is consecutive or simultaneous, (II) how pre-activated CXCR3$^+$ and CCR5$^+$ CD8$^+$ T cells migrate or stay within certain areas of the LN promoting specific DC interactions and which other chemokine receptors influence such interactions,

(III) how and when accessory cells like NK cells interact and modulate CD8⁺ T cell differentiation from a spatio-temporal perspective. These future studies will provide critical insights into how memory CD8⁺ T cell differentiation can be enhanced and thus, which may allow us to optimize vaccination strategies in the future.

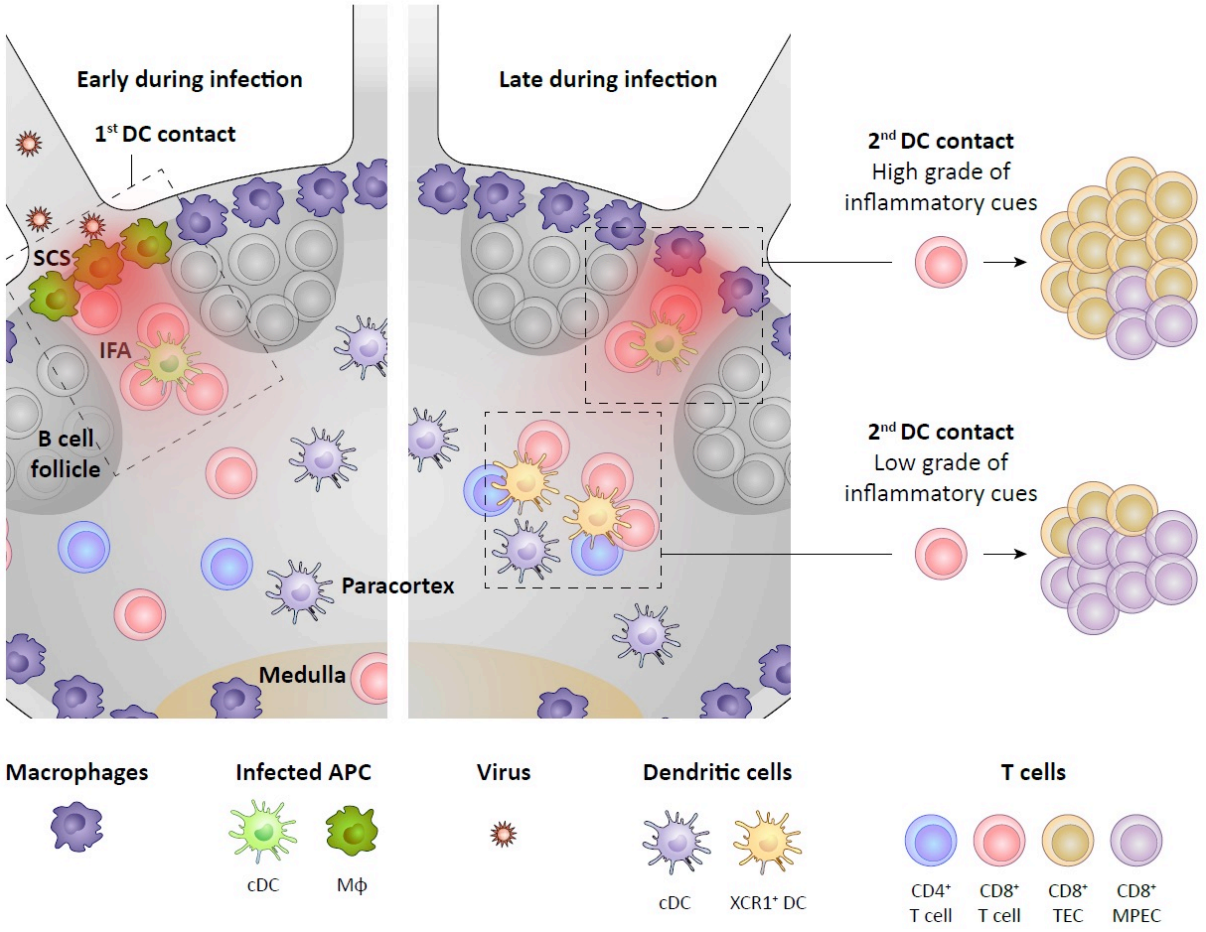

Figure 4.2. A spatio-temporal model for CD8⁺ T cell differentiation.
The picture shows a model of CD8⁺ T cell differentiation based on multiple DC interactions and localization in the LN. Early during viral infection, first DC contact occurs through directly infected APC within the SCS and IFA, which activates antigen-specific CD8⁺ T cells. Later during the infection, pre-activated CD8⁺ T cells have a second DC contact before they undergo proliferation. Depending on the area of the second DC contact, CD8⁺ T cells develop preferentially into TEC (IFA/SCS: high grade of inflammatory cues) or MPEC (paracortex: low grade of inflammatory cues). IFA: interfollicular area; SCS: subcapsular sinus; APC: antigen-presenting cell; Mϕ: macrophage; cDC: conventional dendritic cell; TEC: terminal effector cell; MPEC: memory precursor effector cell. Figure is adapted from Eickhoff et al., 2015.

References

Ahmed, R., Bevan, M.J., Reiner, S.L., and Fearon, D.T. (2009). The precursors of memory: models and controversies. Nat Rev Immunol *9*, 662–668.

Allison, J.P. (1994). CD28-B7 interactions in T-cell activation. Current Opinion in Immunology *6*, 414–419.

Andrian, von, U.H., and Mempel, T.R. (2003). Homing and cellular traffic in lymph nodes. Nat Rev Immunol *3*, 867–878.

Arens, R., and Schoenberger, S.P. (2010). Plasticity in programming of effector and memory CD8 T-cell formation. Immunol Rev *235*, 190–205.

Bajénoff, M., Egen, J.G., Koo, L.Y., Laugier, J.P., Brau, F., Glaichenhaus, N., and Germain, R.N. (2006). Stromal cell networks regulate lymphocyte entry, migration, and territoriality in lymph nodes. Immunity *25*, 989–1001.

Bajénoff, M., Granjeaud, S., and Guerder, S. (2003). The strategy of T cell antigen-presenting cell encounter in antigen-draining lymph nodes revealed by imaging of initial T cell activation. J. Exp. Med. *198*, 715–724.

Banchereau, J., Briere, F., Caux, C., Davoust, J., Lebecque, S., Liu, Y.J., Pulendran, B., and Palucka, K. (2000). Immunobiology of dendritic cells. Annu. Rev. Immunol. *18*, 767–811.

Barnden, M., Allison, J.P., Heath, W.R., and Carbone, F.R. (1998). Defective TCR expression in transgenic mice constructed using cDNA-based [agr]- and [bgr]-chain genes under the control of heterologous regulatory elements. Immunol Cell Biol *76*, 34–40.

Bedoui, S., Heath, W.R., and Mueller, S.N. (2016). CD4(+) T-cell help amplifies innate signals for primary CD8(+) T-cell immunity. Immunol Rev *272*, 52–64.

Behrens, G., Li, M., Smith, C.M., Belz, G.T., Mintern, J., Carbone, F.R., and Heath, W.R. (2004). Helper T cells, dendritic cells and CTL Immunity. Immunol Cell Biol *82*, 84–90.

Belz, G.T., and Nutt, S.L. (2012). Transcriptional programming of the dendritic cell network. Nat Rev Immunol *12*, 101–113.

Bennett, S.R., Carbone, F.R., Karamalis, F., Miller, J.F., and Heath, W.R. (1997). Induction of a CD8+ cytotoxic T lymphocyte response by cross-priming requires cognate CD4+ T cell help. J. Exp. Med. *186*, 65–70.

Benoit, M., Desnues, B., and Mege, J.-L. (2008). Macrophage polarization in bacterial infections. J. Immunol. *181*, 3733–3739.

Bevan, M.J. (2004). Helping the CD8(+) T-cell response. Nat Rev Immunol *4*, 595–602.

Bluestone, J.A., Mackay, C.R., O'Shea, J.J., and Stockinger, B. (2009). The functional plasticity of T cell subsets. Nat Rev Immunol *9*, 811–816.

Bourgeois, C., and Tanchot, C. (2003). Mini-review CD4 T cells are required for CD8 T cell memory generation. Eur. J. Immunol. *33*, 3225–3231.

Bousso, P., and Robey, E. (2003). Dynamics of CD8+ T cell priming by dendritic cells in intact lymph nodes. Nat Immunol *4*, 579–585.

Böttcher, J.P., Beyer, M., Meissner, F., Abdullah, Z., Sander, J., Höchst, B., Eickhoff, S., Rieckmann, J.C., Russo, C., Bauer, T., et al. (2015). Functional classification of memory CD8(+) T cells by CX3CR1 expression. Nat Commun *6*, 8306.

Brewitz, A., Eickhoff, S., Dähling, S., Quast, T., Bedoui, S., Kroczek, R.A., Kurts, C., Garbi, N., Barchet, W., Iannacone, M., et al. (2017). CD8(+) T Cells Orchestrate pDC-XCR1(+) Dendritic Cell Spatial and Functional Cooperativity to Optimize Priming. Immunity *46*, 205–219.

Brincks, E.L., Katewa, A., Kucaba, T.A., Griffith, T.S., and Legge, K.L. (2008). CD8 T cells utilize TRAIL to control influenza virus infection. J. Immunol. *181*, 4918–4925.

Brownlie, R.J., and Zamoyska, R. (2013). T cell receptor signalling networks: branched, diversified and bounded. Nat Rev Immunol *13*, 257–269.

Butcher, E.C., and Picker, L.J. (1996). Lymphocyte homing and homeostasis. Science *272*, 60–66.

Calabro, S., Liu, D., Gallman, A., Nascimento, M.S.L., Yu, Z., Zhang, T.-T., Chen, P., Zhang, B., Xu, L., Gowthaman, U., et al. (2016). Differential Intrasplenic Migration of Dendritic Cell Subsets Tailors Adaptive Immunity. CellReports *16*, 2472–2485.

Caminschi, I. (2012). Targeting dendritic cells in vivo for cancer therapy. 1–13.

Cassell, D., and Forman, J. (1988). Linked recognition of helper and cytotoxic antigenic determinants for the generation of cytotoxic T lymphocytes. Ann N Y Acad Sci *532*, 51–60.

Castellino, F., and Germain, R.N. (2006). Cooperation between CD4+ and CD8+ T cells: when, where, and how. Annu. Rev. Immunol. *24*, 519–540.

Castellino, F., Huang, A.Y., Altan-Bonnet, G., Stoll, S., Scheinecker, C., and Germain, R.N. (2006). Chemokines enhance immunity by guiding naive CD8+ T cells to sites of CD4+ T cell–dendritic cell interaction. Nature *440*, 890–895.

Cebrian, M., Yague, E., Rincon, M., Lopez-Botet, M., de Landazuri, M.O., and Sanchez-Madrid, F. (1988). Triggering of T cell proliferation through AIM, an activation inducer molecule expressed on activated human lymphocytes. J. Exp. Med. *168*, 1621–1637.

Chang, J.T., Palanivel, V.R., Kinjyo, I., Schambach, F., Intlekofer, A.M., Banerjee, A., Longworth, S.A., Vinup, K.E., Mrass, P., Oliaro, J., et al. (2007). Asymmetric T lymphocyte division in the initiation of adaptive immune responses. Science *315*, 1687–1691.

Cook, K.D., Waggoner, S.N., and Whitmire, J.K. (2014). NK cells and their ability to modulate T cells during virus infections. Crit Rev Immunol *34*, 359–388.

Cruz-Guilloty, F., Pipkin, M.E., Djuretic, I.M., Levanon, D., Lotem, J., Lichtenheld, M.G., Groner, Y., and Rao, A. (2009). Runx3 and T-box proteins cooperate to establish the transcriptional program of effector CTLs. J. Exp. Med. *206*, 51–59.

Cui, W., and Kaech, S.M. (2010). Generation of effector CD8+ T cells and their conversion to memory T cells. Immunol Rev *236*, 151–166.

Curtsinger, J.M., Johnson, C.M., and Mescher, M.F. (2003a). CD8 T cell clonal expansion and development of effector function require prolonged exposure to antigen, costimulation, and signal 3 cytokine. J. Immunol. *171*, 5165–5171.

Curtsinger, J.M., Lins, D.C., and Mescher, M.F. (2003b). Signal 3 determines tolerance versus full activation of naive CD8 T cells: dissociating proliferation and development of effector function. J. Exp. Med. *197*, 1141–1151.

Curtsinger, J.M., Valenzuela, J.O., Agarwal, P., Lins, D., and Mescher, M.F. (2005). Type I IFNs provide a third signal to CD8 T cells to stimulate clonal expansion and differentiation. J. Immunol. *174*, 4465–4469.

Cyster, J.G. (2005). Chemokines, sphingosine-1-phosphate, and cell migration in secondary lymphoid organs. Annu. Rev. Immunol. *23*, 127–159.

D'Souza, W.N., and Hedrick, S.M. (2006). Cutting edge: latecomer CD8 T cells are imprinted with a unique differentiation program. J. Immunol. *177*, 777–781.

Davis, M.M., and Bjorkman, P.J. (1988). T-cell antigen receptor genes and T-cell recognition. Nature *334*, 395–402.

Dorner, B.G., Dorner, M.B., Zhou, X., Opitz, C., Mora, A., Guttler, S., Hutloff, A., Mages, H.W., Ranke, K., Schaefer, M., et al. (2009). Selective expression of the chemokine receptor XCR1 on cross-presenting dendritic cells determines cooperation with CD8+ T cells. Immunity *31*, 823–833.

Dorner, B.G., Scheffold, A., Rolph, M.S., Huser, M.B., Kaufmann, S.H.E., Radbruch, A., Flesch, I.E.A., and Kroczek, R.A. (2002). MIP-1alpha, MIP-1beta, RANTES, and ATAC/lymphotactin function together with IFN-gamma as type 1 cytokines. Proc Natl Acad Sci U S A *99*, 6181–6186.

Dorner, B.G., Smith, H.R.C., French, A.R., Kim, S., Poursine-Laurent, J., Beckman, D.L., Pingel, J.T., Kroczek, R.A., and Yokoyama, W.M. (2004). Coordinate expression of cytokines and chemokines by NK cells during murine cytomegalovirus infection. J. Immunol. *172*, 3119–3131.

Eickhoff, S., Brewitz, A., Gerner, M.Y., Klauschen, F., Komander, K., Hemmi, H., Garbi, N., Kaisho, T., Germain, R.N., and Kastenmüller, W. (2015). Robust Anti-viral Immunity Requires Multiple Distinct T Cell-Dendritic Cell Interactions. Cell *162*, 1322–1337.

Feau, S., Garcia, Z., Arens, R., Yagita, H., Borst, J., and Schoenberger, S.P. (2012). The CD4+ T-cell help signal is transmitted from APC to CD8+ T-cells via CD27–CD70 interactions. Nat Commun *3*, 948–949.

Frenz, T., Waibler, Z., Hofmann, J., Hamdorf, M., Lantermann, M., Reizis, B., Tovey, M.G., Aichele, P., Sutter, G., and Kalinke, U. (2010). Concomitant type I IFN receptor-triggering of T cells and of DC is required to promote maximal modified vaccinia virus Ankara-induced T-cell expansion. Eur. J. Immunol. *40*, 2769–2777.

Garcia, K.C., and Adams, E.J. (2005). How the T cell receptor sees antigen--a structural view. Cell *122*, 333–336.

Garcia, Z., Lemaitre, F., van Rooijen, N., Albert, M.L., Levy, Y., Schwartz, O., and Bousso, P. (2012). Subcapsular sinus macrophages promote NK cell accumulation and activation in response to lymph-borne viral particles. Blood *120*, 4744–4750.

Gatto, D., Wood, K., Caminschi, I., Murphy-Durland, D., Schofield, P., Christ, D., Karupiah, G., and Brink, R. (2013). The chemotactic receptor EBI2 regulates the homeostasis, localization and immunological function of splenic dendritic cells. Nat Immunol *14*, 446–453.

Gerlach, C., Moseman, E.A., Loughhead, S.M., Alvarez, D., Zwijnenburg, A.J., Waanders, L., Garg, R., la Torre, de, J.C., and Andrian, von, U.H. (2016). The Chemokine Receptor CX3CR1 Defines Three Antigen-Experienced CD8 T Cell Subsets with Distinct Roles in Immune Surveillance and Homeostasis. Immunity *45*, 1270–1284.

Gerlach, C., van Heijst, J.W.J., Swart, E., Sie, D., Armstrong, N., Kerkhoven, R.M., Zehn, D., Bevan, M.J., Schepers, K., and Schumacher, T.N.M. (2010). One naive T cell, multiple fates in CD8+ T cell differentiation. J. Exp. Med. *207*, 1235–1246.

Gerner, M.Y., Casey, K.A., Kastenmüller, W., and Germain, R.N. (2017). Dendritic cell and antigen dispersal landscapes regulate T cell immunity. J. Exp. Med.

Gerner, M.Y., Kastenmüller, W., Ifrim, I., Kabat, J., and Germain, R.N. (2012). Histo-cytometry: a method for highly multiplex quantitative tissue imaging analysis applied to dendritic cell subset microanatomy in lymph nodes. Immunity *37*, 364–376.

Gowans, J.L., and Knight, E.J. (1964). The Route of Re-Circulation of Lymphocytes in the Rat. Proc R Soc Lond B Biol Sci *159*, 257–282.

Greenwald, R.J., Freeman, G.J., and Sharpe, A.H. (2005). The B7 family revisited. Annu. Rev. Immunol. *23*, 515–548.

Greyer, M., Whitney, P.G., Stock, A.T., Davey, G.M., Tebartz, C., Bachem, A., Mintern, J.D., Strugnell, R.A., Turner, S.J., Gebhardt, T., et al. (2016). T Cell Help Amplifies Innate Signals in

CD8(+) DCs for Optimal CD8(+) T Cell Priming. CellReports *14*, 586–597.

Gutierrez-Martinez, E., Planes, R., Anselmi, G., Reynolds, M., Menezes, S., Adiko, A.C., Saveanu, L., and Guermonprez, P. (2015). Cross-Presentation of Cell-Associated Antigens by MHC Class I in Dendritic Cell Subsets. Front Immunol *6*, 363.

Harding, F.A., McArthur, J.G., Gross, J.A., Raulet, D.H., and Allison, J.P. (1992). CD28-mediated signalling co-stimulates murine T cells and prevents induction of anergy in T-cell clones. Nature *356*, 607–609.

Haring, J.S., Badovinac, V.P., and Harty, J.T. (2006). Inflaming the CD8+ T cell response. Immunity *25*, 19–29.

Hassin, D., Garber, O.G., Meiraz, A., Schiffenbauer, Y.S., and Berke, G. (2011). Cytotoxic T lymphocyte perforin and Fas ligand working in concert even when Fas ligand lytic action is still not detectable. Immunology *133*, 190–196.

Helft, J., Manicassamy, B., Guermonprez, P., Hashimoto, D., Silvin, A., Agudo, J., Brown, B.D., Schmolke, M., Miller, J.C., Leboeuf, M., et al. (2012). Cross-presenting CD103+ dendritic cells are protected from influenza virus infection. J Clin Invest *122*, 4037–4047.

Hendriks, J., Gravestein, L.A., Tesselaar, K., van Lier, R.A., Schumacher, T.N., and Borst, J. (2000). CD27 is required for generation and long-term maintenance of T cell immunity. Nat Immunol *1*, 433–440.

Hendriks, J., Xiao, Y., and Borst, J. (2003). CD27 promotes survival of activated T cells and complements CD28 in generation and establishment of the effector T cell pool. J. Exp. Med. *198*, 1369–1380.

Heng, T.S., and Painter, M.W. (2008). The Immunological Genome Project: networks of gene expression in immune cells. Nat Immunol *9*, 1091-1094.

Hickman, H.D., Takeda, K., Skon, C.N., Murray, F.R., Hensley, S.E., Loomis, J., Barber, G.N., Bennink, J.R., and Yewdell, J.W. (2008). Direct priming of antiviral CD8+ T cells in the peripheral interfollicular region of lymph nodes. Nat Immunol *9*, 155–165.

Hildner, K., Edelson, B.T., Purtha, W.E., Diamond, M., Matsushita, H., Kohyama, M., Calderon, B., Schraml, B.U., Unanue, E.R., Diamond, M.S., et al. (2008). Batf3 Deficiency Reveals a Critical Role for CD8 + Dendritic Cells in Cytotoxic T Cell Immunity. Science *322*, 1097–1100.

Hirst, C.E., Buzza, M.S., Bird, C.H., Warren, H.S., Cameron, P.U., Zhang, M., Ashton-Rickardt, P.G., and Bird, P.I. (2003). The intracellular granzyme B inhibitor, proteinase inhibitor 9, is up-regulated during accessory cell maturation and effector cell degranulation, and its overexpression enhances CTL potency. J. Immunol. *170*, 805–815.

Hogquist, K.A., Jameson, S.C., Heath, W.R., Howard, J.L., Bevan, M.J., and Carbone, F.R. (1994). T cell receptor antagonist peptides induce positive selection. Cell *76*, 17–27.

Hor, J.L., Whitney, P.G., Zaid, A., Brooks, A.G., Heath, W.R., and Mueller, S.N. (2015). Spatiotemporally Distinct Interactions with Dendritic Cell Subsets Facilitates CD4+ and CD8+ T Cell Activation to Localized Viral Infection. Immunity *43*, 554–565.

Hu, J.K., Kagari, T., Clingan, J.M., and Matloubian, M. (2011). Expression of chemokine receptor CXCR3 on T cells affects the balance between effector and memory CD8 T-cell generation. Proc Natl Acad Sci U S A *108*, E118–E127.

Itano, A.A., and Jenkins, M.K. (2003). Antigen presentation to naive CD4 T cells in the lymph node. Nat Immunol *4*, 733–739.

Iyoda, T., Shimoyama, S., Liu, K., Omatsu, Y., Akiyama, Y., Maeda, Y., Takahara, K., Steinman, R.M., and Inaba, K. (2002). The CD8+ dendritic cell subset selectively endocytoses dying cells in culture and in vivo. J. Exp. Med. *195*, 1289–1302.

John, B., Harris, T.H., Tait, E.D., Wilson, E.H., Gregg, B., Ng, L.G., Mrass, P., Roos, D.S., Dzierszinski, F., Weninger, W., et al. (2009). Dynamic Imaging of CD8(+) T cells and dendritic cells during infection with Toxoplasma gondii. PLoS Pathog *5*, e1000505.

Kaech, S.M., and Cui, W. (2012). Transcriptional control of effector and memory CD8+ T cell differentiation. Nat Rev Immunol *12*, 749–761.

Kalia, V., Sarkar, S., Subramaniam, S., Haining, W.N., Smith, K.A., and Ahmed, R. (2010). Prolonged interleukin-2Ralpha expression on virus-specific CD8+ T cells favors terminal-effector differentiation in vivo. Immunity *32*, 91–103.

Kamala, T. (2007). Hock immunization: A humane alternative to mouse footpad injections. Journal of Immunological Methods *328*, 204–214.

Kastenmüller, W., Brandes, M., Wang, Z., Herz, J., Egen, J.G., and Germain, R.N. (2013). Peripheral prepositioning and local CXCL9 chemokine-mediated guidance orchestrate rapid memory CD8+ T cell responses in the lymph node. Immunity *38*, 502–513.

Kastenmüller, W., Torabi-Parizi, P., Subramanian, N., Lammermann, T., and Germain, R.N. (2012). A spatially-organized multicellular innate immune response in lymph nodes limits systemic pathogen spread. Cell *150*, 1235–1248.

Kennedy, M.K., Glaccum, M., Brown, S.N., Butz, E.A., Viney, J.L., Embers, M., Matsuki, N., Charrier, K., Sedger, L., Willis, C.R., et al. (2000). Reversible defects in natural killer and memory CD8 T cell lineages in interleukin 15-deficient mice. J. Exp. Med. *191*, 771–780.

Kim, M.T., and Harty, J.T. (2014). Impact of Inflammatory Cytokines on Effector and Memory CD8+ T Cells. Front Immunol *5*, 295.

Kissenpfennig, A., Henri, S., Dubois, B., Laplace-Builhe, C., Perrin, P., Romani, N., Tripp, C.H., Douillard, P., Leserman, L., Kaiserlian, D., et al. (2005). Dynamics and function of Langerhans cells in vivo: dermal dendritic cells colonize lymph node areas distinct from slower migrating Langerhans cells. Immunity *22*, 643–654.

Klauschen, F., Ishii, M., Qi, H., Bajénoff, M., Egen, J.G., Germain, R.N., and Meier-Schellersheim, M. (2009). Quantifying cellular interaction dynamics in 3D fluorescence microscopy data. Nat Protoc *4*, 1305–1311.

Kohlmeier, J.E., Reiley, W.W., Perona-Wright, G., Freeman, M.L., Yager, E.J., Connor, L.M., Brincks, E.L., Cookenham, T., Roberts, A.D., Burkum, C.E., et al. (2011). Inflammatory chemokine receptors regulate CD8(+) T cell contraction and memory generation following infection. J. Exp. Med. *208*, 1621–1634.

Kolumam, G.A., Thomas, S., Thompson, L.J., Sprent, J., and Murali-Krishna, K. (2005). Type I interferons act directly on CD8 T cells to allow clonal expansion and memory formation in response to viral infection. J. Exp. Med. *202*, 637–650.

Kurachi, M., Kurachi, J., Suenaga, F., Tsukui, T., Abe, J., Ueha, S., Tomura, M., Sugihara, K., Takamura, S., Kakimi, K., et al. (2011). Chemokine receptor CXCR3 facilitates CD8(+) T cell differentiation into short-lived effector cells leading to memory degeneration. J. Exp. Med. *208*, 1605–1620.

Kurts, C., Heath, W.R., Carbone, F.R., Allison, J., Miller, J.F., and Kosaka, H. (1996). Constitutive class I-restricted exogenous presentation of self antigens in vivo. J. Exp. Med. *184*, 923–930.

Lanzavecchia, A., and Sallusto, F. (2002). Progressive differentiation and selection of the fittest in the immune response. Nat Rev Immunol *2*, 982–987.

Lenschow, D.J., Walunas, T.L., and Bluestone, J.A. (1996). CD28/B7 system of T cell costimulation. Annu. Rev. Immunol. *14*, 233–258.

Lindquist, R.L., Shakhar, G., Dudziak, D., Wardemann, H., Eisenreich, T., Dustin, M.L., and Nussenzweig, M.C. (2004). Visualizing dendritic cell networks in vivo. Nat Immunol *5*, 1243–1250.

Lucas, M., Schachterle, W., Oberle, K., Aichele, P., and Diefenbach, A. (2007). Dendritic cells prime natural killer cells by trans-presenting interleukin 15. Immunity *26*, 503–517.

Ma, A., Koka, R., and Burkett, P. (2006). Diverse functions of IL-2, IL-15, and IL-7 in lymphoid homeostasis. Annu. Rev. Immunol. *24*, 657–679.

Madsen, L., Labrecque, N., Engberg, J., Dierich, A., Svejgaard, A., Benoist, C., Mathis, D., and Fugger, L. (1999). Mice lacking all conventional MHC class II genes. Proceedings of the National Academy of Sciences *96*, 10338–10343.

Mandl, J.N., Liou, R., Klauschen, F., Vrisekoop, N., Monteiro, J.P., Yates, A.J., Huang, A.Y., and Germain, R.N. (2012). Quantification of lymph node transit times reveals differences in antigen surveillance strategies of naive CD4+ and CD8+ T cells. Proc Natl Acad Sci U S A *109*, 18036–18041.

Manjunath, N., Shankar, P., Wan, J., Weninger, W., Crowley, M.A., Hieshima, K., Springer,

T.A., Fan, X., Shen, H., Lieberman, J., et al. (2001). Effector differentiation is not prerequisite for generation of memory cytotoxic T lymphocytes. J Clin Invest *108*, 871–878.

Mantovani, A., Sozzani, S., Locati, M., Allavena, P., and Sica, A. (2002). Macrophage polarization: tumor-associated macrophages as a paradigm for polarized M2 mononuclear phagocytes. Trends Immunol *23*, 549–555.

Martín-Fontecha, A., Thomsen, L.L., Brett, S., Gerard, C., Lipp, M., Lanzavecchia, A., and Sallusto, F. (2004). Induced recruitment of NK cells to lymph nodes provides IFN-gamma for T(H)1 priming. Nat Immunol *5*, 1260–1265.

Mathieu, C., Beltra, J.-C., Charpentier, T., Bourbonnais, S., Di Santo, J.P., Lamarre, A., and Decaluwe, H. (2015). IL-2 and IL-15 regulate CD8+ memory T-cell differentiation but are dispensable for protective recall responses. Eur. J. Immunol. *45*, 3324–3338.

Matloubian, M., Lo, C.G., Cinamon, G., Lesneski, M.J., Xu, Y., Brinkmann, V., Allende, M.L., Proia, R.L., and Cyster, J.G. (2004). Lymphocyte egress from thymus and peripheral lymphoid organs is dependent on S1P receptor 1. Nature *427*, 355–360.

Matzinger, P., and Kamala, T. (2011). Tissue-based class control: the other side of tolerance. Nat Rev Immunol *11*, 221–230.

Maudsley, D.J., and Pound, J.D. (1991). Modulation of MHC antigen expression by viruses and oncogenes. Immunol Today *12*, 429–431.

McHeyzer-Williams, L.J., Malherbe, L.P., and McHeyzer-Williams, M.G. (2006). Checkpoints in memory B-cell evolution. Immunol Rev *211*, 255–268.

Medzhitov, R., and Janeway, C.J. (2000). Innate immune recognition: mechanisms and pathways. Immunol Rev *173*, 89–97.

Mempel, T.R., Henrickson, S.E., and Andrian, von, U.H. (2004). T-cell priming by dendriticcells in lymph nodes occurs in three distinct phases. Nature *427*, 154–159.

Merad, M., Ginhoux, F., and Collin, M. (2008). Origin, homeostasis and function of Langerhans cells and other langerin-expressing dendritic cells. Nat Rev Immunol *8*, 935–947.

Merad, M., Sathe, P., Helft, J., Miller, J., and Mortha, A. (2013). The dendritic cell lineage: ontogeny and function of dendritic cells and their subsets in the steady state and the inflamed setting. Annu. Rev. Immunol. *31*, 563–604.

Mescher, M.F., Curtsinger, J.M., Agarwal, P., Casey, K.A., Gerner, M., Hammerbeck, C.D., Popescu, F., and Xiao, Z. (2006). Signals required for programming effector and memory development by CD8+ T cells. Immunol Rev *211*, 81–92.

Miles, J.J., Elhassen, D., Borg, N.A., Silins, S.L., Tynan, F.E., Burrows, J.M., Purcell, A.W., Kjer-Nielsen, L., Rossjohn, J., Burrows, S.R., et al. (2005). CTL recognition of a bulged viral peptide involves biased TCR selection. J. Immunol. *175*, 3826–3834.

Miller, M.J., Safrina, O., Parker, I., and Cahalan, M.D. (2004). Imaging the single cell dynamics of CD4+ T cell activation by dendritic cells in lymph nodes. J. Exp. Med. *200*, 847–856.

Miller, M.J., Wei, S.H., Parker, I., and Cahalan, M.D. (2002). Two-photon imaging of lymphocyte motility and antigen response in intact lymph node. Science *296*, 1869–1873.

Mitchison, N.A., and O'Malley, C. (1987). Three-cell-type clusters of T cells with antigen-presenting cells best explain the epitope linkage and noncognate requirements of the in vivo cytolytic response. Eur. J. Immunol. *17*, 1579–1583.

Murphy, K., and Weaver, C. (2016). Janeway´s Immunbiology 9th Edition (Garland Science).

Norbury, C.C., Princiotta, M.F., Bacik, I., Brutkiewicz, R.R., Wood, P., Elliott, T., Bennink, J.R., and Yewdell, J.W. (2001). Multiple antigen-specific processing pathways for activating naive CD8+ T cells in vivo. J. Immunol. *166*, 4355–4362.

Oppermann, M. (2004). Chemokine receptor CCR5: insights into structure, function, and regulation. Cell Signal *16*, 1201–1210.

Oxenius, A., Bachmann, M.F., Zinkernagel, R.M., and Hengartner, H. (1998). Virus-specific MHC-class II-restricted TCR-transgenic mice: effects on humoral and cellular immune responses after viral infection. Eur. J. Immunol. *28*, 390–400.

Parish, I.A., and Kaech, S.M. (2009). Diversity in CD8(+) T cell differentiation. Current Opinion in Immunology *21*, 291–297.

Pearce, E.L., and Shen, H. (2007). Generation of CD8 T cell memory is regulated by IL-12. J. Immunol. *179*, 2074–2081.

Pham, T.H.M., Baluk, P., Xu, Y., Grigorova, I., Bankovich, A.J., Pappu, R., Coughlin, S.R., McDonald, D.M., Schwab, S.R., and Cyster, J.G. (2010). Lymphatic endothelial cell sphingosine kinase activity is required for lymphocyte egress and lymphatic patterning. J. Exp. Med. *207*, 17–27.

Pircher, H., Burki, K., Lang, R., Hengartner, H., and Zinkernagel, R.M. (1989). Tolerance induction in double specific T-cell receptor transgenic mice varies with antigen. Nature *342*, 559–561.

Prlic, M., Hernandez-Hoyos, G., and Bevan, M.J. (2006). Duration of the initial TCR stimulus controls the magnitude but not functionality of the CD8+ T cell response. J. Exp. Med. *203*, 2135–2143.

Qi, H., Kastenmüller, W., and Germain, R.N. (2014). Spatiotemporal basis of innate and adaptive immunity in secondary lymphoid tissue. Annu Rev Cell Dev Biol *30*, 141–167.

Randolph, G.J., Angeli, V., and Swartz, M.A. (2005). Dendritic-cell trafficking to lymph nodes through lymphatic vessels. Nat Rev Immunol *5*, 617–628.

Ratner, A., and Clark, W.R. (1993). Role of TNF-alpha in CD8+ cytotoxic T lymphocyte-

mediated lysis. J. Immunol. *150*, 4303–4314.

Reinhardt, R.L., Liang, H.-E., and Locksley, R.M. (2009). Cytokine-secreting follicular T cells shape the antibody repertoire. Nat Immunol *10*, 385–393.

Ridge, J.P., Di Rosa, F., and Matzinger, P. (1998). A conditioned dendritic cell can be a temporal bridge between a CD4+ T-helper and a T-killer cell. Nature *393*, 474–478.

Rudensky, A.Y., Preston-Hurlburt, P., Hong, S.C., Barlow, A., and Janeway, C.A.J. (1991). Sequence analysis of peptides bound to MHC class II molecules. Nature *353*, 622–627.

Rudolph, M.G., Stanfield, R.L., and Wilson, I.A. (2006). How TCRs bind MHCs, peptides, and coreceptors. Annu. Rev. Immunol. *24*, 419–466.

Rydyznski, C., Daniels, K.A., Karmele, E.P., Brooks, T.R., Mahl, S.E., Moran, M.T., Li, C., Sutiwisesak, R., Welsh, R.M., and Waggoner, S.N. (2015). Generation of cellular immune memory and B-cell immunity is impaired by natural killer cells. Nat Commun *6*, 1–14.

Sanchez, P.J., McWilliams, J.A., Haluszczak, C., Yagita, H., and Kedl, R.M. (2007). Combined TLR/CD40 stimulation mediates potent cellular immunity by regulating dendritic cell expression of CD70 in vivo. J. Immunol. *178*, 1564–1572.

Schaefer, B.C., Schaefer, M.L., Kappler, J.W., Marrack, P., and Kedl, R.M. (2001). Observation of antigen-dependent CD8+ T-cell/ dendritic cell interactions in vivo. Cell Immunol *214*, 110–122.

Schoenberger, S.P., Toes, R.E., van der Voort, E.I., Offringa, R., and Melief, C.J. (1998). T-cell help for cytotoxic T lymphocytes is mediated by CD40-CD40L interactions. Nature *393*, 480–483.

Schulze, D.H., Pease, L.R., Geier, S.S., Reyes, A.A., Sarmiento, L.A., Wallace, R.B., and Nathenson, S.G. (1983). Comparison of the cloned H-2Kbm1 variant gene with the H-2Kb gene shows a cluster of seven nucleotide differences. Proceedings of the National Academy of Sciences *80*, 2007–2011.

Semmling, V., Lukacs-Kornek, V., Thaiss, C.A., Quast, T., Hochheiser, K., Panzer, U., Rossjohn, J., Perlmutter, P., Cao, J., Godfrey, D.I., et al. (2010). Alternative cross-priming through CCL17-CCR4-mediated attraction of CTLs toward NKT cell-licensed DCs. Nat Immunol *11*, 313–320.

Shiow, L.R., Rosen, D.B., Brdickova, N., Xu, Y., An, J., Lanier, L.L., Cyster, J.G., and Matloubian, M. (2006). CD69 acts downstream of interferon-alpha/beta to inhibit S1P1 and lymphocyte egress from lymphoid organs. Nature *440*, 540–544.

Shortman, K., and Heath, W.R. (2010). The CD8+ dendritic cell subset. Immunol Rev *234*, 18–31.

Sixt, M., Kanazawa, N., Selg, M., Samson, T., Roos, G., Reinhardt, D.P., Pabst, R., Lutz, M.B., and Sorokin, L. (2005). The conduit system transports soluble antigens from the afferent

lymph to resident dendritic cells in the T cell area of the lymph node. Immunity *22*, 19–29.

Stabenow, D., Frings, M., Truck, C., Gartner, K., Forster, I., Kurts, C., Tuting, T., Odenthal, M., Dienes, H.-P., Cederbrant, K., et al. (2010). Bioluminescence imaging allows measuring CD8 T cell function in the liver. Hepatology *51*, 1430–1437.

Stachowiak, A.N., Wang, Y., Huang, Y.-C., and Irvine, D.J. (2006). Homeostatic lymphoid chemokines synergize with adhesion ligands to trigger T and B lymphocyte chemokinesis. J. Immunol. *177*, 2340–2348.

Staib, C., Drexler, I., and Sutter, G. (2004). Construction and isolation of recombinant MVA. Methods Mol Biol *269*, 77–100.

Steinman, R.M. (2012). Decisions about dendritic cells: past, present, and future. Annu. Rev. Immunol. *30*, 1–22.

Steinman, R.M., and Cohn, Z.A. (1973). Identification of a novel cell type in peripheral lymphoid organs of mice. I. Morphology, quantitation, tissue distribution. J. Exp. Med. *137*, 1142–1162.

Steinman, R.M., and Cohn, Z.A. (1974). Identification of a novel cell type in peripheral lymphoid organs of mice. II. Functional properties in vitro. J. Exp. Med. *139*, 380–397.

Stemberger, C., Huster, K.M., Koffler, M., Anderl, F., Schiemann, M., Wagner, H., and Busch, D.H. (2007). A single naive CD8+ T cell precursor can develop into diverse effector and memory subsets. Immunity *27*, 985–997.

Stoll, S., Delon, J., Brotz, T.M., and Germain, R.N. (2002). Dynamic imaging of T cell-dendritic cell interactions in lymph nodes. Science *296*, 1873–1876.

Surh, C.D., and Sprent, J. (2008). Homeostasis of naive and memory T cells. Immunity *29*, 848–862.

Tan, P., Anasetti, C., Hansen, J.A., Melrose, J., Brunvand, M., Bradshaw, J., Ledbetter, J.A., and Linsley, P.S. (1993). Induction of alloantigen-specific hyporesponsiveness in human T lymphocytes by blocking interaction of CD28 with its natural ligand B7/BB1. J. Exp. Med. *177*, 165–173.

Trambas, C.M., and Griffiths, G.M. (2003). Delivering the kiss of death. Nat Immunol *4*, 399–403.

van Stipdonk, M.J., Lemmens, E.E., and Schoenberger, S.P. (2001). Naive CTLs require a single brief period of antigenic stimulation for clonal expansion and differentiation. Nat Immunol *2*, 423–429.

Villadangos, J.A., and Young, L. (2008). Antigen-presentation properties of plasmacytoid dendritic cells. Immunity *29*, 352–361.

Waggoner, S.N., Cornberg, M., Selin, L.K., and Welsh, R.M. (2012). Natural killer cells act as

rheostats modulating antiviral T cells. Nature *481*, 394–398.

Watts, T.H. (2005). TNF/TNFR family members in costimulation of T cell responses. Annu. Rev. Immunol. *23*, 23–68.

Weninger, W., Crowley, M.A., Manjunath, N., and Andrian, von, U.H. (2001). Migratory properties of naive, effector, and memory CD8(+) T cells. J. Exp. Med. *194*, 953–966.

Williams, M.A., and Bevan, M.J. (2007). Effector and memory CTL differentiation. Annu. Rev. Immunol. *25*, 171–192.

Woolf, E., Grigorova, I., Sagiv, A., Grabovsky, V., Feigelson, S.W., Shulman, Z., Hartmann, T., Sixt, M., Cyster, J.G., and Alon, R. (2007). Lymph node chemokines promote sustained T lymphocyte motility without triggering stable integrin adhesiveness in the absence of shear forces. Nat Immunol *8*, 1076–1085.

Yamazaki, C., Sugiyama, M., Ohta, T., Hemmi, H., Hamada, E., Sasaki, I., Fukuda, Y., Yano, T., Nobuoka, M., Hirashima, T., et al. (2013). Critical Roles of a Dendritic Cell Subset Expressing a Chemokine Receptor, XCR1. J.I. *190*, 6071–6082.

Zecher, D., Li, Q., Oberbarnscheidt, M.H., Demetris, A.J., Shlomchik, W.D., Rothstein, D.M., and Lakkis, F.G. (2010). NK cells delay allograft rejection in lymphopenic hosts by downregulating the homeostatic proliferation of CD8+ T cells. J. Immunol. *184*, 6649–6657.

Zhang, N., and Bevan, M.J. (2011). CD8+ T Cells: Foot Soldiers of the Immune System. Immunity *35*, 161–168.

Index of Figures

Abbreviations

°C	Degree Celsius
^{137}Cs	Caesium-137
ACK	Ammonium Chlorid Kalium
Ad	Adenovirus
APC	antigen-presenting-cells
$B8R_{20}$	Immuno-dominant epitope against Vaccinia virus, presented via MHCI
Batf3	basic leucine zipper transcription factor, ATF-like 3
BHI	brain heart infusion
BM	bone marrow
BSA	bovine serum albumin
CCL	CC chemokine ligand
CCR	CC chemokine rezeptor
CD	cluster of differentiation
cDC	conventional dendritic cell
CFSE	carboxy fluorescein succinimidyl ester
CFU	colony forming units
CS	cortical sinus
CTL	cytotoxic T lymphocytes
CTB/ G/ O	cell tracker blue/ green/ orange
CTLA4	cytotoxic T-lymphocyte-associated protein 4
CXCL	CXC chemokine ligand
CXCR	CXC chemokine rezeptor
DC	dendritic cells
DMSO	Dimethylsulfoxid
DNA	Deoxyribonucleic acid
DTR	diphtheria toxin receptor
DTX	diphtheria toxin
EDTA	Ethylendiamintetraacetat
EMA	Ethidium monoazide bromide E1374
et al.	*et alii;* and others
FACS	fluorescence activated cell sorting
FBS	fetal bovine serum
FDC	follicular dendritic cells
f.p.	foot-pad
FRC	fibroblastic reticular cells
g	gram or gravity accerelation
GFP	green flourescent protein

GP	glycoprotein of lymphocytic choriomeningitis virus
Gy	Gray
h	hour/hours
HEV	high endothelial venules
hi	high expression
KLRG1	killer cell lectin-like receptor G1
KO	knockout
ICAM1	intracellular adhesion molecule 1
IFA	interfollicular area
IFN	interferon
IL	interleukine
IL-xR	interleukine x receptor
i.p.	intraperitoneal
i.v.	intravenously
IVM	intravital two-photon microscopy
L	liter or ligand
LCMV	lymphocytic choriomeningitis virus
LFA-1	leukocyte function-associated antigen 1
L.m.	*Listeria monocytogenes*
LN	lymph node
LPS	lipopolysaccharid
M	molar
m	milli
MACS	magnetic activated cell sorting
MALT	mucosa-associated lymphoid tissues
MFI	mean fluorescence intensity
MHC	major histocompatibility complex
Mϕ	macrophages
MPEC	memory precursor effector cells
MS	medullary sinus
MVA	modified Vaccinia virus Ankara
min	minute/s
NK cells	natural killer cells
NKT cells	natural killer T cells
NMS	normal mouse serum
NRaS	normal rabbit serum
NRS	normal rat serum
OT-I/OT-II	ovalbumin specific T cells, restricted to MHCI or MHCII, respectively
OVA	ovalbumin
P	P-value

P14	LCMV glycoprotein specific $CD8^+$ T cells, restricted to MHCI
PAMP	pathogen-associated molecular pattern
PBS	phosphate buffered saline
pDC	plasmacytoid dendritic cell
PFA	paraformaldehyd
PFU	plaque forming units
pH	potentia Hydrogenii
pLN	popletial lymph node
PLP	P-buffer L-lysin Paraformaldehyd
p:MCH	peptide load MHC
PNAD	peripheral node addressins
PRR	pattern recognition receptors
s	second/s
S1P	sphingosine 1-phosphate
S1PR1	sphingosine 1-phosphate receptor 1
SCS	subcapsular sinus
sec	second/s
SD	standard deviation
SEM	standard error of the mean
SIINFEKL	$OVA_{257-264}$ peptide sequence
SLEC	short-lived effector cells
SMARTA	LCMV glycoprotein specific $CD4^+$ T cells, restricted to MHCII
T_{CM}	central memory T cells
TCR	T cell receptor
TEC	terminal effector cells
T_{EM}	effector memory T cells
TNF	Tumor-necrose factor
TRAIL	TNF-related apoptosis-inducing ligand
T_{RM}	tissue-resident memory T cells
U	Unit
Ub	ubiquitin
VV	Vaccinia virus
WT	wildtype
YFP	yellow fluorescent protein
α	anti
µ	micro